

Politecnico di Torino (POLITO)

Warsaw University of Technology (WUT)

Master degree in Mechanical engineering

**Determination of main parameters of plug-in hybrid
powertrain components for a passenger car**



SUPERVISORS:

Prof. Ezio Spessa (POLITO)

Prof. Daniela Misul (POLITO)

Prof. Chang Yuhua (WUT)

STUDENT:

Ferriero Simone (254194)

OCTOBER 2020

to my family

Contents

Abstract	V
Abstract (italian version)	VI
Acknowledgements	VII
Acknowledgements (Italian version)	VIII
Chapter 1: Introduction and classification of hybrid vehicles	1
1.1 Introductions to HEV and PHEV _____	1
1.2 Series configuration _____	2
1.3 Parallel configuration _____	5
1.4 Complex configuration: series-parallel _____	9
Chapter 2: Analysis methods	12
2.1 Longitudinal dynamic _____	12
2.2 Backward method and forward method _____	14
2.3 Quasistatic approach _____	15
Chapter 3: Vehicle modelling in Simulink	17
3.1 Vehicle modelling introduction _____	17
3.2 Models for calculating input parameters to the powertrain _____	17
3.3 Transmission models _____	19
3.4 ICE and electric machine models _____	23
3.5 Energy source model _____	25
3.6 Parameter control model _____	26
Chapter 4: Design requirements and calculation of CO₂ emissions and fuel consumption according to EU regulations	27
4.1 NEDC and WLTP results for the reference vehicle _____	27
4.2 Design requirements _____	29
4.3 Charge-depleting test _____	30
4.4 Charge-sustaining test _____	32
4.5 Weighted final results _____	32
4.6 Performance analysis _____	33
Chapter 5: PHEV: Series powertrain	34
5.1 Presentation main component _____	34

5.2 NEDC cycle CD test _____	38
5.3 WLTP cycle CD test _____	39
5.4 NEDC cycle CS test _____	41
5.5 WLTP cycle CS test _____	43
5.6 CO ₂ emissions, FC and electric range calculated for NEDC and WLTP cycle _____	44
5.7 Performance analysis _____	46
Chapter 6: PHEV: Parallel powertrain	50
6.1 Presentation main component _____	50
6.2 NEDC cycle CD test _____	53
6.3 WLTP cycle CD test _____	54
6.4 NEDC cycle CS test _____	56
6.5 WLTP cycle CS test _____	57
6.6 CO ₂ emissions, FC and electric range calculated for NEDC and WLTP cycle _____	58
6.7 Performance analysis _____	60
Chapter 7: PHEV: Series-parallel powertrain	64
7.1 Presentation main component _____	64
7.2 NEDC cycle CD test _____	67
7.3 WLTP cycle CD test _____	69
7.4 NEDC cycle CS test _____	71
7.5 WLTP cycle CS test _____	72
7.6 CO ₂ emissions, FC and electric range calculated for NEDC and WLTP cycle _____	73
7.7 Performance analysis _____	75
Chapter 8: Conclusions	80
Appendix A	82
Bibliography	85

Nomenclature

A_f - Front Area of the Vehicle

C_d - Aerodynamic Drag Coefficient

c_r - Rolling Resistance Coefficient

CD - Charge Depleting

CO₂ - Carbon Dioxide

CS - Charge Sustaining

EC - Electric Energy Consumption

EMS - Energy Management System

EU - European Union

FC - Fuel Consumption

g - Gravity acceleration

GTR - Global Technical Regulation

ICE - Internal Combustion Engine

NEDC - New European Driving Cycle

OEM - Original Equipment Manufacturer

PHEV - Plug-in Hybrid Electric Vehicles

r_w - Wheel Radius

REEC - Relative Electric Energy Change

REESS - Rechargeable Electric Energy Storage System

SOC - State Of Charge

TA - Type Approval

UF - Utility Factor

UNECE - United Nations Economic Commission for Europe

WLTC - Worldwide Harmonized Light Vehicles Test Cycle

WLTP - Worldwide Harmonized Light Vehicles Test Procedure

ρ_a - Air density

γ - Total Gear Ratio

Abstract

The main objective of the following thesis work is to identify and analyze, through the use of the Matlab-simulink simulation software, the behavior of the various elements that make up a hybrid powertrain with plug-in configuration (PHEV). It is necessary to specify the type of configuration since there are particular peculiarities that differentiate it from a traditional hybrid vehicle (HEV), on top of all, the possibility of recharging the batteries through the normal electricity network or public columns.

The thesis work was born thanks to Prof. Chang Yuhua, professor of “Electric and hybrid vehicles engineering” at the Warsaw University of Technology and subsequently continued under the supervision of prof. Ezio Spessa and Prof. Daniela Misul at the Polytechnic of Turin. Starting from a traditional vehicle, with internal combustion engine, belonging to the city-car category, we moved on to the sizing of the main components of a hybrid vehicle: electric motor, electric generator and battery pack, obviously passing through a careful analysis of downsizing of the internal combustion engine and transmission, in order to make it a hybrid vehicle with plug-in configuration. Making the heat engine work in combination with one or more electric motors / generators allows you to select a wide range of vehicle operating modes in order to limit pollutant emissions and better manage the flow of power from the various energy sources present.

In hybrid vehicles it is possible to combine these different powertrains in different ways: in series, in parallel and a mixed series / parallel combination. During the thesis, these various configurations will be explained and deepened, assessing which of these allows better energy management, through specific control strategies, lower fuel consumption and lower emission of pollutants, obviously referring to comfort, driving and vehicle performance.

The idea of taking a city car as an object of study was born from my study experience in Turin and Warsaw. These two cities lend themselves a lot to the use of hybrid vehicles or purely electric vehicles given their territorial compliance, purely flat and to the possible inclusion of the infrastructures required for charging these vehicles given their importance in their respective countries.

The division of the chapters was created in such a way as to carefully follow the logical and design steps and the reasons that led to the choice of the operating parameters of the various components of the powertrain.

Abstract (italian version)

L'obiettivo principale del seguente lavoro di tesi è quello di individuare ed analizzare, attraverso l'utilizzo del software di simulazione Matlab-Simulink, il comportamento dei vari elementi che compongono un powertrain ibrido con configurazione plug-in (PHEV). Risulta necessario specificare il tipo di configurazione dal momento che sono presenti particolari peculiarità che lo differenziano da un ibrido tradizionale (HEV), una fra tutte, la possibilità di ricaricare le batterie attraverso la normale rete elettrica oppure colonnine pubbliche.

Il lavoro di tesi è nato grazie alla prof.ssa Chang Yuhua, docente di "Electric and hybrid vehicles engineering" presso il Warsaw University of Technology e proseguito successivamente sotto la supervisione del prof. Ezio Spessa e della prof.ssa Daniela Misul presso il Politecnico di Torino. Partendo da un veicolo tradizionale, con motore a combustione interna, facente parte della categoria city-car, si è passati al dimensionamento dei principali componenti di un veicolo ibrido: motore elettrico, generatore elettrico e pacco batterie, passando ovviamente attraverso un'attenta analisi di ridimensionamento del motore a combustione interna e della trasmissione, al fine di renderlo un veicolo ibrido con configurazione plug-in. Far lavorare il motore termico in combinazione con uno o più motori/generatori elettrici permette di selezionare una vasta gamma di modi di funzionamento del veicolo con il fine di limitare le emissioni di inquinanti e gestire al meglio il flusso di potenza proveniente dalle varie sorgenti energetiche presenti.

Nei veicoli ibridi è possibile combinare questi diversi propulsori in diversi modi: in serie, in parallelo e una combinazione mista serie/parallelo. Nel corso della tesi saranno spiegate ed approfondite queste varie configurazioni, andando a valutare quale di queste permette una migliore gestione dell'energia, attraverso delle specifiche strategie di controllo, un minor consumo di combustibile e una minore emissione di inquinanti, facendo ovviamente riferimento al confort di guida e alle prestazioni del veicolo.

L'idea di prendere come oggetto di studio una city-car è nata dalla mia esperienza di studio a Torino e Varsavia. Queste due città si prestano molto all'utilizzo di veicoli ibridi o veicoli puramente elettrici data la loro conformità territoriale, prettamente pianeggianti e al possibile inserimento delle infrastrutture richieste per la ricarica di questi veicoli data la loro importanza nei rispettivi paesi.

La divisione dei capitoli è stata creata in modo da seguire minuziosamente i passaggi logici e progettuali e le motivazioni che hanno portato alla scelta dei parametri di funzionamento dei vari componenti del powertrain.

Acknowledgements

I would like to thank my family for the affection, love and support shown me not only during my university studies but throughout my life. They are for me models to follow in the long journey that is life. I would like to thank my uncles and cousins who have never stopped cheering me on and welcoming me warmly every time I returned home. I would like to thank my grandmother, a tenacious, strong woman who never broke down despite the thousands of obstacles faced, with her life lessons she passed on a lot to me and I'm sure she will continue to do so.

A big thank you goes to my girlfriend Marika, who has never made me lack love and affection throughout my university career despite the distance. She endured my anxieties and my fears giving me the strength to never give up and always managing to find a word of comfort and encouragement in the less happy moments.

I would like to thank my roommates Alessandro, Christian and Francesco, with them I shared joys and fears, happy moments and sad moments, but all under the sign of sincere friendship. I also thank all my friends of the "paesello" who have never lacked their support even from afar, always ready to celebrate every time I return and always ready to lend me a hand in case of need. I would like to thank all those guys I met at university and during my study period in Turin.

A special thanks goes to Omar Cavuoto and to all Cus Torino for allowing me to continue living my basketball passion both as a player and as head of university basketball.

I also thank the guys on the third floor of the DS Akademik in Warsaw, with them I shared the Erasmus experience.

I also thank all my university professors and especially my supervisor prof. Ezio Spessa and Prof. Daniela Misul for the final help in the last steps of the thesis and Prof. Chang Yuhua of the WUT who directed and guided me at the beginning of this work.

Acknowledgements (Italian version)

Un ringraziamento particolarmente sentito va alla mia famiglia per l'affetto, l'amore e il sostegno mostratomi non soltanto durante il percorso universitario ma durante tutta la vita. Sono per me modelli da seguire nel lungo viaggio che è la vita. Un sentito ringraziamento va anche ai miei zii e ai miei cugini che non hanno mai smesso di incitarmi ed accogliermi calorosamente ogni qualvolta ritornavo a casa. Un sentito ringraziamento va a mia nonna, una donna tenace, forte che non si è mai abbattuta nonostante i mille ostacoli affrontati, con le sue lezioni di vita mi ha trasmesso tanto e sono sicuro continuerà a farlo.

Un grandissimo ringraziamento va alla mia fidanzata Marika, la quale non mi ha fatto mai mancare l'amore e l'affetto durante tutto il mio percorso universitario nonostante la lontananza. Ha sopportato le mie ansie e le mie paure dandomi la forza di non mollare mai e riuscendo sempre a trovare una parola di conforto e di incoraggiamento nei momenti meno felici.

Un sentito ringraziamento va anche ai miei coinquilini Alessandro, Christian e Francesco, con i quali ho condiviso gioie e paure, momenti felici e momenti tristi, ma tutti sotto il segno di una sincera amicizia. Ringrazio anche tutti i miei amici del "paesello" che anche da lontano non hanno mai fatto mancare il loro sostegno, sempre pronti a far festa ad ogni mio ritorno e sempre pronti a darmi una mano in caso di bisogno. Un sentito ringraziamento va a tutti quei ragazzi conosciuti tra i banchi universitari e durante la mia permanenza a Torino.

Un particolare ringraziamento va ad Omar Cavuoto e a tutto il Cus Torino per avermi permesso di continuare a vivere la mia passione cestistica sia come giocatore che come responsabile del basket universitario.

Ringrazio anche i ragazzi del terzo piano del DS Akademik di Varsavia, con i quali ho condiviso l'esperienza dell'Erasmus.

Ringrazio anche tutti i miei professori universitari e soprattutto i miei relatori il prof. Ezio Spessa e la prof.ssa Daniela Misul per l'aiuto finale nella stesura del lavoro di tesi e la prof.ssa Chang Yuhua del Politecnico di Varsavia la quale mi ha indirizzato e guidato all'inizio di questo lavoro.

Chapter 1: Introduction and classification of hybrid vehicles

1.1 Introductions to HEV and PHEV

Today we are witnessing an increasing demand from the world population for ease of mobility and it is one of the key factors for economic growth and development. Since 2012, Europe has seen a growth in the transport of people and goods and estimates that it will grow by a further 10% by 2030 [1]. Nearly a quarter of greenhouse gas emissions and one of the main causes of pollution is due to the transport sector, in fact the European Union has issued increasingly stringent regulations to deal with this problem before it becomes irreversible. On 1 January of this year, European legislation came into force [2] requiring light vehicle manufacturers to reach an average of 95g/km of CO₂ by the end of this year, 80 g/km of CO₂ by 2025 and 60 g/km of CO₂ by 2030.

One of the ways to reach the target is that of hybridization and electrification of vehicles. These vehicles are able to ensure mobility by significantly reducing the emission of harmful substances, but although these are the best way to overcome the pollution problem, there is still no marked depth of integration within the market. In the last two years alone, there has been an increase in the models of BEV, HEV and PHEVs available on the market, going from a value of about sixty in 2018 to a value of almost 180 models available in 2020 [3].

The vehicles called HEVs are vehicles in which, alongside the thermal engine, there are one or more electric cars that can assist the engine during the traction of the vehicle, accelerating and exploiting kinetic energy from the braking and deceleration phases. They can be divided into different categories depending on the level of electrification used:

- Mild Hybrid: this technology uses a small electric motor that acts as a support to the thermal powertrain in the phases of ignition, acceleration and obviously taking advantage of the energy from regenerative braking.
- Full Hybrid: this technology has an electric motor larger than the previous one, it performs essentially the same functions but compared to the mild hybrid allows you to move for a short kilometer range in pure electric.

The last category is plug-in vehicles (PHEVs), these represent a kind of transition model between a hybrid vehicle and a purely electric vehicle. This type of hybrid vehicle has batteries with higher capacity and power of electric cars superior to traditional HEVs, resulting in improvements in the electric range. This type is also distinguished by the ability to recharge the battery through an external source that can be both the normal home network, and through columns specially designed for charging these vehicles. However, due to the lack of infrastructure required to load these vehicles in a reasonable time, their penetration into the automotive market is still low.

The architecture of a hybrid vehicle is defined by the connections of the various components that make up the powertrain, which define the flow of energy and the logic of control of the system.

- Having to size the electric motor to ensure maximum demand for power, it will also add a significant weight and cost on the vehicle;
- The system of storage of electricity, the battery pack, also weighs on the weight of the vehicle having to power an electric motor of not negligible size.

It therefore appears that the series architecture is not particularly suitable as an alternative solution to traditional vehicles but can be applied with good results to vehicles used for public transport where the already large dimensions do not place particular limits in the use of this architecture and it is also possible to adopt targeted control strategies since these tend to follow established urban routes.

Energy flows are now presented during the various phases of operation that this type of architecture can guarantee:

- Purely electric mode: the power to move the vehicle comes only from the electric motor powered by the battery pack;

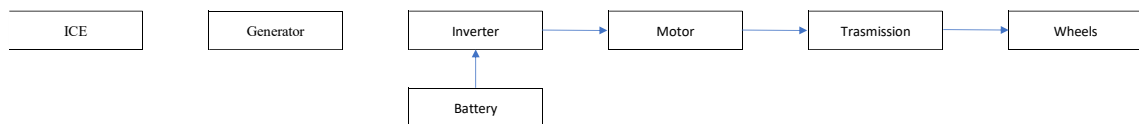


Figure 2

- Purely thermal mode: the power to move the vehicle comes only from the thermal engine through the generator;

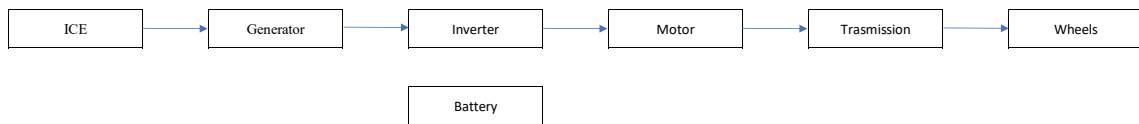


Figure 3

- Hybrid mode: The power to move the vehicle is provided by both electric and thermal thrusters;

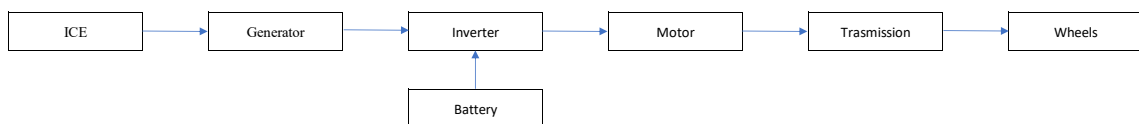


Figure 4

- Battery charging mode and thermal engine traction mode: Thermal power provides the power needed for the vehicle's propulsion and the power to charge the batteries, to use this mode it is not possible to downsizing the thermal engine;

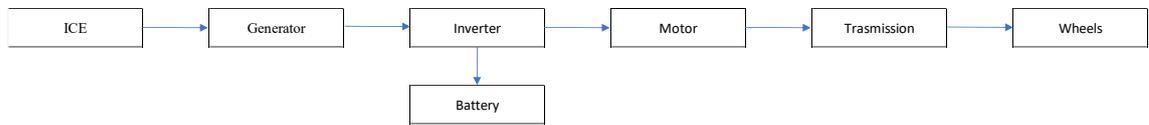


Figure 5

- Regenerative braking: The mechanically connected electric machine works as a generator to recover the kinetic energy dissipated during braking.

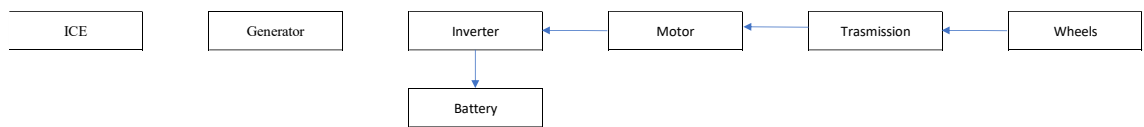


Figure 6

- Battery charge: the vehicle is stationary, the thermal engine provides power to the generator to recharge the batteries;

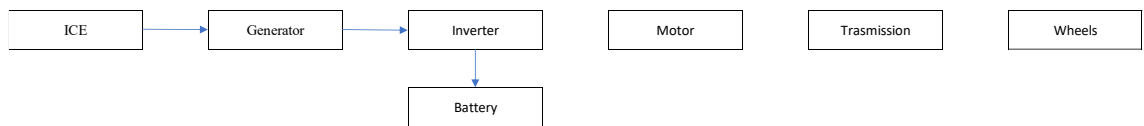


Figure 7

- Hybrid battery charge: The vehicle is decelerating, the thermal engine and energy from regenerative braking compete in charging batteries;

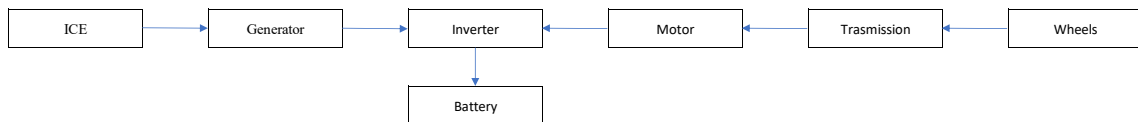


Figure 8

1.3 Parallel configuration

The hybrid vehicle with parallel architecture is a vehicle where there are two distinct thrusters, thermal and electric, which are connected in parallel and are able to provide the power needed for traction independently of each other. The greatest advantages of this architecture over the series architecture are:

- No electric generator required;
- The traction engine is smaller;
- There is no need for a multi-conversion of energy resulting in losses along the transmission line;

This architecture has multiple ways of combining the operation of the two thrusters depending on where the mechanical connection between the two is inserted [4]:

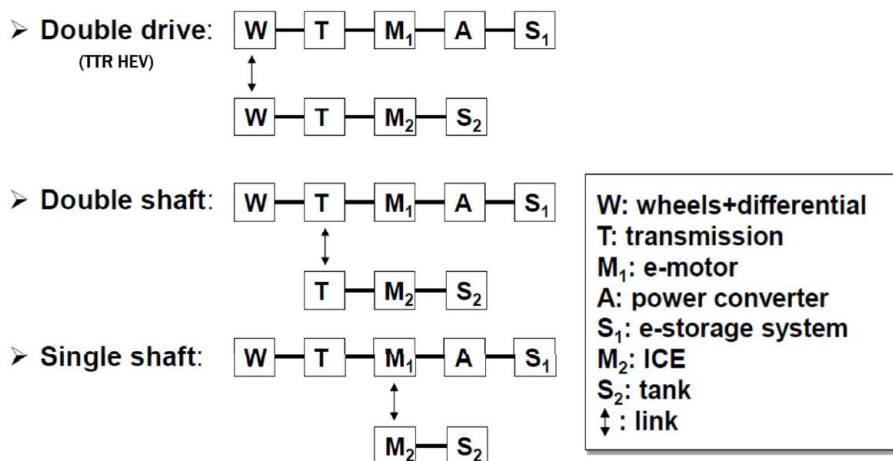


Figure 9

The single shaft configuration has a connection to the machine level, the thermal engine is mechanically connected to the electric machine, it is the configuration most used due to the lower cost compared to the other two types.

The double shaft configuration enables mechanical connection at the transmission level, so you have two distinct powertrains up to the transmission level. This type of configuration is used quite infrequently, although there are some advantages being able to insert two different gearboxes for each machine, due to the high cost.

The double drive or TTR (through the road) configuration has the mechanical link even further downstream, at the wheels level, in this configuration a powertrain is connected to the front axle while the other is connected to the rear axle is therefore the road to ensure the mechanical connection. This solution allows the adoption of four-wheel drive. This solution is also expensive, but at the market level this higher cost is justified by the presence of the four-wheel drive.

Since the single shaft configuration is the most used, it is worth focusing on the adoptable solutions.

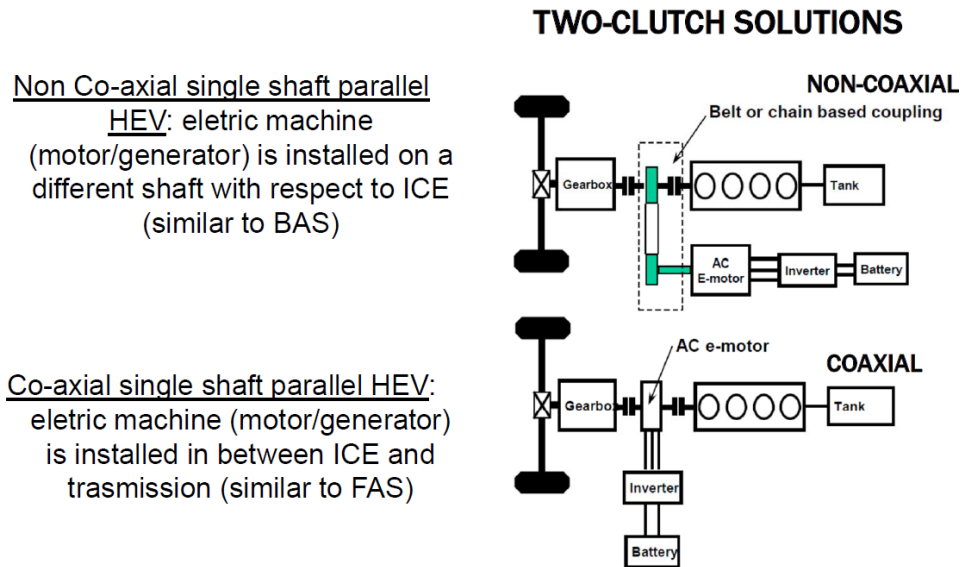


Figure 10

The single shaft configuration can be implemented by adopting two different ways of pairing the two powertrains:

- Not co-axial: in this case the two thrusters are located on two non-coaxial trees precisely, the connection between the two takes place through mechanical organs such as belts or chains. This configuration resembles a conventional powertrain, since if I thought about replacing the electric motor with an alternator, the inverter with a diode bridge and eliminating the downstream clutch of ice we can find the configuration of a traditional vehicle. The limitation of such a solution is the mechanical connection through the belt, since this dictates the constraints on the maximum torque transmitted by the electric machine both when working as an engine and when working as a generator, so limits are placed on the size of the electric machine. It also presents challenges with belt design. But it also has the advantage of not having to drastically change the engineering of the thermal engine.
- Co-axial: in this configuration the two powertrains are placed on the same axis, precisely to overcome the problems imposed by the use of the straps. However, this configuration has the disadvantage, in the case of the use of the start and stop, that the electric machine must provide all the torque necessary to start the thermal engine. This disadvantage can be overcome by using start-up for inertia. It has excellent modes of operation going to open and close the two clutches depending on the operating modes.

For both configurations, the two clutches are necessary because they allow you to take advantage of all the operating modes of hybrid vehicles.

The analysis of the various configurations that a parallel hybrid vehicle can take has served to understand the advantages and disadvantages of this architecture, among the advantages we can remember that the electric motor can be sized with a lower power since it is not the only powertrain to provide the necessary power to traction, therefore you can also reduce the size and capacity of the battery pack , earning in terms of footprint and vehicle costs. Among the disadvantages is certainly that of not being able to make the thermal engine, which boasts a low performance compared to electric cars, in points of maximum efficiency, so there will be fewer reductions in consumption and emissions at the same time. The last disadvantage is the control of these two components, in order to make both work optimally the control strategies to be implemented are more complex.

For example, the energy flows related to the various modes of operation that this architecture can guarantee are presented, a single shaft co-axial architecture is used since it is the one used for subsequent simulations:

- Purely electric mode: the clutch1 is open the clutch2 is closed, the power to move the vehicle comes only from the electric motor powered by the battery pack;

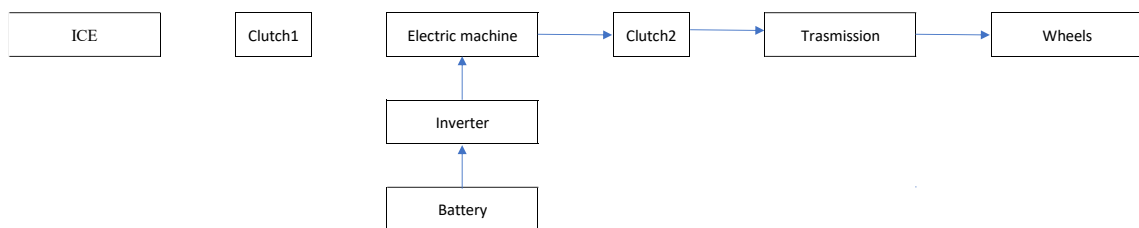


Figure 11

- Purely thermal mode: both clutches are closed, the power to move the vehicle comes only from the thermal engine ;

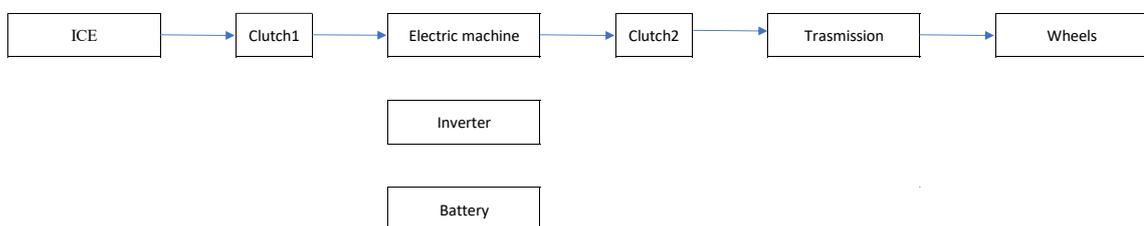


Figure 12

- Hybrid mode: both clutches are closed and the power to move the vehicle is provided by both electric and thermal machine;

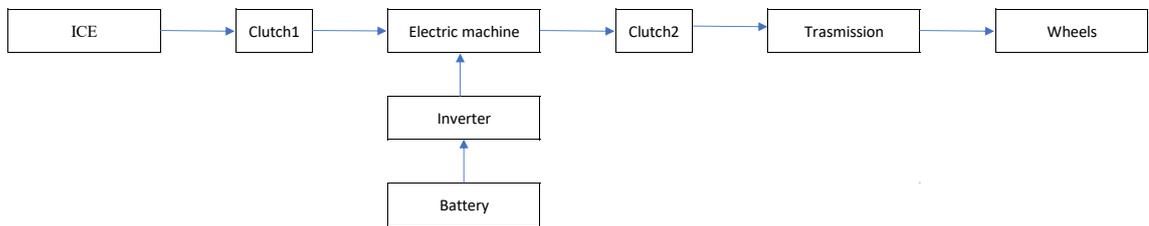


Figure 13

- Acceleration: vehicle acceleration is ensured by both thrusters while keeping the two clutches closed;

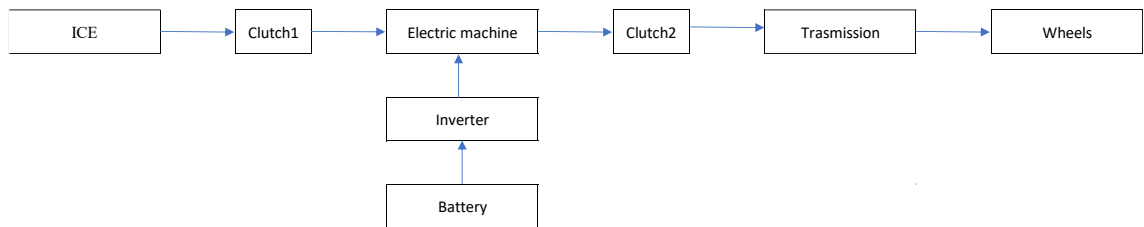


Figure 14

- Regenerative brake: the clutch1 is opened and the electric machine mechanically connected to the wheels having closed the clutch2 works as a generator to recover the kinetic energy dissipated during braking.

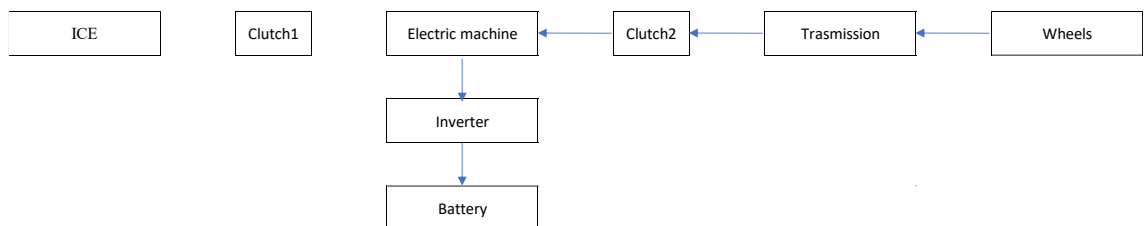


Figure 15

- Battery charge: the vehicle is stationary, the thermal engine provides power to the electric machine that acts as a generator to recharge the batteries;

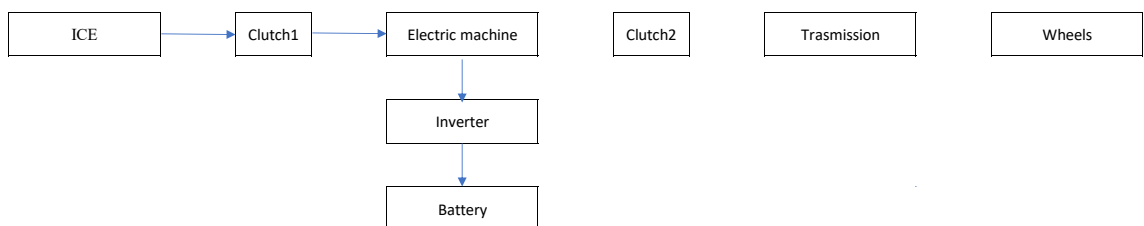


Figure 16

1.4 Complex configuration: series-parallel

This configuration encloses the potential of both previously analyzed configurations. Energy flows can follow the paths dictated by the series or parallel configuration depending on how the vehicle operates. Can be obtained with three different technology ways [4]:

- By increasing the number of traction motors/ICEs;
- By increasing the number of energy and power sources;
- By coupling parallel and series concepts on the same powertrain architecture;

The first and the third technology ways are the most investigated in order to:

- Improve market penetration of hybrid vehicles;
- Improve fuel consumption;
- Enable further functions like 4-wheel drive or HVAC on when ICE is off;

Figure 17 shows a conceptual scheme to understand what energy flows can look like depending on which path is used, whether the electrical or the mechanical.

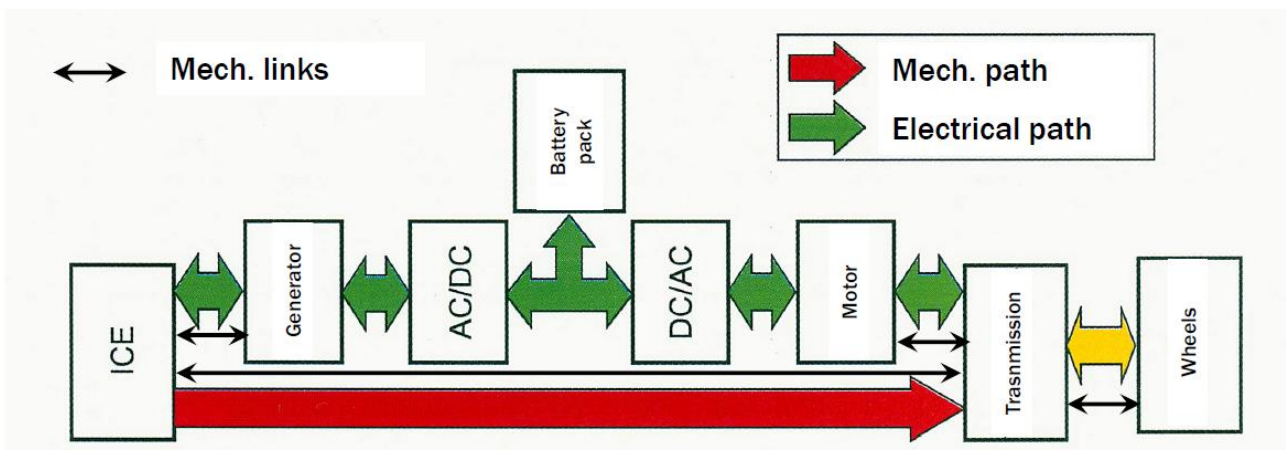


Figure 17

It is now important to understand how the two electric machines and the thermal engine are connected to each other, these connections are implemented through the use of power split systems that can take on various configurations.

The best known example is the system developed and implemented in the Toyota Prius, another drive line system of the input power split type is the Ford Hybrid System [5]. In this system a planetary gearbox is used in order to pair the three machines. The use of this mechanical system allows, as needed, different operating conditions operating on the speeds of the three elements of the system: carrier, ring and sun. Figure 18 [4] shows the starting situation of the vehicle, adjusting the speed of the solar it is possible to accelerate through the system ring, while keeping the carrier connected to ICE still.

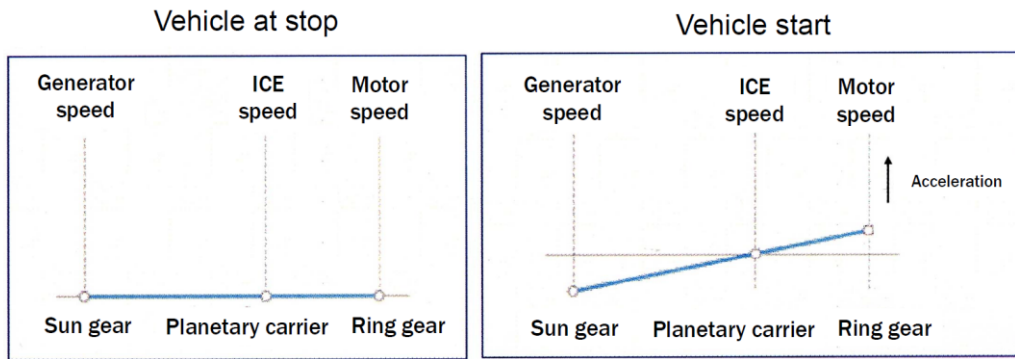


Figure 18

Figure 19 shows the case where the thermal engine is turned on to a stationary vehicle, note the speed of the ring nothing, I use the generator to start the thermal engine. This situation can be easily adapted to the case where the vehicle is moving. Next in normal driving conditions you just need to adjust the speed of the sun to vary the speed of the ICE, in Figure 19 is shown the case in on you want to keep the sun still.

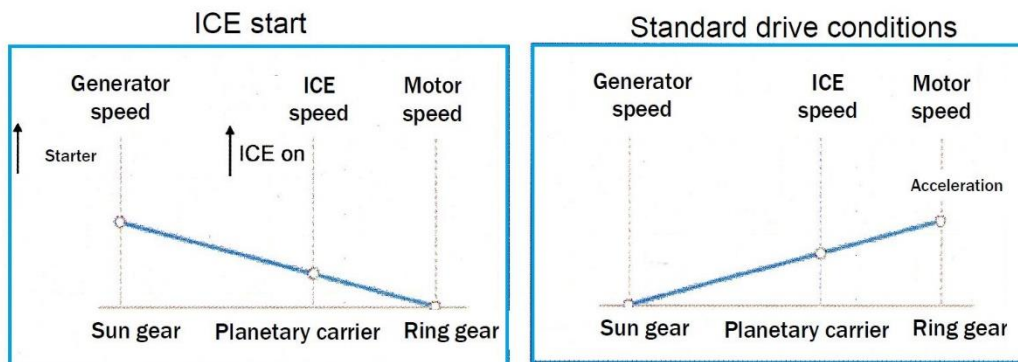


Figure 19

Another solution to obtain a power split device is similar is show in figure 20 to e-CVT and is called electrical variable transmission (EVT) [7]. In this system the power split effect is obtained by mean of the combination of two electric machine, the first machine is coupled to the engine at the stator, which is rotating and supplied through slip rings by a first inverter. A great advantage of the EVT is the wide range of the speed regulation that can be obtained between the engine and the wheels. The main drawback of the EVT is the high torque sizing of the electric machines which must be sized for the engine maximum torque, leading to high volume and weight.

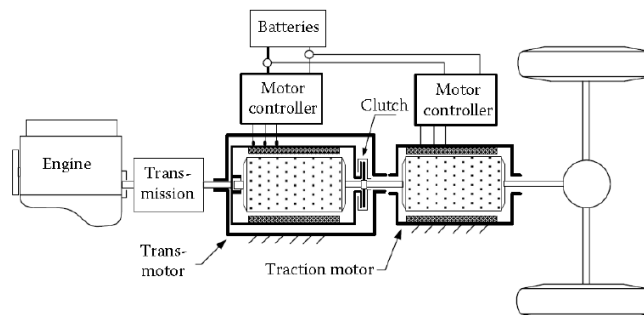


Figure 20

Another solutions for connect the machines is represented by dual mode power split driveline or also called compound power split. There are a lot complex solutions based on the use of at least epicyclical gear trains and one or more locking system. These configuration can be classified as *compound type power split*, one example is the solution developed by Allison [8].

In figure 19 are show an example, in the second planetary gear unit, one element can be stopped or can be connected to one gear of input power split through the use of mechanical clutches or hydraulic brakes. This system can work in low range mode when R2 is stopped and high range mode when R2 rotates as S1 and MG/1.

This yields to a minimum sizing of the electric components, and applies satisfactory torque level at the final drive both at low and high speed range, but is characterized by a relevant complexity of the mechanical layout [9].

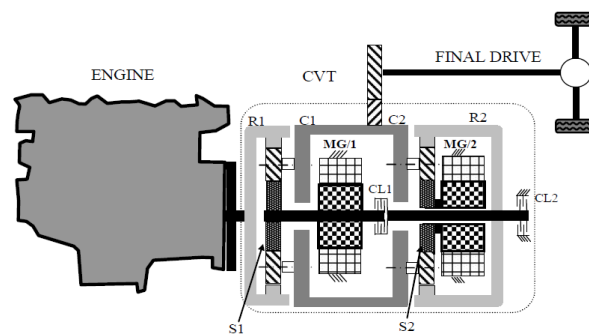


Figure 21

Chapter 2: Analysis methods

2.1 Longitudinal dynamic

The concept of longitudinal dynamics allows to represent the vehicle through a model that takes into account the different operating conditions. Generally it is easy to set up a model that describes the vehicle, with a few degrees of freedom. Dynamically the vehicle looks like it looks like it's in figure 22:

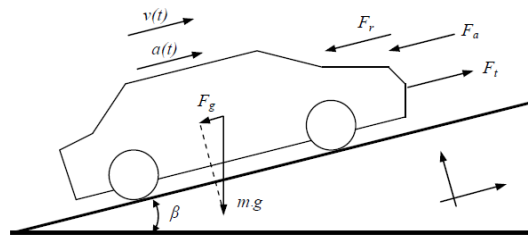


Figure 22

The following terms are identified::

- $v(t)$: instant speed of the vehicle m/s;
- $a(t)$: instant acceleration of the vehicle in m/s^2 ;
- $F_t(t)$: force developed by the propulsion system;

Formally these terms should be expressed with vector notation, but since the motion develops along a plane parallel to those terms, a scalar notation will be used.

Remembering II Newton's Law the motion of the vehicle can be described as:

$$m_r \cdot \frac{dv}{dt} = F_t(t) - [F_a(t) + F_r(t) + F_g(t)] \quad (2.1)$$

For simplicity of notation, the sum of the motion-resistant forces of the vehicle was indicated by F_{res} .

Where m_r is expressed as [10]:

$$m_r = m_{vehicle} + \Theta_w \cdot \frac{1}{r_w^2} + \Theta_e \cdot \frac{\gamma^2}{r_w^2} \quad (2.2)$$

- Aerodynamic resistance:

$$F_a = \frac{1}{2} \cdot \rho_a \cdot A_f \cdot C_d \cdot v^2 \quad (2.3)$$

- Rolling friction force:

$$F_r = m_{vehicle} \cdot g \cdot c_r \cdot \cos \beta \quad (2.4)$$

- Gravity force:

$$F_g = m_{vehicle} \cdot g \cdot \sin \beta \quad (2.5)$$

The goal now is to compute $P_{required}$, power required for vehicle traction:

$$P_{required} = F_{res} \cdot v + m_r \cdot \frac{dv}{dt} \cdot v \quad (2.6)$$

During the simulations carried out, it was found that using the (2.1) to calculate F_t you were getting some $P_{required}$ slightly lower than those calculated using the typical coast-down coefficients of the vehicle under consideration, for the calculation of the above coefficients, refer to [11]

$$F_{res} = F_0 + F_1 \cdot v + F_2 \cdot v^2 \quad (2.7)$$

- F_0 : coast down coefficient in N;
- F_1 : coast down coefficient in N/(km/h);
- F_2 : coast down coefficient in N/(km/h)²;

2.2 Backward method and forward method

To study energy and power flows in a vehicle, different methods of analysis can be used. A first classification that can be done is based on the direction of the calculation method adopted.

A backward method is a method in which the analysis starts going backwards from the wheels to the thruster passing through all the organs that make up the powertrain, such as: the differential, the gearbox.

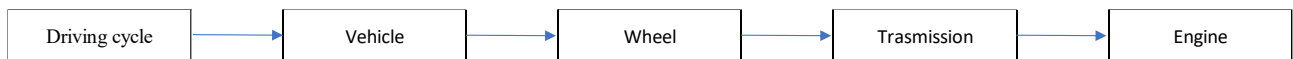


Figure 23

A forward method conducts the analysis in the opposite direction to the previous method, i.e. from the engine to the wheels of the vehicle, always passing through the organs that make up the drive train. The starting point remains the driving cycle, but in this case there is the introduction of the block called "pilot" that represents the behavior of a hypothetical driver precisely acting on the drive controls of the vehicle as: accelerator, brake and clutch so that the vehicle follows the selected driving cycle. The difference between the instant speed of the vehicle and the theoretical speed imposed by the driving cycle is calculated, in case of discrepancy an error is generated that through a feedback corrects the actions of the driver, obviously through the passage of information from one block to another are calculated the fundamental sources that describe the behavior of each block.

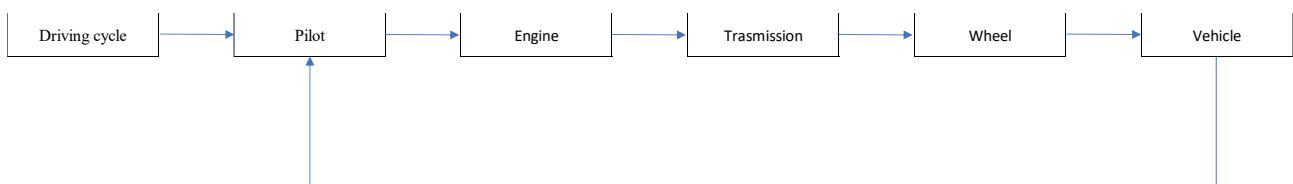


Figure 24

Among the backward methods most used are: the midpoint method of operation and the quasi-static method, which are used by software such as QSS-ToolBox [12], which has been used as an aid to Simulink modeling. Forward methods include dynamic methods. Here, the quasi-static method for in-depth analysis of the other methods mentioned is used and explained [10].

2.3 Quasistatic approach

The method used in this in this weaving work is a backward-type method called "Quasistatic method", this method assumes as input variables, coming from the cycle driving the v velocity , deriving this acceleration a and in some cases the grade angle of the road β . Through these input values, using the (2.6) and the (2.7) you can estimate the power required for the traction of the vehicle and the corresponding force. Approaching the problem with this method assumes that the vehicle develops its motion through a finite succession of static states, in which speed, acceleration and all the sizes derived from these are constant. The almost static method implicitly preserves some peculiarities of the method of the midpoint of operation in fact, the guide cycle is divided into short temporal moments, at each moment the typical relationships of the method of the midpoint of operation are applied.

Take the speed profile in the figure below as an example:

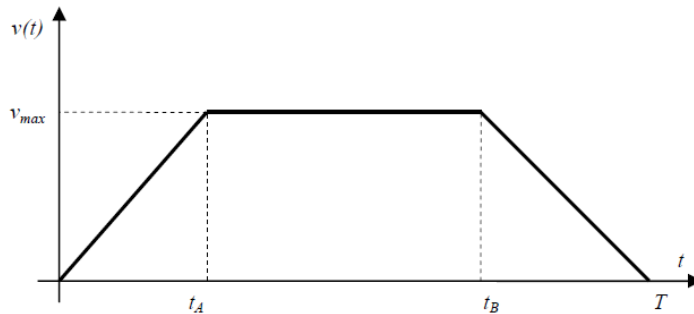


Figure 25

At this point a discretization of the time axis is made, through the definition of a fixed step h , so given the T duration of the cycle you can identify the intervals T/h and the moments that t_i separate them. Once discretization is done, you can apply the midpoint method to each identified range.

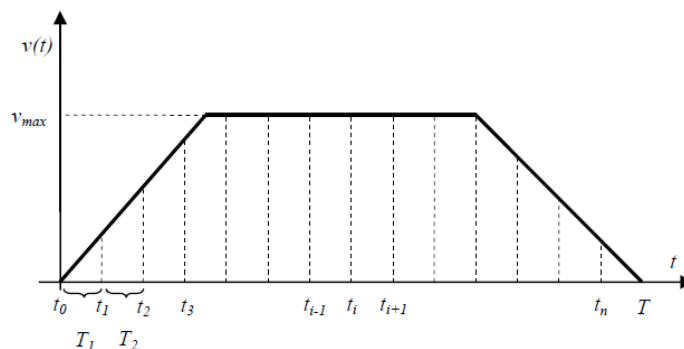


Figure 26

Using the same notation as [10] you get a speed profile defined as:

$$v_f(t) = \frac{(v(k \cdot h + h) + v(k \cdot h))}{2} \quad (2.8)$$

$$\forall t \in [k \cdot h, k \cdot h + h[\quad \text{con } k = 1, \dots, \left(\frac{T}{h} - 1\right)$$

The speed profile then became:

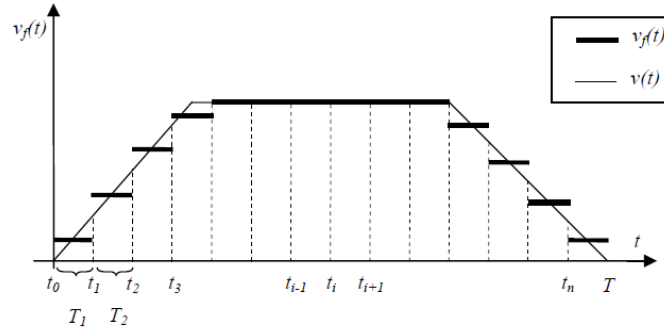


Figure 27

At this point the integral/differential equations that describe the motion of the vehicle can be treated as equations to finite differences, which lend themselves to be processed to the computer.

By deriving the (2.8) it is possible to derive the acceleration of the vehicle:

$$a_f(t) = \frac{(v_f(k \cdot h + h) - v_f(k \cdot h))}{h} \quad (2.9)$$

In order to implement this method to the computer, not particularly high computing capabilities are required, but these are dependent on the step h used.

This method, however, inevitably leads to disadvantages: for the calculation of v it is necessary to know the entire driving cycle in advance and therefore it is not possible to carry out analysis on random routes and the use of relationships that would be valid under static conditions but are used in dynamic situations.

Chapter 3: Vehicle modelling in Simulink

3.1 Vehicle modelling introduction

All simulations carried out here were conducted in Simulink, the graphic programming environment associated with Matlab, it is particularly suitable for simulating systems of any type (mechanical, thermal, electrical, etc.) through the construction of linear and non-linear block schemes. The software has a large library of libraries with preset models representative of the most diverse dynamic systems and mathematical operations to use. In this thesis work, no models already present in the library are used, but the various blocks are built from scratch with the help of the QSS Toolbox.

The models of the vehicle built in the Simulink environment are flanked by two different types of scripts in Matlab, in the first are initialized the parameters used for the calculation of sizes in each block representative of the vehicle and the maps of efficiency and consumption of the various types of thrusters analyzed, the second type instead allows the processing of the results obtained in the Simulink environment in order to display the operating points during the driving cycle.

3.2 Models for calculating input parameters to the powertrain

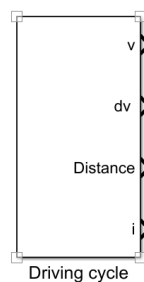


Figure 28

The first model implemented concerns the definition of the driving cycle, loaded within the Matlab script it is represented as an array containing the vectors with the time values of the cycle duration, speeds and in case the architecture needs a gearbox the gears used by the vehicle, this block provides as output the speed of the vehicle, acceleration, gearbox gears and the distance traveled during the driving cycle.

The speed, acceleration and gear values of the gearbox in the case of a vehicle equipped with this element are the inputs of the representative block of the longitudinal dynamics of the vehicle, this through the relationships (2.6) and (2.7) $P_{required}$ computed and F_{res} . The other terms that make up the output of the *vehicle* block represent: angular wheel speed, angular wheel acceleration and torque on wheels, calculated as:

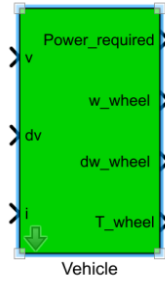


Figure 29

$$\omega_{wheel} = \frac{v}{r_w} \quad \left[\frac{rad}{s} \right] \quad (3.1)$$

$$d\omega_{wheel} = \frac{dv}{dt} \cdot \frac{1}{r_w} = \frac{a}{r_w} \quad \left[\frac{rad}{s^2} \right] \quad (3.2)$$

$$T_{wheel} = \left(F_{res} + m_r \frac{dv}{dt} \right) \cdot r_w \quad [Nm] \quad (3.3)$$

Within the above block, the energy required to follow the driving cycle is also calculated, by integrating power and saving the results in the Matlab workspace for subsequent analysis during post processing.

3.3 Transmission models

The transmission of speeds and pairs from wheels to powertrains is guaranteed thanks to a series of elements inserted upstream of the various thrusters. The output values of the *vehicle* block are the input of the representative block of the differential.

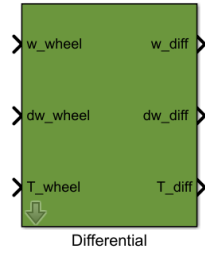


Figure 30

The differential allows the twisting moment to be distributed between the two-wheel drive when they rotate at different speeds, in this study it behaves like a simple speed reducer since it is considered only the longitudinal motion and the perfect grip of the tires on the ground. The differential is characterized by a final ratio τ_{diff} and a performance that depending on the architecture analyzed will assume certain η_{diff} values. The output terms are calculated as:

$$\omega_{diff} = \omega_{wheel} \cdot \tau_{diff} \quad \left[\frac{rad}{s} \right] \quad (3.4)$$

$$d\omega_{diff} = d\omega_{wheel} \cdot \tau_{diff} \quad \left[\frac{rad}{s^2} \right] \quad (3.5)$$

$$T_{diff} = \frac{T_{wheel}}{\tau_{diff} \cdot \eta_{diff}} \quad [Nm] \quad (3.6)$$

Downstream of the differential depending on the architecture you are analyzing we find different blocks. For the series configuration, the electric motor is mechanically connected to the differential through a mechanical organ (belts or gears), in this configuration there is also the transmission that connects the thermal engine to the generator.

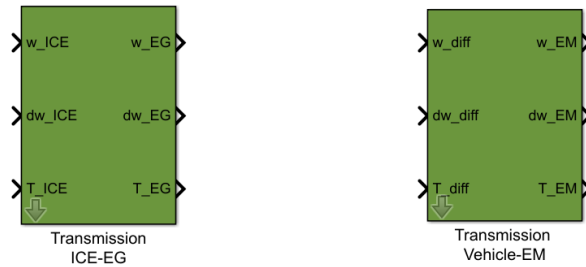


Figure 31

For our treatment these two transmissions are represented as the differential characterized therefore by a fixed transmission ratio and a performance. Relationships (3.4) and (3.5) are used to calculate the torque, which takes into account whether the energy flow goes from the wheels to the engine or vice versa.

For the parallel vehicle, a block was built that represents an automatic 5-speed gearbox.

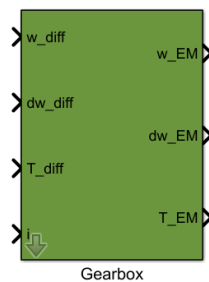


Figure 32

This block, in addition to receiving as input the speeds, acceleration and torque from the differential, also receives the ratio to be used coming from the *driving cycle* block, within the aforementioned block is implemented a Matlab function which, depending on the gear inserted adopts a certain value of the transmission ratio. The usual known relationships are used to calculate output sizes.

A more detailed analysis is reserved for the device present in the complex series-parallel configuration, it is an planetary gear that perfects to make three machines work through three different components of the system.

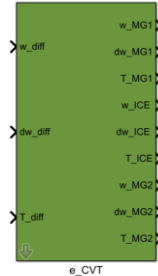


Figure 33

The best-known example was developed and implemented on the Toyota Prius by Toyota Motor Company [5]. Usually in this type of architecture the electric machine of greater size and connected to the reducer ring, which in turn is mechanically connected to the wheels of the vehicle through an appropriate transmission, the second electric machine is connected to the sun and finally the thermal engine is connected to the carrier of the planetary gear.

The advantages of this system can be:

- high power density;
- multiple kinematic combinations;
- large reduction ratio in a small volume and coaxial shafting;

The disadvantages can instead be represented by [13]:

- high bearing loads;
- inaccessibility and design complexity;

The relationships used for this type of element are different from ordinary gearbox. The fundamental parameter of this system is the fundamental ratio [9]:

$$\tau_0 = -\frac{R}{S} \quad (3.7)$$

- R is the number of teeth of the ring;
- S is the number of teeth of the ring;

As can be seen from the (3.7) it depends, like all the transmissions in which there are gears, on the number of teeth of the ring, the sun and the carrier. The relationship between these is expressed by:

$$R = S + 2P \quad (3.8)$$

- R : number of teeth of the ring;
- S : number of teeth of the sun;
- P : number of teeth of the satellites;

The kinematic relationships that governate this type of gearbox are obtained by choosing a fixed reference system, in fact the fundamental gear ratio represents the ratio between sun and ring when the carrier is stationary. To define the relationships between the three cogwheel wheels, the notorius Willis's formulas are used [14]:

$$\tau_0 = \frac{\omega_{SC}}{\omega_{RC}} = \frac{\omega_S - \omega_C}{\omega_R - \omega_C} = -\frac{R}{S} \quad (3.9)$$

$$\omega_C = \omega_S \cdot \left(\frac{1}{1 - \tau_0} \right) - \omega_R \cdot \left(\frac{\tau_0}{1 - \tau_0} \right) \quad (3.10)$$

Where:

- ω_C carrier rotational speed;
- ω_S sun rotational speed;
- ω_R ring rotational speed;

As for couples, however, the following relationship was used:

$$T_R = \left(\frac{\tau_0}{1 - \tau_0} \right) \cdot T_C = -\tau_0 \cdot T_S \quad (3.11)$$

Figure 34 is show with a diagram of how the three elements are paired using the planetary gear set.

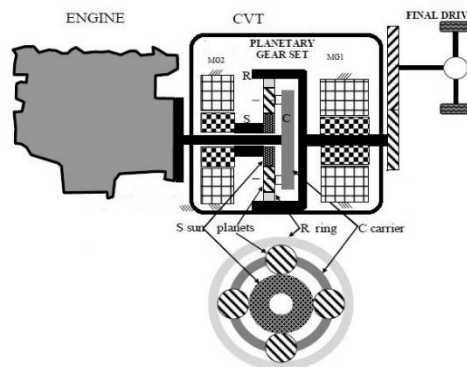


Figure 34

3.4 ICE and electric machine models

The reports governing the operation of an internal combustion engine are dependent on various factors, but with the method adopted here it is possible to consider a limited number of them allowing a fairly realistic modelling of operating conditions. It does not present all the reports in the literature [15], that govern the operation of an internal combustion engine, but only those actually implemented in this block.

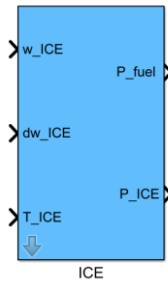


Figure 35

The block used in the Simulink environment receives as input the speed, acceleration and torque values of the thermal engine and presents in output P_{fuel} and P_{ICE} representing respectively: the power actually produced by the combustion of fuel and the power made available to the shaft net of all losses.

$$P_{fuel} = H_i \cdot \dot{m}_{fuel} \quad (3.12)$$

- H_i : lower calorific power in J/(kg K);
- \dot{m}_{fuel} : fuel flow in kg/s;

$$P_{ICE} = \omega_{ICE} \cdot T_{ICE} = \eta_{ICE} \cdot P_{fuel} \quad (3.13)$$

Within the block is implemented a 2D look-up table representing the heat engine consumption map: providing the values of ω_{ICE} e T_{ICE} the system through an interpolation process estimation \dot{m}_{fuel} . Subsequently, Through the reports in the literature [15] you can obtain the map that represents the BSFC in order to accurately analyze the results obtained.

It is worth noting that fuel consumption maps, specific consumption and those of the efficiency of electric machines describe the behavior of these components under regimen conditions, so working with the almost static method, they lend themselves well to the description of the operation of the aforementioned machines.

A similar treatment can be used to explain the operation of the block representing the electric machine, whether it is functioning as a generator or as an engine.

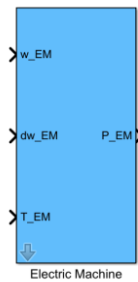


Figure 36

As with the thermal machine, the electric machine also receives input speed, acceleration and torque values and outputs the electrical power developed.

$$P_{EM} = \omega_{EM} \cdot T_{EM} \cdot \eta_{EM} \quad (3.14)$$

It should be noted that with regard to the series configuration and the complex configuration parallel series for simplicity of reasoning on the part of the subscriber, sign conventions explained in the chapter dedicated to architecture itself have been adopted.

3.5 Energy source model

The battery is the beating heart of hybrid and electric vehicles, and it depends on the operation of the entire powertrain and the mileage range that can be used in electric mode. The battery is a device capable of creating a reversible energy storage system and its behavior can be described using different models present in literature [16]. In this study we used the model implemented within the *QSS-Toolbox*, for this reason, all the relationships used in this block are not reported in order not to weigh down the treatment, for the consultation of the same refer to [10] [12].

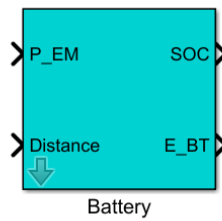


Figure 37

In summary, the reasoning behind the relationships within the block is based on instant-by-moment knowledge of the voltage at the battery clamps and stored charge. Note these two sizes and integrating the power taken over time derives the energy taken and consequently the remaining charge. Please note that a submodel representing the inverter, which is the interface between the battery and the electric machines, can be described in the following reports:

$$\eta_{inv} = \frac{P_{EM}}{P_{BT}} \quad (3.15)$$

$$\eta_{inv} = \frac{P_{BT}}{P_{EM}} \quad (3.16)$$

As a function of the inverter, the two relationships (3.13) and (3.14) are valid in the case of engine operation and generator operation, respectively.

Another submodel implemented within the battery block concerns the possibility of the vehicle to perform regenerative braking, which is crucial for proper energy management on board. The model recognizes whether the vehicle is in a traction condition, with positive torque and therefore power, or in braking conditions use the power produced to recharge the batteries.

The block representing the battery receives as input the output generated by the electric machines and through the relationships present in [10] calculates the SOC as the output of the system.

The second input is the distance traveled during the driving cycle, coming from the driving cycle block, is used to calculate energy consumption in kWh/(100km).

The equivalent of the battery as far as the thermal engine is the tank, the block representing its operation receives input the power produced by combustion and the distance traveled, to provide as output the fuel consumption in l/100km calculated as suggested by [15] direct consequence of fuel consumption are the CO₂ emissions calculated through the report [17].

$$m_{CO_2} = \frac{\rho_f}{0,0315} \cdot V \quad (3.17)$$

- ρ_f è la densità del combustibile in [kg/dm³];
- V è il consumo di combustibile in [l/100km];

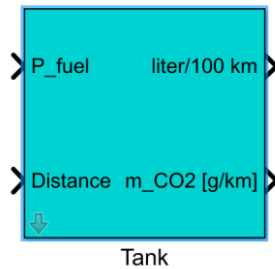


Figure 38

3.6 Parameter control model

The last remaining block to present is the block that controls the powertrain's operation parameters depending on the simulation performed. It should be noted that these are not real control strategies since the aim of this thesis work is not to investigate what is the best strategy to adopt, for this type of analysis is postponed to [18].

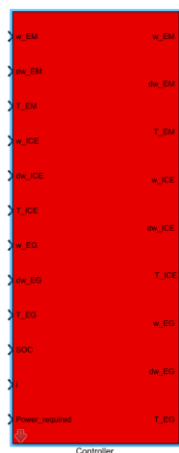


Figure 39

Chapter 4: Design requirements and calculation of CO₂ emissions and fuel consumption according to EU regulations

4.1 NEDC and WLTP results for the reference vehicle

The reference vehicle is a category A vehicle, equipped with an internal combustion engine compression ignition with a 5-speed manual transmission.

Table 1 shows the technical data of the reference vehicle:

MASS	1063 kg
ICE	Compression ignition Displacement: 1248 ccm Rated power: 52 kW @ 3500-4000 rpm Rated torque: 178 Nm @ 1750-2000 rpm
GEARBOX	Gears: 5 Final drive ratio: 3,563 Gear shift #1 trans. Ratio: 3,909 Gear shift #2 trans. Ratio: 2,238 Gear shift #3 trans. Ratio: 1,444 Gear shift #4 trans. Ratio: 1,029 Gear shift #5 trans. Ratio: 0,767

Table 1

For this vehicle, simulations were performed through the NEDC and WLTP cycles according to the procedures prescribed by [19] in table 2 shows the data useful for simulation, test mass and coast-down coefficient.

	Unit	NEDC	WLTP
Test mass	<i>kg</i>	1063	1210
F0	<i>N</i>	114,2	166
F1	$\frac{N}{km/h}$	0	0
F2	$\frac{N}{(km/h)^2}$	0,0344	0,039

Table 2

Below are the simulations of the aforementioned vehicle subjected to the NEDC and WLTP approval cycles, presenting operational points, fuel consumption and CO₂ emissions.

In the figure 40 are show the operating points of the ICE in NEDC cycle:

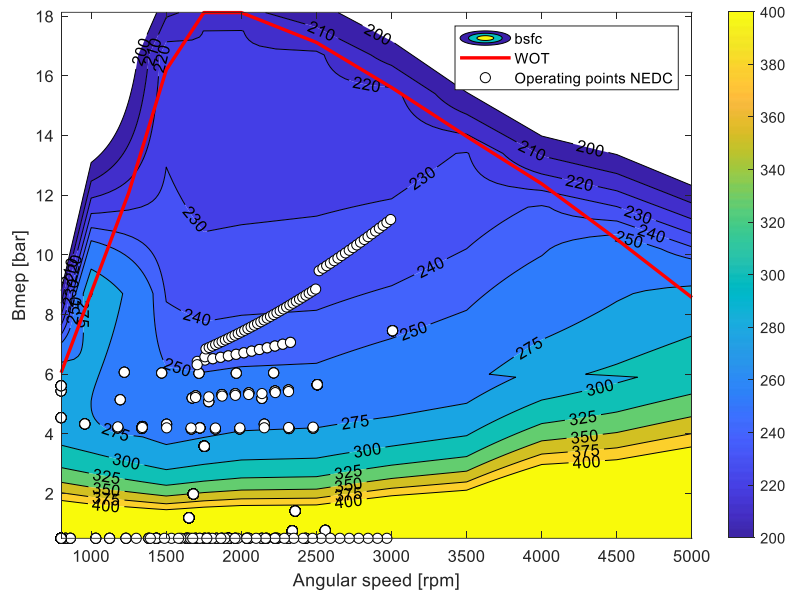


Figure 40

In the figure 42 are show the operating points of the ICE in WLTP cycle:

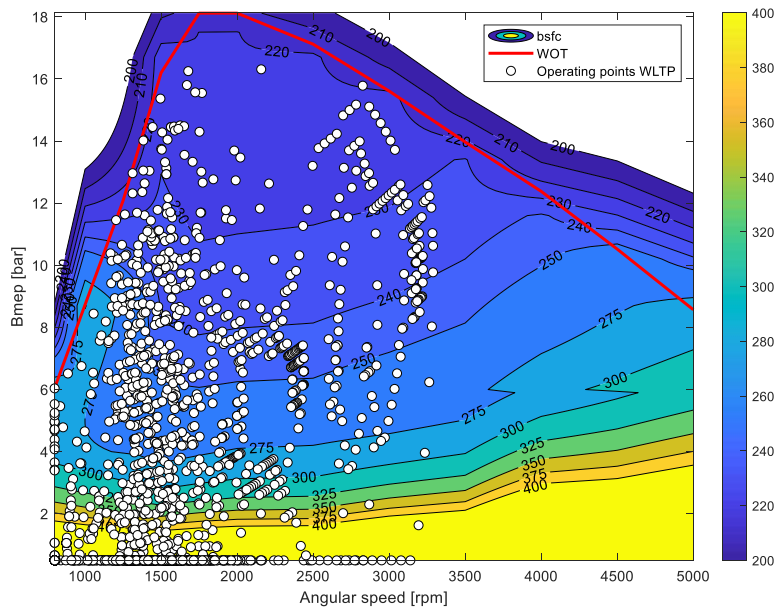


Figure 41

The WLTP cycle is much more aggressive than the NEDC cycle, as can be seen clearly from the comparison of the two figures. Thermal engine work points during the WLTP cycle are present in a larger area of the consumption map while those of the NEDC cycle thicken in a limited area.

In the figure 2 the value of fuel consumption in $\frac{l}{100 km}$ and CO₂ emissions in $\frac{g}{km}$ for NEDC cycle and WLTP cycle:

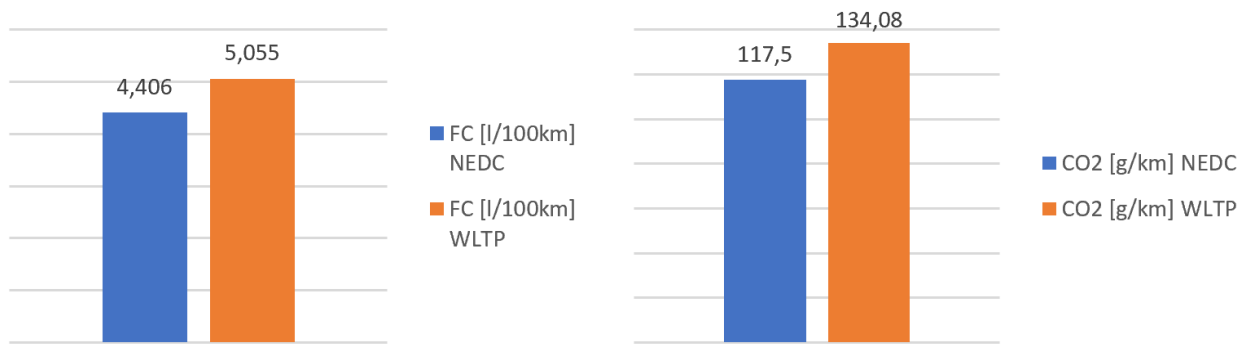


Figure 42

The results obtained following the WLTP cycle are higher precisely because of the fact that the above cycle goes to engage the vehicle in situations that more reflect the normal driving conditions in the real world.

4.2 Design requirements

Now the goal is to turn this traditional vehicle into a plug-in vehicle, recalling the peculiarities highlighted in previous chapters that set it apart from traditional hybrid vehicles.

In order to proceed with the design of the powertrain for the various configurations, it is necessary that two fundamental parameters of the project be established: the performance of the vehicle and the distance traveled in pure electric (AER).

Vehicle performance refers to the top speed easily determinable intersecting the curve of the resistant forces with the characteristic of the electric motor, and the time to accelerate from 0-100 $\frac{km}{h}$.

The design requirement are show in the next table:

Top Speed	140 km/h
Acceleration 0-100 km/h	16 s
All electric range (AER)	60 km

Table 3

For each powertrain configuration, the following tests were carried out to calculate FC, CO₂ emissions and AER, the above tests are prescribed in [19].

4.3 Charge-depleting test

In the NEDC if AER is longer than 1 NEDC the manufacturer has the ability to request the CD mode test in pure electric. Since most PHEVs on the market have a higher range of 11 km CD mode CO₂ emissions resulting from NEDC testing are equal to 0 $\frac{g}{km}$.

With the introduction of the WLTP approval cycle, this option has been eliminated since during this test there is the possibility of having a non-negligible increase of CO₂ emissions.

In the WLTP, CD CO₂ emissions and FC of each phase of WLTP test (low, medium, high and extra-high) have a different weighting final CD CO₂ emissions according to:

$$M_{CO_2CD}^{WLTP} = \frac{\sum_{j=1}^k (UF_j \cdot M_{CO_2,CD_j})}{\sum_{j=1}^k UF_j} \quad (3.1)$$

- $M_{CO_2CD}^{WLTP}$: is the WLTP's utility factor-weighted CD CO₂ emissions in $\frac{g}{km}$;
- UF_j : is the utility factor for WLTP's CD phase j;
- M_{CO_2,CD_j} : is the CO₂ mass emissions of CD phase j in $\frac{g}{km}$;

A method to calculate UF at each phase is shown in [19]. Utility factors represent the ratio of the distance covered in CD mode to the total distance covered between 2 subsequent charges. The UF curve is developed based on driving statistics described in SAE J2841 [19].

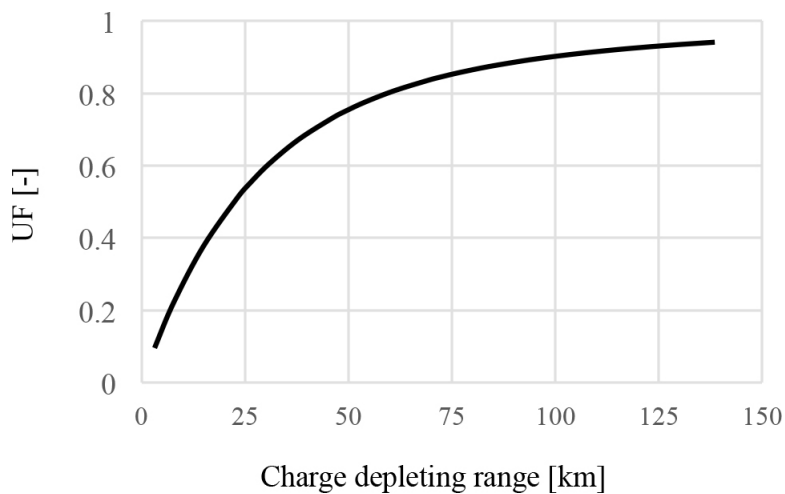


Figure 43

The Regulation 101 of the United Nation Economic Commission for Europe (UNECE) has been applied for NEDC testing [20] CD testing is composed by a number of NEDC tests carried out with a fully charged battery. CD ends after termination of NEDC cycle during which the battery has reached the minimum state of charge.

The battery minimum state of charge is reached in NEDC cycle N if the electricity balance measured during the cycle N+1 is not more than 3% discharge, therefore, for each NEDC cycle, you must verify that the following relationship is satisfied:

$$\frac{\int_{t_{0,k}}^{t_{1,k}} I_{REESS} dt}{REESS \max \text{ capacity} \cdot 3600} \cdot 100 < 3\% \quad (3.2)$$

- $t_{0,k}$ $t_{1,k}$: is the time (s) at the beginning and at the end of NEDC cycle, number k is the charge depleting sequence;
- I_{REESS} : is the current measured at the battery output;
- $REESS \max \text{ capacity}$: is the max capacity of the battery expressed in Ah ;

For the WLTP test instead applies the [21] this regulation is more complicated than the previous one. The break-off criteria is different: this is reached when the relative electric energy change (REEC) for the i -th WLTP is lower than 0,04 according to the following relationship:

$$REEC_i = \frac{|\Delta E_{REESS,i}|}{E_{cycle}} < 0,04 \quad (3.3)$$

- $\Delta E_{REESS,i}$: is the change of battery energy content expressed in Wh ;
- E_{cycle} : is the cycle energy demand for the specific vehicle expressed in Wh

The cycle in which the break-off criteria is fulfilled is called the confirmation cycle and after that the vehicle is ready and preconditioned for the CS testing.

4.4 Charge-sustaining test

CS test is performed according to the standard type 1 test for the standard European Certification test.

As explained in Chapter 1, the WLTP test is more energy-intensive, CO₂ emissions and FC than the NEDC cycle. However, remember that you can introduce a fix for results obtained during the WLTP test, which you cannot do for the NEDC test.

The correction is present in the following formula:

$$M_{CO_2,CS}^{WLTP} = M_{CO_2,CS_{nb}} - K_{CO_2} \cdot EC_{DC,CS} \quad (3.4)$$

- K_{CO_2} : is the correction coefficient in $\frac{g/km}{Wh/km}$;
- $EC_{DC,CS}$: is the electric energy consumption of CS test $\frac{Wh}{km}$;
- $M_{CO_2,CS_{nb}}$: is the non-balanced CO₂ result in $\frac{g}{km}$ obtained in CS cycle, which does not consider whether the battery is recharged or discharged during the test;

For compute FC it is possible following the same procedure.

4.5 Weighted final results

In the NEDC cycle, for compute weighted final results for CO₂ emissions, FC, and electric energy consumption (EC) you use the following:

$$M_{CO_2}^{NEDC} = \frac{D_{OVC} \cdot M_1 + D_{av} \cdot M_2}{D_{OVC} + D_{av}} \quad (3.5)$$

- D_{OVC} : can be described as the distance driven in the charge depleting test until the end of the transition cycle.
- D_{av} : represent the average distance covered in CS mode prior the next battery charge, it is equal to 25 km;
- M_1 : is the CD CO₂, FC or EC consumption;
- M_2 : is the CS CO₂, FC or EC consumption;

In the WLTP cycle, for compute weighted final results for CO₂ emissions, FC, and electric energy consumption (EC) you use the following:

$$M_{i,weighted}^{WLTP} = \sum_{j=1}^k (UF_j \cdot M_{i,CD,j}) + \left(1 - \sum_{j=1}^k UF_j \right) \cdot M_{i,CS} \quad (3.6)$$

4.6 Performance analysis

After running the CD and CS test and calculating AER, CO₂ emissions, FC, EC performance simulations were performed to verify the correct behavior of the various powertrains, in particular the following simulations were performed:

- Acceleration up to the speed of $100 \frac{km}{h}$ in pure electric;
- Emergency overtaking on suburban road: sudden acceleration from $50 \frac{km}{h}$ to $90 \frac{km}{h}$;
- Acceleration to the speed of $140 \frac{km}{h}$ with maintenance;

Chapter 5: PHEV: Series powertrain

5.1 Presentation main component

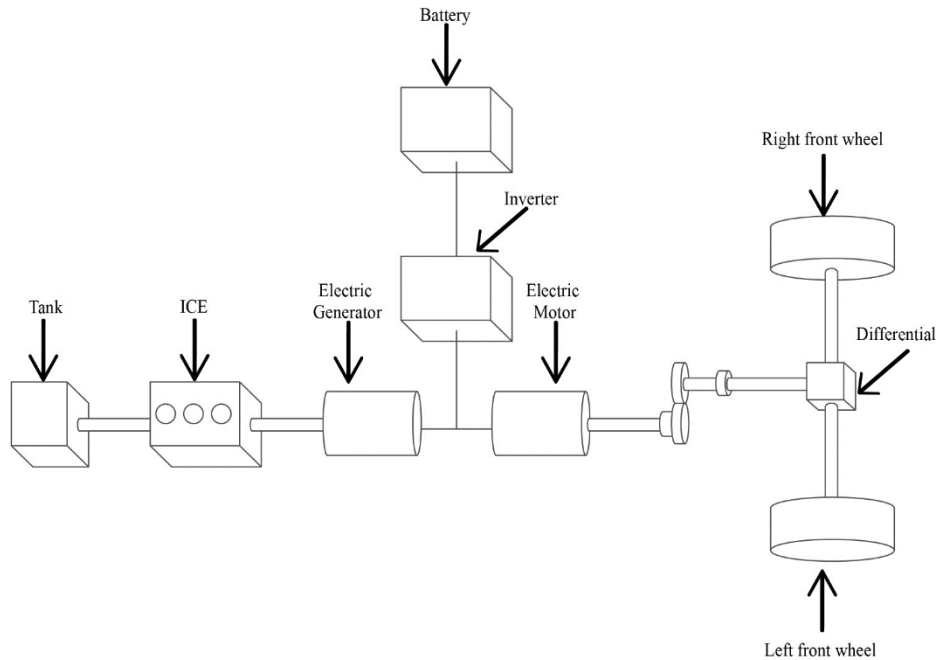


Figure 44

In Chapter 2, models and under models were presented, of the various components of a vehicle, developed in the Simulink environment,. Assembling these models appropriately it is possible to model different types of powertrains, in particular in this thesis work, starting from the same reference vehicle, three were developed, in order to assess and analyze their behavior by simulating the conditions described in the previous chapter.

The author decided to present and describe only the final components of the various powertrains, it was preferred not to insert all the tests carried out with ICE, EM and EG having different values of power and nominal torque in order not to weigh down and lengthen the treatment.

The series configuration allows a reduction in the size of the ICE, operating a slight downsizing in order to make it work in its optimal points. The characteristics of the ICE are presented in table 4 and figure 45 shows the bmep, speed and BSFC characteristic.

Max bmep	14,5 bar @ 1750-2000 rpm
Max Power	25 kW @ 3500-4000 rpm
Displacement	0,748 ccm
Idle speed	800 rpm

Table 4

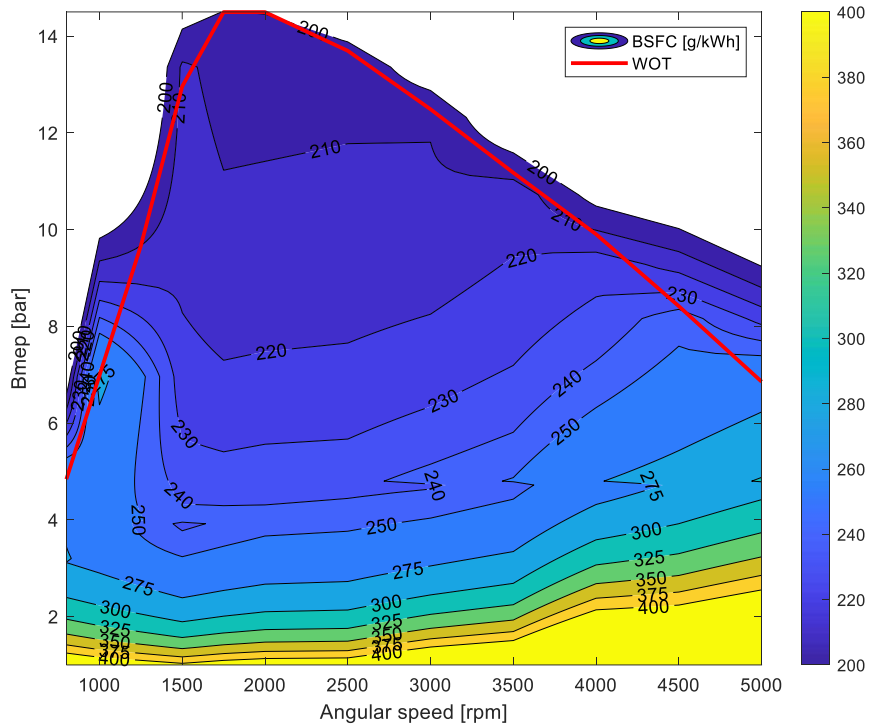


Figure 45

In this configuration, the internal combustion engine is paired with a generator that is tasked with converting mechanical energy into electrical energy. With a correct control strategy, it allows ICE to work in its optimal points, below are presented license plate data and mechanical feature.

Max torque EG	115 Nm
Max Power EG	19 kW

Table 4

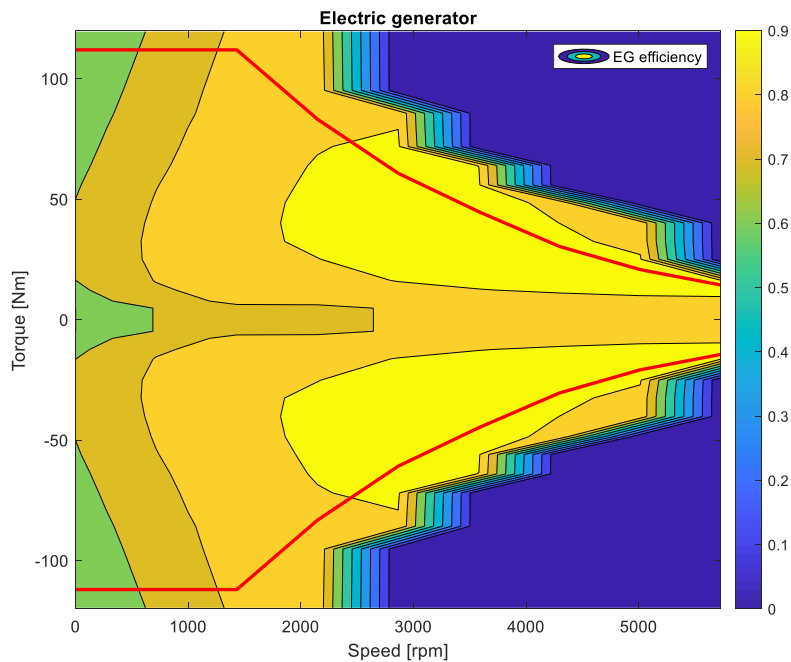


Figure 46

The generator being an electric machine has higher performance values so it is necessary to optimize the operation of the ICE. For this purpose, several transmission ratios were evaluated for the ICE/generator coupling in addition to the differential transmission ratio and the transmission ratio close to the electric motor (EM). The transmission has no gearbox. In the end, the selected transmission ratios are shown in table 5.

Gear ratio ICE/EG	0,9
Gear ratio EM	2,2
Gear ratio differential	1,8

Table 5

The electric motor is the engine directly connected to the wheels through an appropriate transmission. It is responsible for the primary traction of the vehicle. The EM has been sized to meet the design requirements expressed in the previous chapter, then it will be evaluated during the course of the simulations, if indeed this component allows proper traction of the vehicle by also assessing efficiency during performance analysis.

The nominal data of the electric motor and its characteristic torque-speed are presented in next table .

Max torque EM	260 Nm
Max Power EM	87 kW

Table 6

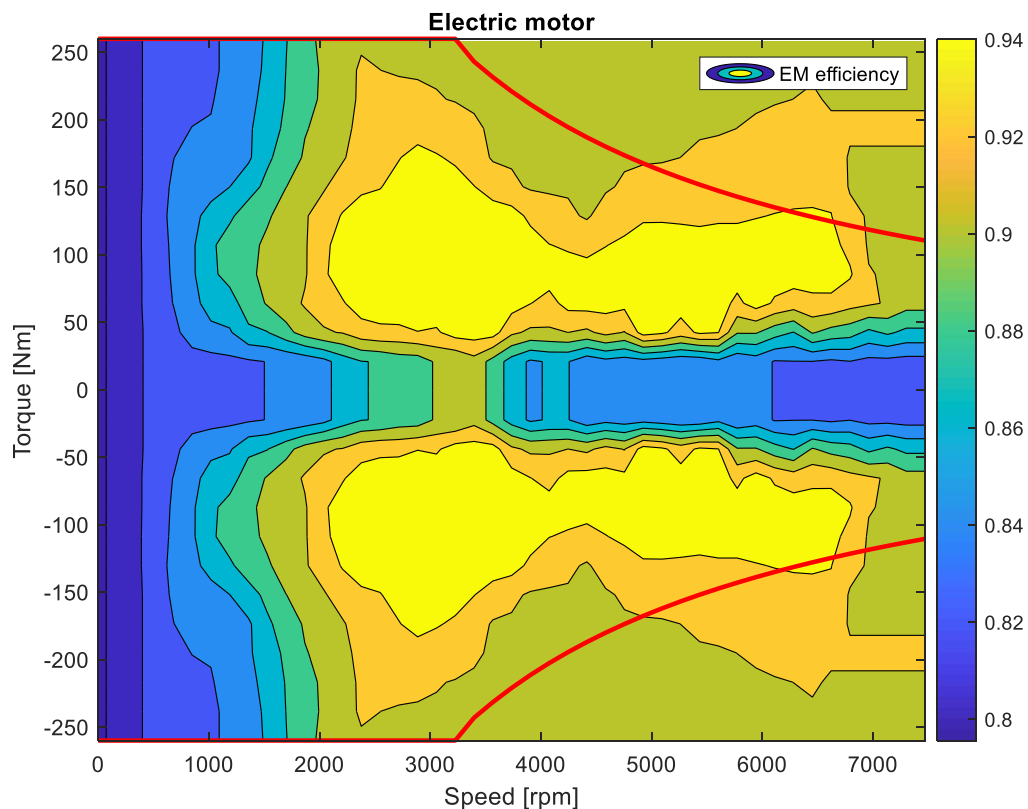
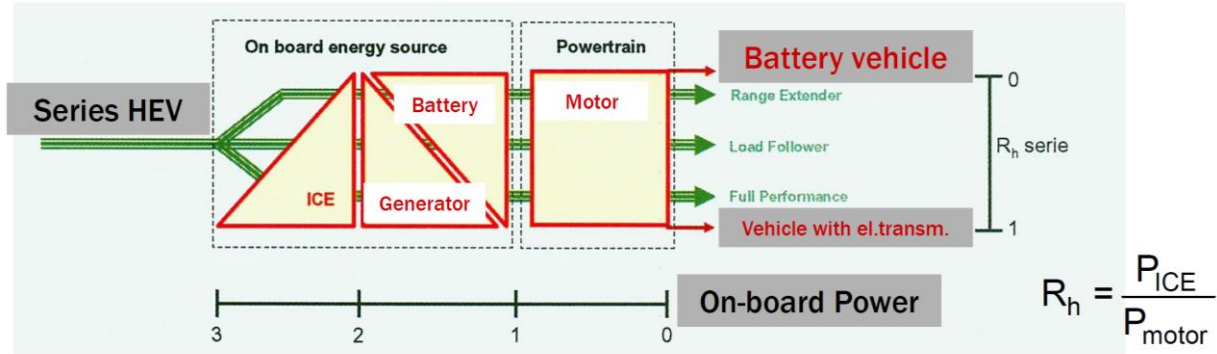


Figure 47

For comparison with the different hybrid architectures in this thesis work, it was decided to calculate the R_h hybridization factor, calculated as [4]:

$$R_h = \frac{P_{ICE}}{P_{EM}} \quad (4.1)$$



$R_h = 0$: pure electric vehicle; $R_h = 1$: vehicle with electric transmission.

Figure 48

For this configuration $R_h = \frac{P_{ICE}}{P_{EM}} = 0,28$, as show in the figure 46 this value corresponds to having designed a range extender vehicle. It is a sort of thermally assisted electric vehicle, in which the ICE works at fixed point (max efficiency) and it is used to charge batteries. The ICE (and the electric machines connected to the ICE line) is designed to provide the average power during the scheduled driving cycle.

The power supply of the electric component is a lithium-ion battery, a type most commonly used in both the automotive and other applications. It has a high energy density and a good capacity of charging hysteria. We can say that the battery is the main component of PHEVs but also one of the most sensitive due to the dependence of its efficiency on multiple factors. The technical data of the battery are show in table 7.

Type	Li-Ion
Capacity	30 Ah
Nominal Voltage	345 V
Energy	11 kWh

Table 7

5.2 NEDC cycle CD test

The first simulation was performed by performing a CD test along several NEDC cycles to assess whether the design requirements for the electric range and to identify the minimum SOC, respecting the equation (3.2). For greater clarity, the operating points on the characteristics of EM, and then the evaluation of the electric range and minimum SOC reported, after CS test for each cycle. Having changed the configuration of the powertrain compared to the main vehicle, to take into account the addition of three elements: battery pack, electric motor and electric generator, you choose to increase the mass tests for the NEDC and WLTP cycle by 230kg, maintaining the coast down coefficients unchanged.

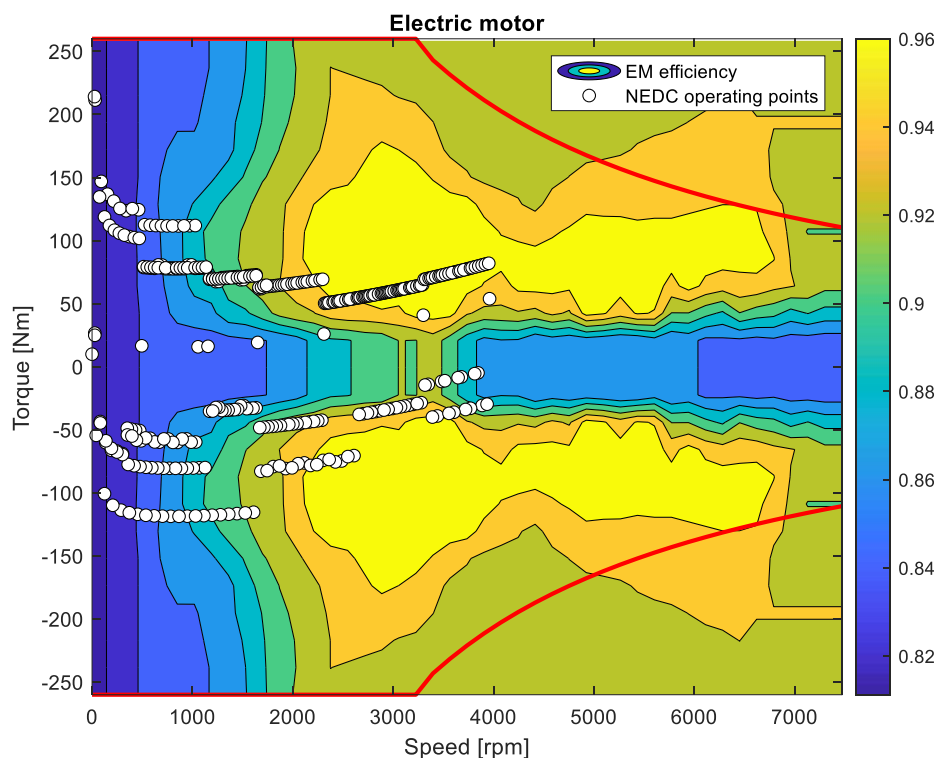


Figure 49

From the operational points present on the EM characteristic you can easily see how, it can safely follow the series of NEDC cycles, indeed at first impact it may seem that it is oversized, but later you will see that this design choice will bring benefits in terms of the performance of the vehicle.

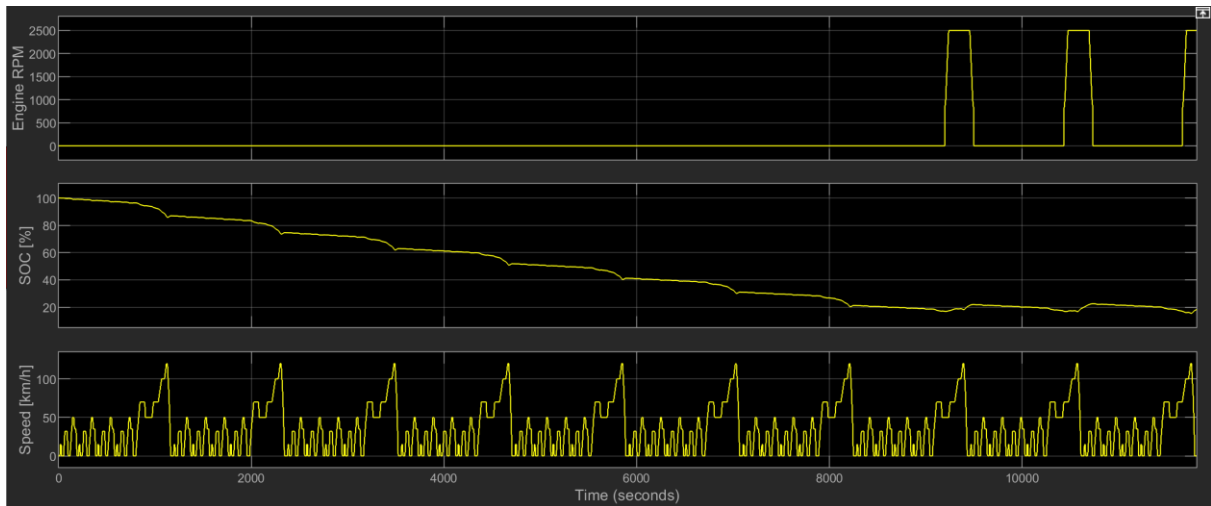


Figure 50

As shown in the figure 50 the ICE first turned on during 8th CD NEDC cycle. The next CD NEDC cycle, confirmed that the minimum SOC was reached, fulfilling the electricity balance criterion. The minimum SOC is around 17%.

5.3 WLTP cycle CD test

By running the CD test along several WLTP cycles, you can easily see that the operating points of the EM are spread over a larger portion of the characteristic, as already shown above, this is due to the different structure of the WLTP cycle, which is closer to a real driving condition than the NEDC cycle.

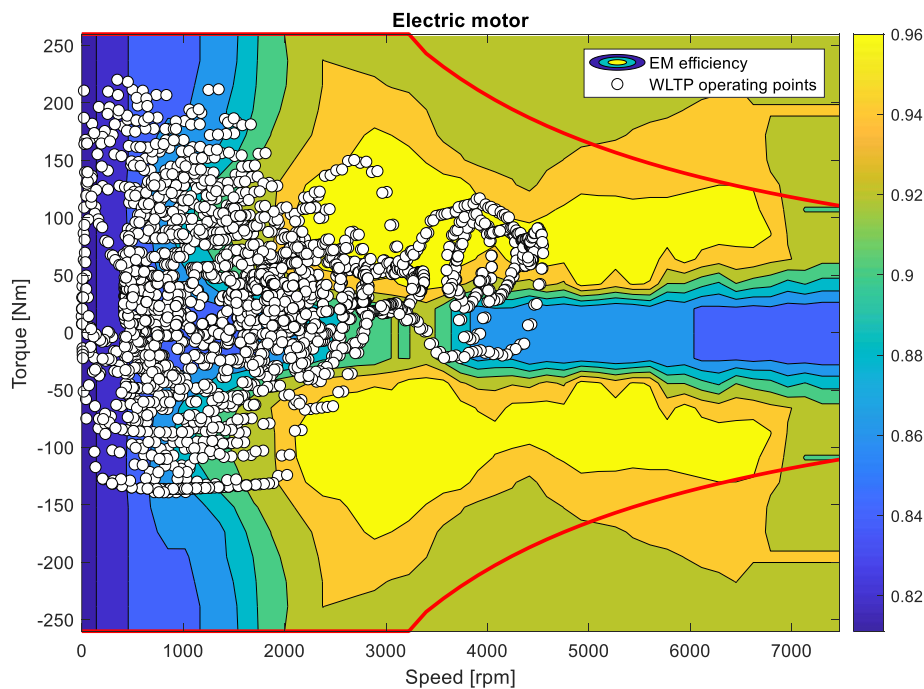


Figure 51

Again, it is possible to see how the EM is not exploited to its full potential, most of the time it works in a low lap and high pairs regime, where it does not perform particularly well, but as mentioned above it was decided to adopt this design solution also to comply with the constraints dictated by the performance of the vehicle.

As show in the figure 52 the ICE first turned on during 3th CD WLTP cycle. The next CD WLTP cycle, confirmed that the minimum SOC was reached, fulfilling the electricity balance criterion. The minimum SOC is around 18%.

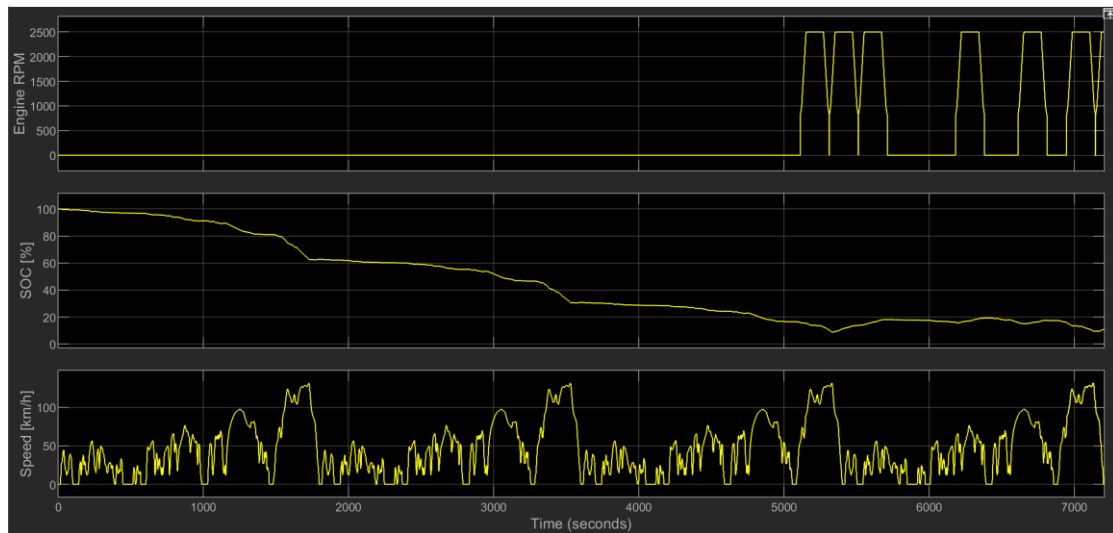


Figure 52

5.4 NEDC cycle CS test

According to [19] CS test should be run after overnight soaking, without charging the battery. In this work, not having a physical vehicle available, the CS test was simulated starting from the charging state reached at the end of the CD test.

In this section, it is considered appropriate to explain the operational points of ICE and the EG. The control strategy adopted, will allow the vehicle to follow the CS test coming to the end of the NEDC cycle with an SOC in the surrounding of the initial SOC, i.e. minimum SOC.

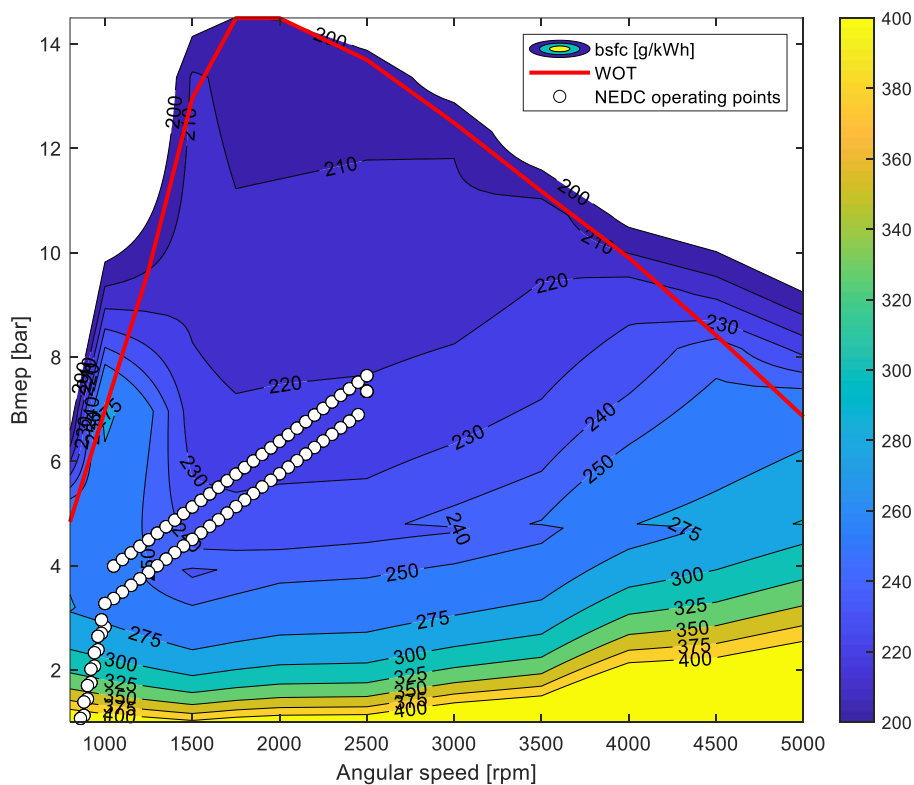


Figure 53

It can be seen that the engine works in a medium BSFC area, because it was decided for the purposes of the thesis work, not to recharge the batteries during the CS test, this would have led to adopting a control strategy in order to make ICE work in the area around the 12 bar of bmeP.

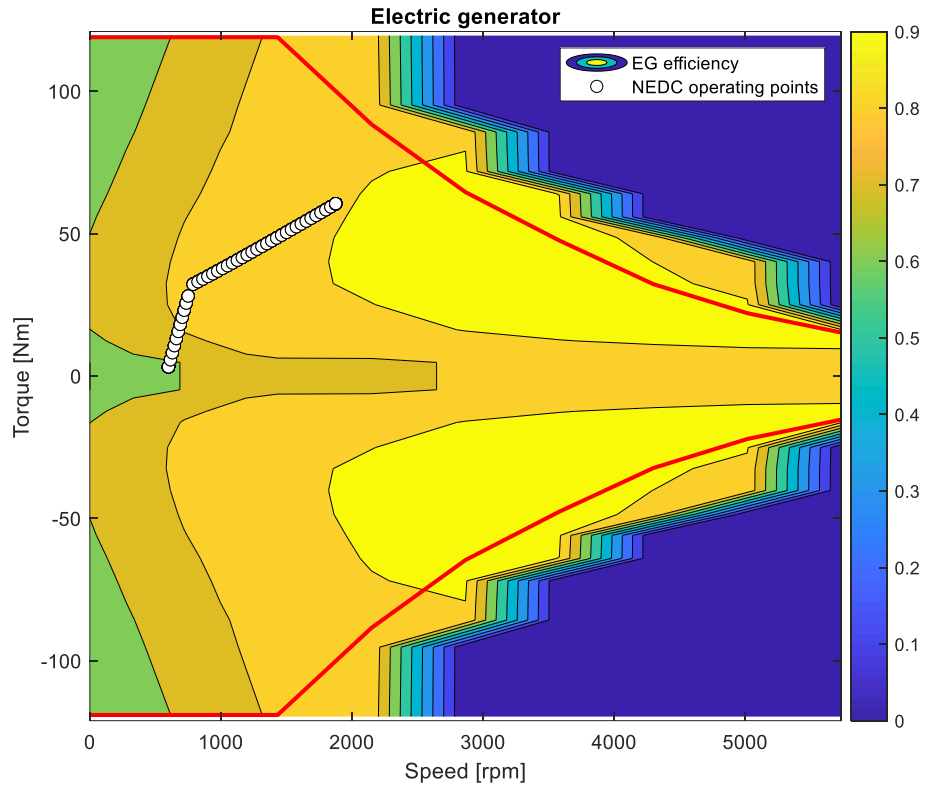


Figure 54

EG's operational points are a direct consequence of ice's choice of operating points. There are no particular efficiency problems as this type of electric car works with excellent performance in a large area of the feature.

5.5 WLTP cycle CS test

The WLTP cycle also chose to adopt the same control strategy adopted for the NEDC as explained in [23] a control strategy for charging the battery could lead to a deviation of the true value of CO_2 emissions, since the correction in the equation (3.4) would be optional, causing manufacturers to take advantage of it. In the WLTP cycle for implementing the control strategy chosen, it is necessary to make the engine work with higher loads, around 10 bar of bmep. This will lead ICE to work in a better bsfc zone than the NEDC cycle, but will then assess the goodness of this choice for CO_2 emissions and FC.

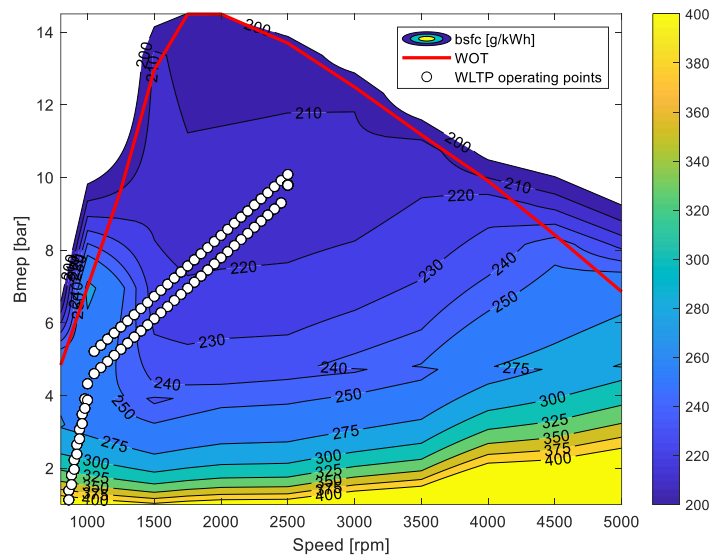


Figure 55

As shown in figure 55, the EG will also work in a more efficient area.

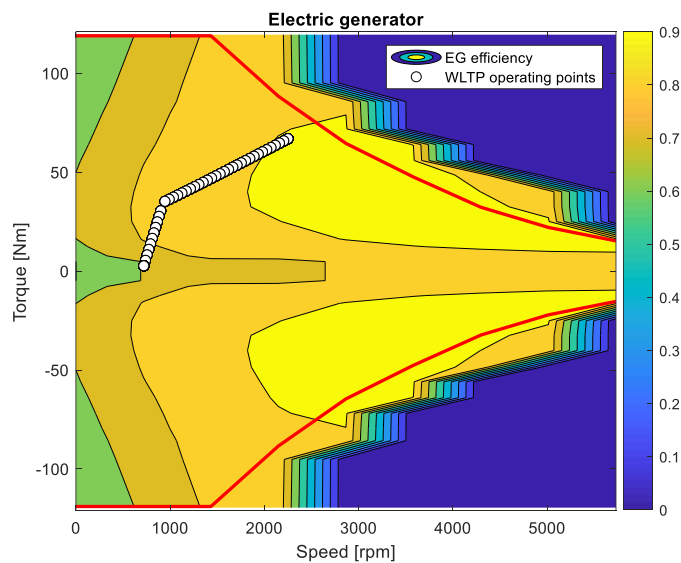


Figure 56

5.6 CO₂ emissions, FC and electric range calculated for NEDC and WLTP cycle

In Chapter 3, reports for the calculation of CO₂ emissions, FC and electric range were presented, in some of them there is UF for the calculation of the various parameters, given its length of calculation the algebraic mathematical steps carried out in the Matlab environment were omitted.

Electric range defined in EU Regulations are reported in table 8.

Ranges [km]	NEDC	WLTP
D _{OVc} /R _{CDC}	88.24	69.81
D _e /AER	85.17	62.05

Table 8

As for the NEDC procedure, there are two definitions of electric range: **D_{ovc}** and **D_e** .

D_{OVc} : is defined as the distance traveled in charge depleting mode to the end of the transition cycle and is always equal to the number of cycles.

D_e :is defined as the distance traveled in charge depleting mode until the ICE turn on for the first time.

In the WLTP procedure, R_{CDC} is equivalent to D_{OVc} and AER is equivalent to D_e. Following faithfully the legislation [19] the WLTP procedure mentions three other definitions of electric range: AER_{city}, R_{CDA} and EAER, which in this thesis work have not been considered since the previous results are considered reliable.

With the reports set out in Chapter 3, it was possible to calculate and weigh the values of CO₂ emissions and FC, it is stated that only one UF was calculated for the CS test, while for each cycle during the CD test, four UFs were calculated, one for each stage [23].

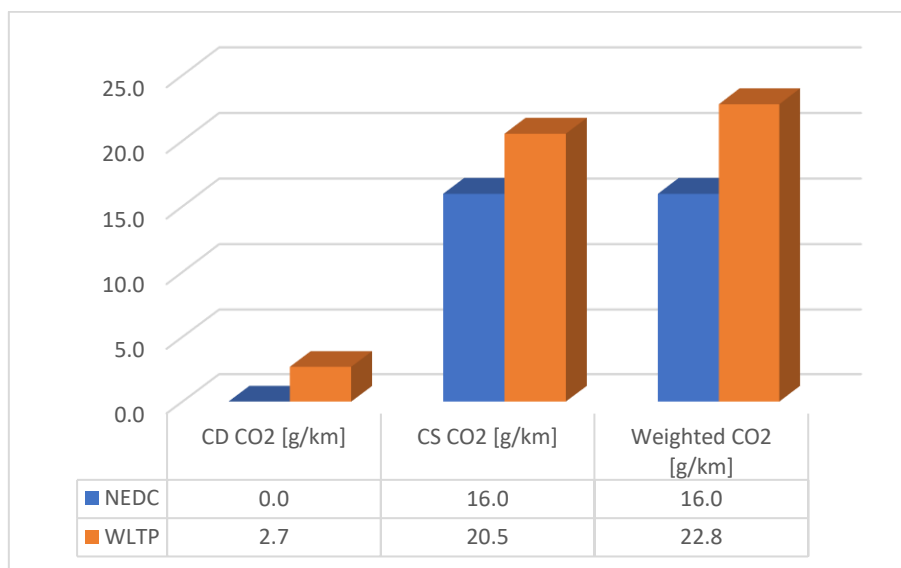


Figure 57

Figure 57 shows the results for CO₂ emissions, as the application of the equation (3.6) brings a higher weighted CO₂ value for the WLTP cycle than in the NEDC cycle. However, it should be remembered that the correction in (3.4) was not used, which would have decreased the value calculated in the CS test.

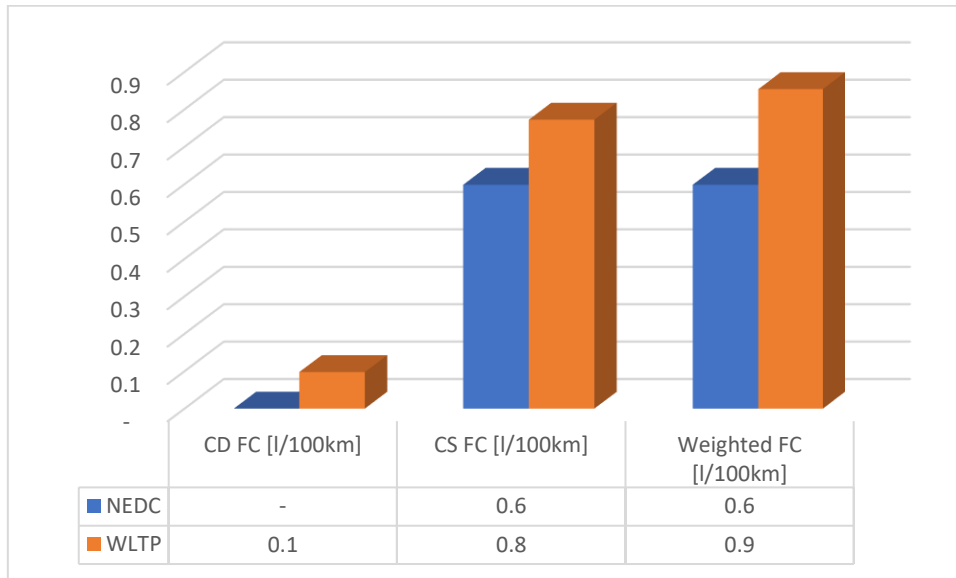


Figure 58

For FC we can apply the same reasoning made for CO₂ emissions, noting again that for the WLTP cycle there are values greater than the NEDC cycle.

The results are due of the control strategy adopted during the CS test, by imposing a different strategy on the control unit, slightly different results could be obtained.

5.7 Performance analysis

The first simulation of the vehicle's performances was to simulate acceleration from 0 to 100 $\frac{km}{h}$ in pure electric, without the help of the thermal engine and generator.

Figure 59 show the operating points of the electric motor. In this simulation, given the low number of seconds, it was decided to adopt a sample time h value of 0.05 in order to make the simulation more accurate.

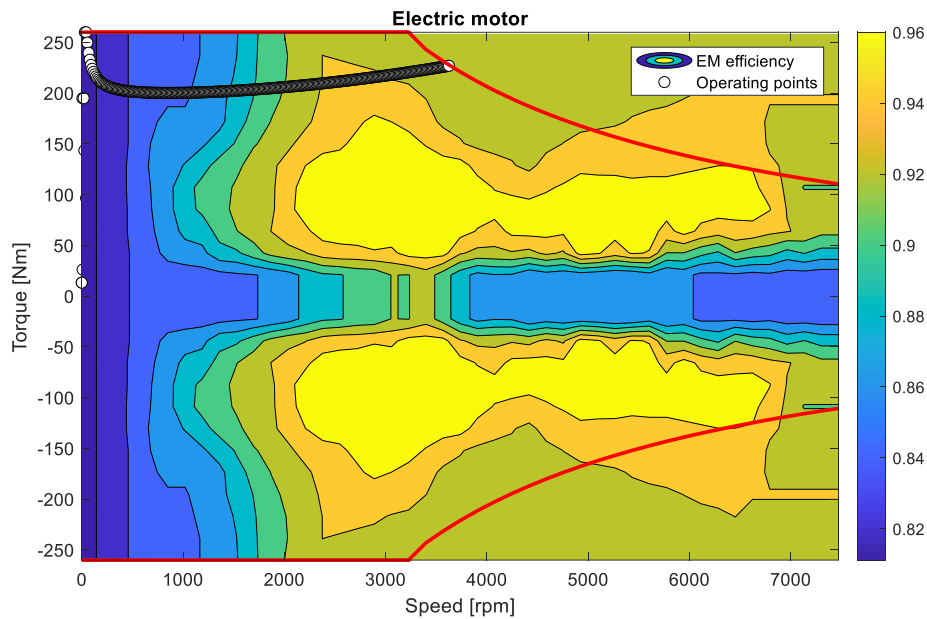


Figure 59

The vehicle to accelerate in pure electric up to 100 km/h takes about 15 s, a value quite in line with other cars of the same segment, since from this type of vehicle is not expected to perform high in terms of accelerations. Figure 60 you can also see that there is not a high expenditure of SOC, in fact for this maneuver we use about 4% of the charge.

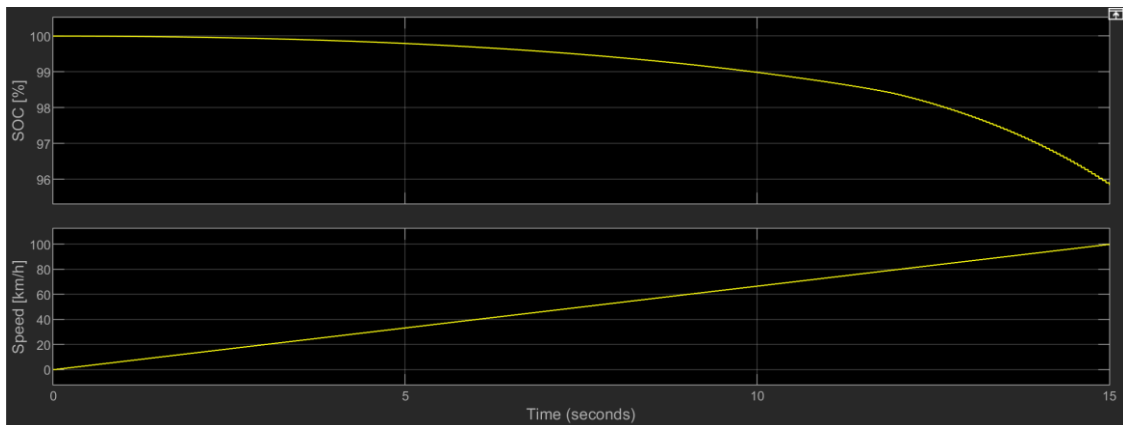


Figure 60

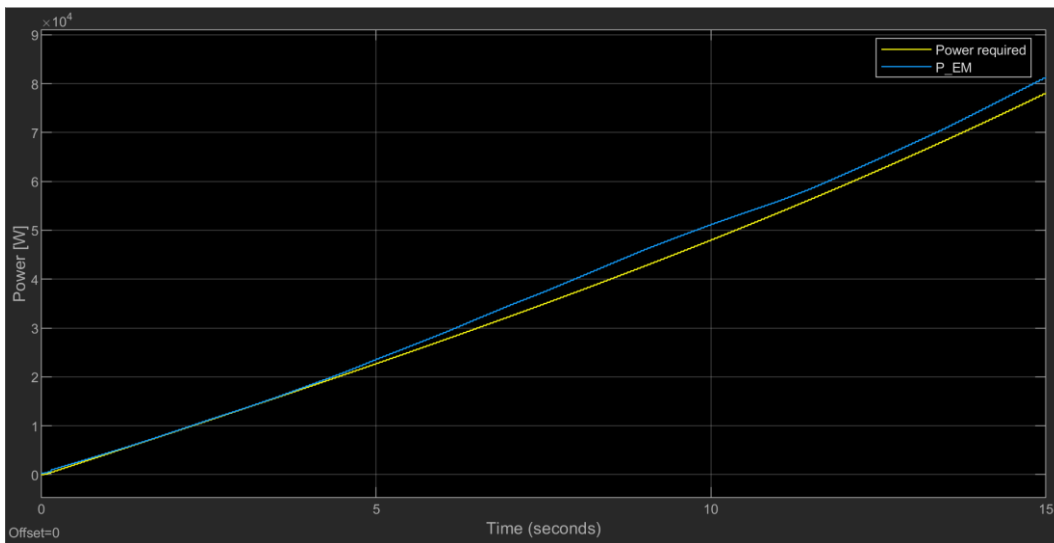


Figure 61

Interesting is the comparison between the power required on the wheels to perform this acceleration maneuver and the power developed by the electric motor. The blue curve that represents the power developed by the electric motor is almost always above the yellow one. A slight overlap can be seen near the initial part of the acceleration, at that stage there is a slight discrepancy between the power developed by the EM and the required power.

It was appropriate to zoom in the area between 10 and 30 km/h, so that you could see how the power developed by the EM is always higher than the required power. This small gap is due to the fact that the engine in the first seconds of acceleration, works in a low-efficiency area. In general, as a control strategy is already implemented the ignition of the thermal engine in cases like this, where the difference between power developed by the thruster and required power is minimal, in this simulation it was preferred not to adopt this method, so as to have a focus on the real behavior of the electric motor.

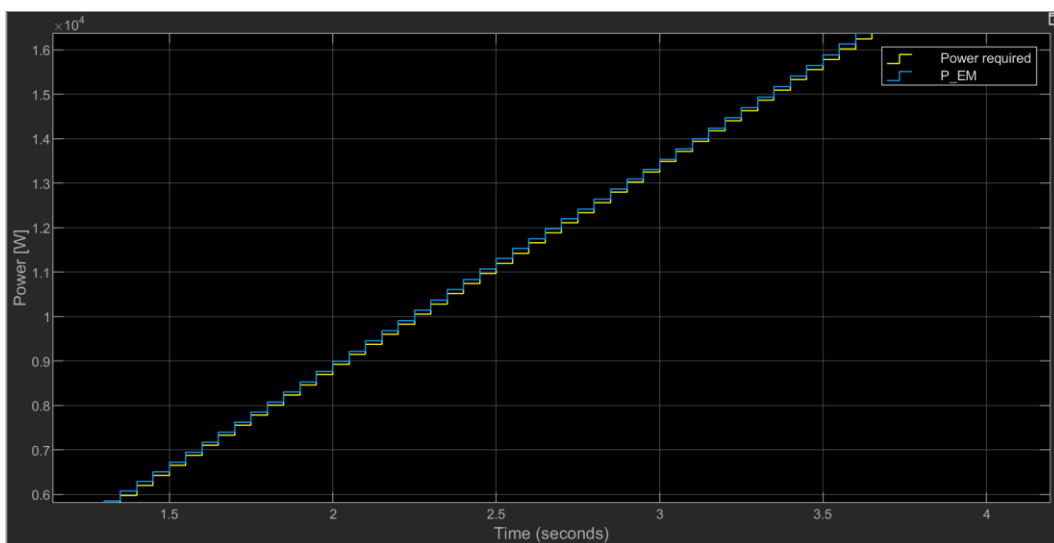


Figure 62

The second performance simulation shows an overtaking manoeuvre on the suburban road. Figure 63 show the driving profile and the vehicle's SOC is illustrated throughout the manoeuvre. Note that at the time when the vehicle is required to accelerate from 50 to 90 km/h, there is a change in slope in the performance of the SOC, an indication that more power has been required. The vehicle is then asked to maintain the speed of 90 km/h for about 5 minutes, during which there is an additional drop of 12% of the SOC.

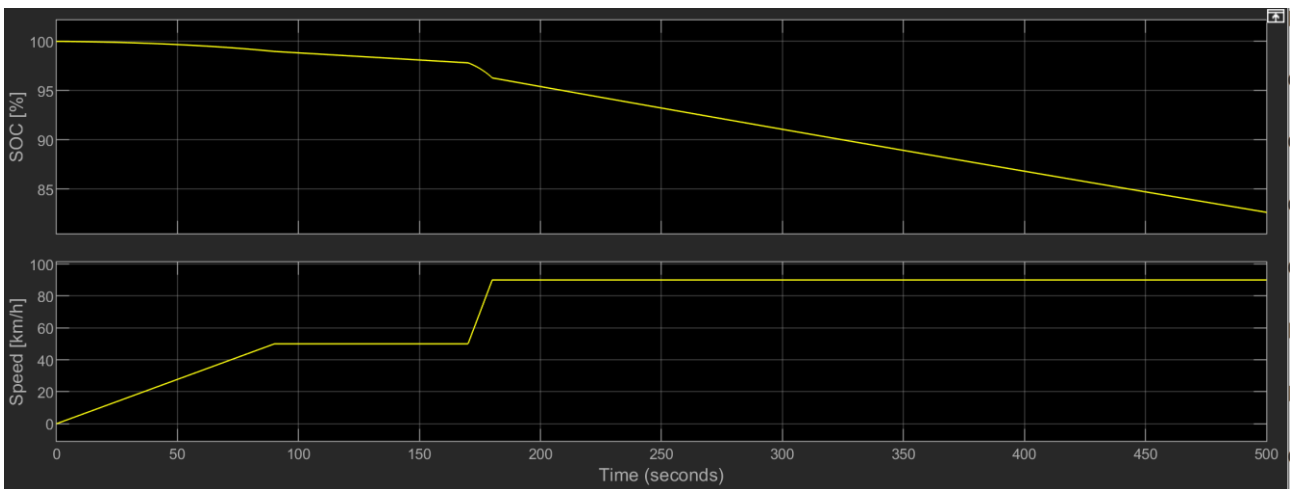


Figure 63

Again, as shown in figure 42 most of the EM's operating points are in the low-efficiency zone during the acceleration maneuver from 0 to 50 km/h, and then stabilize in a maximum-efficiency zone during the second acceleration from 50 to 90 km/h.

In this simulation, it was preferred not turn on ICE and EG.

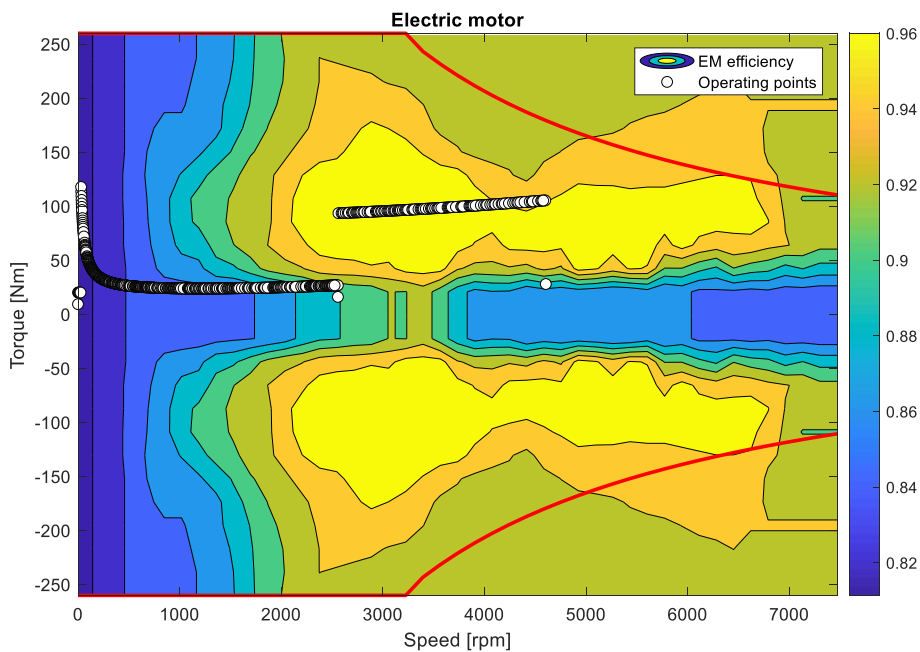


Figure 64

In this last simulation starting from a fully SOC you are asked to the driver of the vehicle to reach a speed of 140 km/h and to keep it up to a value of SOC considered acceptable.

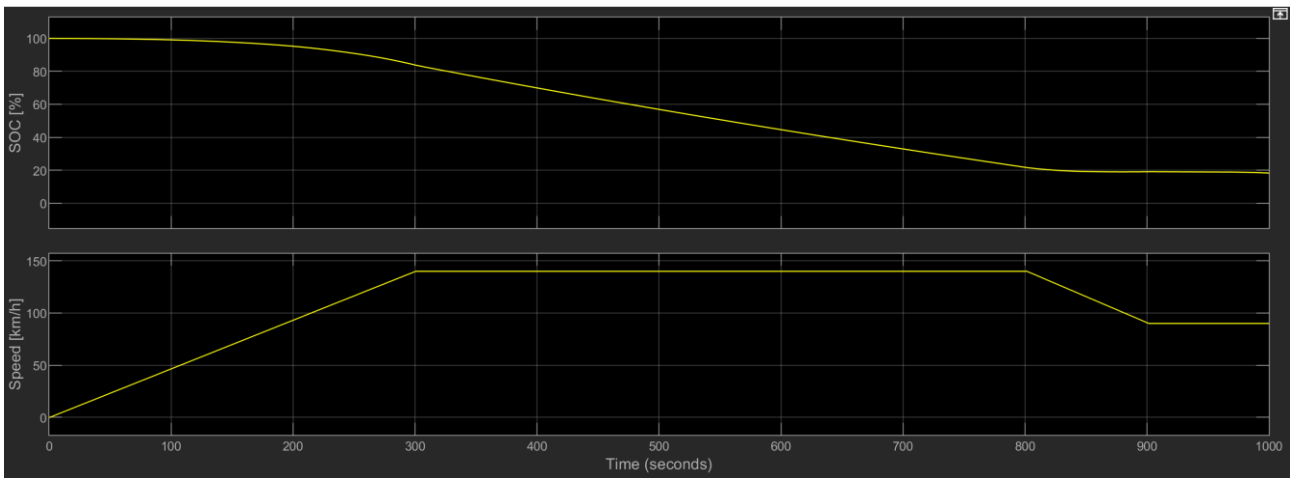


Figure 65

Figure 65 shows the trend of the SOC as a result of the driving profile below. The speed of 140 km/h is maintained for about 8 minutes, up to a charge state of around 20%. Subsequently, the EMS puts the internal combustion engine into operation and the generate to work in CS mode, but accepts a reduction in the vehicle's speed.

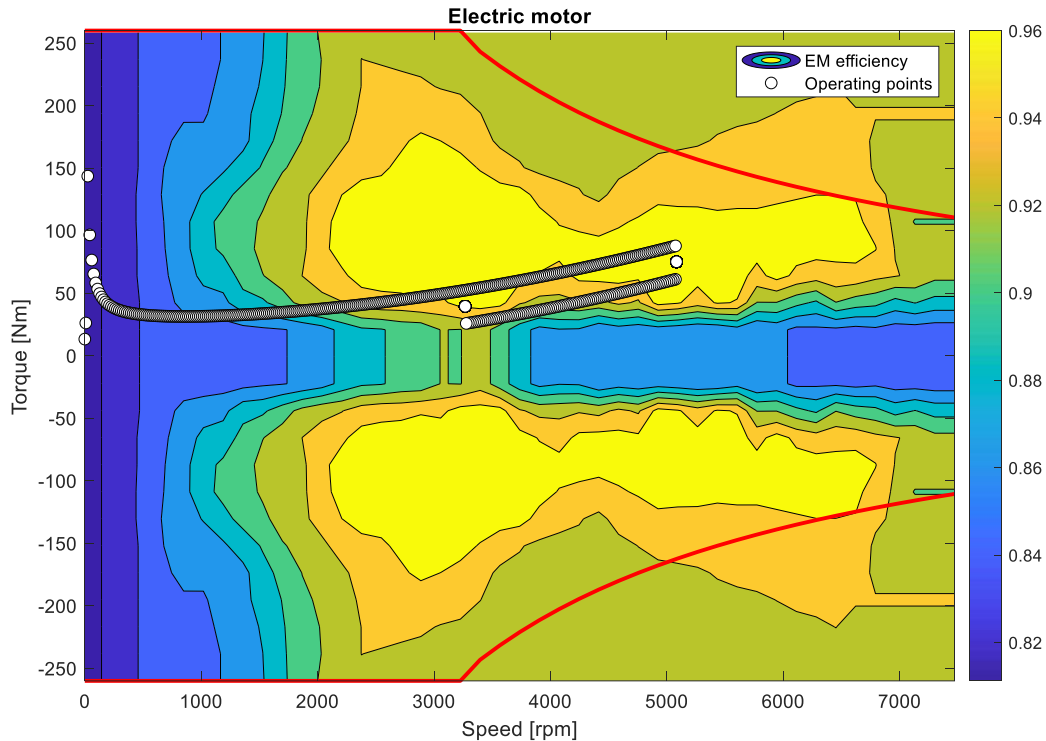


Figure 66

The electric motor is brought to work in points at good efficiency, during the brand at constant speed.

Chapter 6: PHEV: Parallel powertrain

6.1 Presentation main component

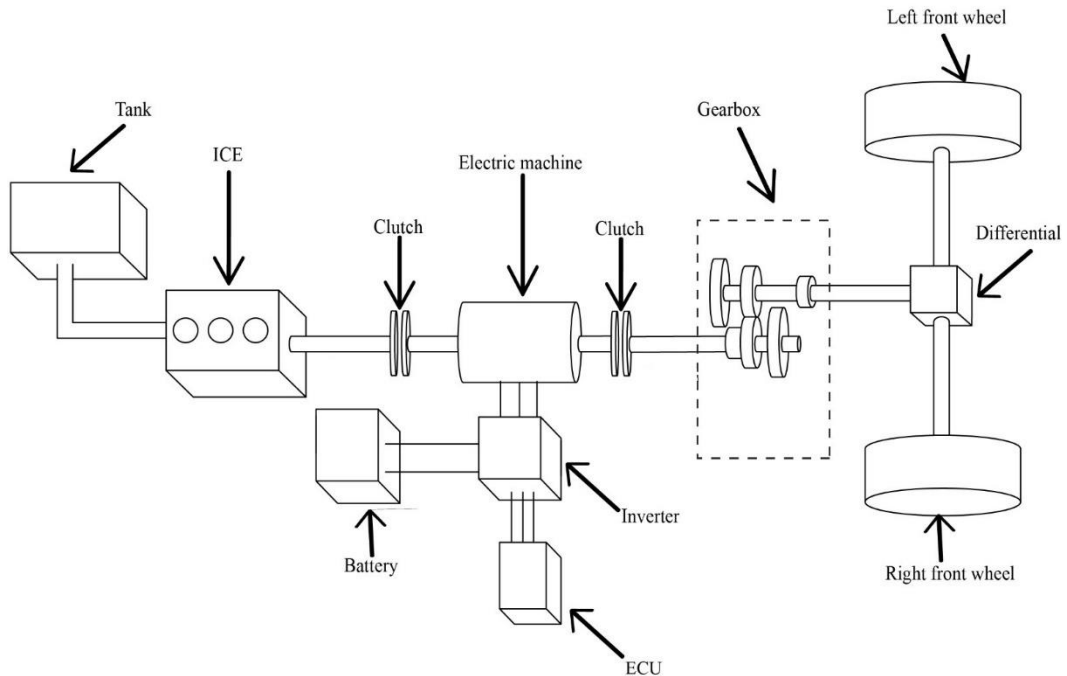


Figure 67

The second architecture analyzed is the parallel configuration. It does not have a second electric machine that acts as a generator, but it is the main electric machine that is used for both functions: motor and generator. Unlike the series configuration, the thermal engine through a transmission chain is affected by the speed of the wheels, but you have to undergo the speeds imposed by the driving cycle.

In the first chapter some variants of the parallel configuration were introduced, for this thesis work it was decided to use a single shaft configuration, in which the gearbox is inserted downstream of the electric machine, this comes to be mechanically connected to the gearbox and ICE through two clutches, as shown in the figure 67.

ICE	Compression ignition Displacement: 1248 ccm Rated power: 52 kW @ 3500-4000 rpm Rated torque: 178 Nm @ 1750-2000 rpm
GEARBOX	Gears: 5 Final drive ratio: 3,563 Gear shift #1 trans. Ratio: 3,909 Gear shift #2 trans. Ratio: 2,238 Gear shift #3 trans. Ratio: 1,444 Gear shift #4 trans. Ratio: 1,029 Gear shift #5 trans. Ratio: 0,767

Table 9

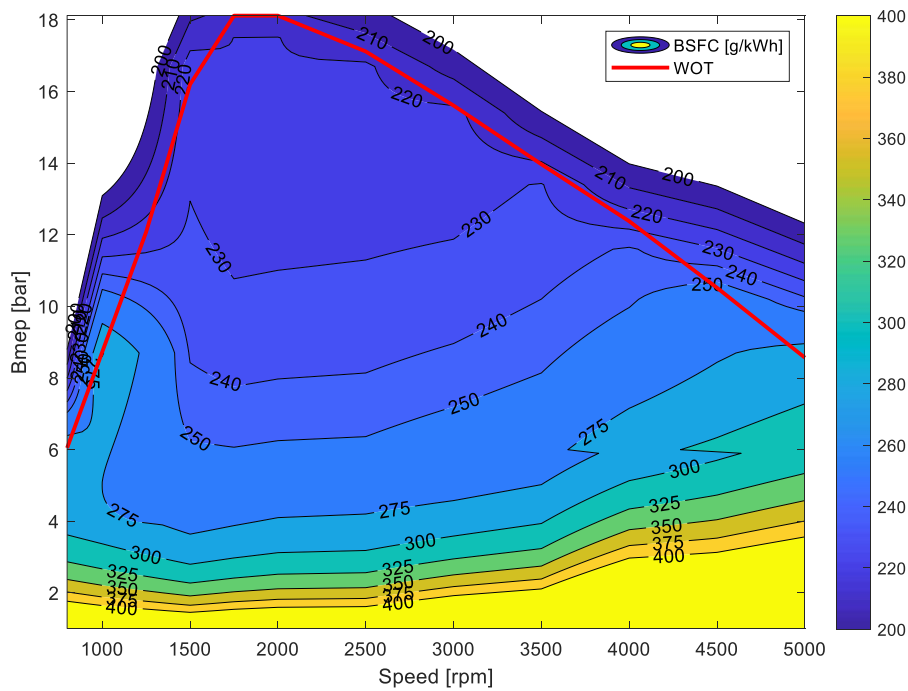


Figure 68

As for the electric powertrain, it is chosen to use an electric car slightly different from the previous one, to try to adapt to the speeds and pairs imposed by the gearbox. The new machine has a lower maximum power than the previous engine of about 15 kW, the rotational regime is about the same, the maximum torque is lower.

Max torque EM	240 Nm
Max Power EM	72 kW

Table 10

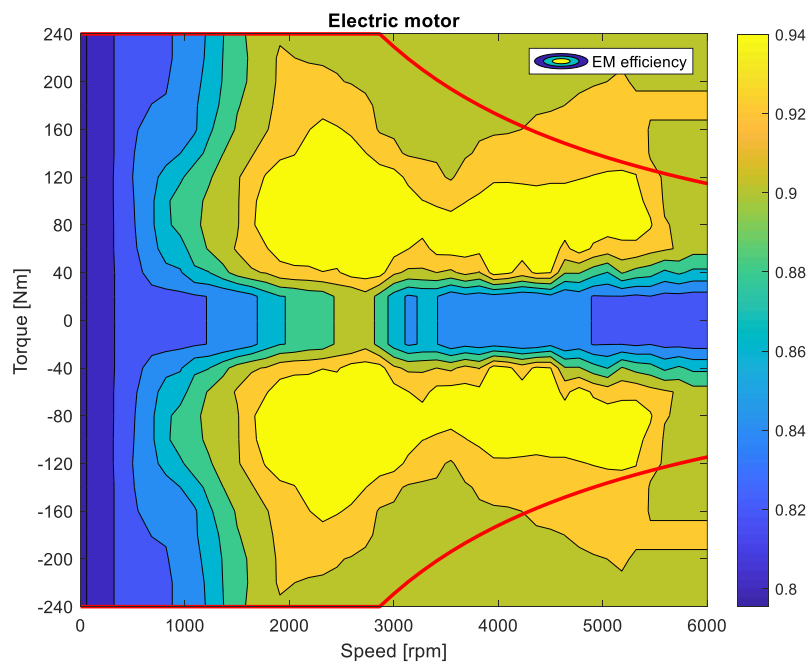


Figure 69

6.2 NEDC cycle CD test

For this simulation the same considerations apply for the hybrid series, again to take into account changes to the powertrain compared to the traditional vehicle the mass tests for the NEDC and WLTP cycle have been increased by about 180 kg, since there is no longer the generator but there is an ICE with a greater displacement.

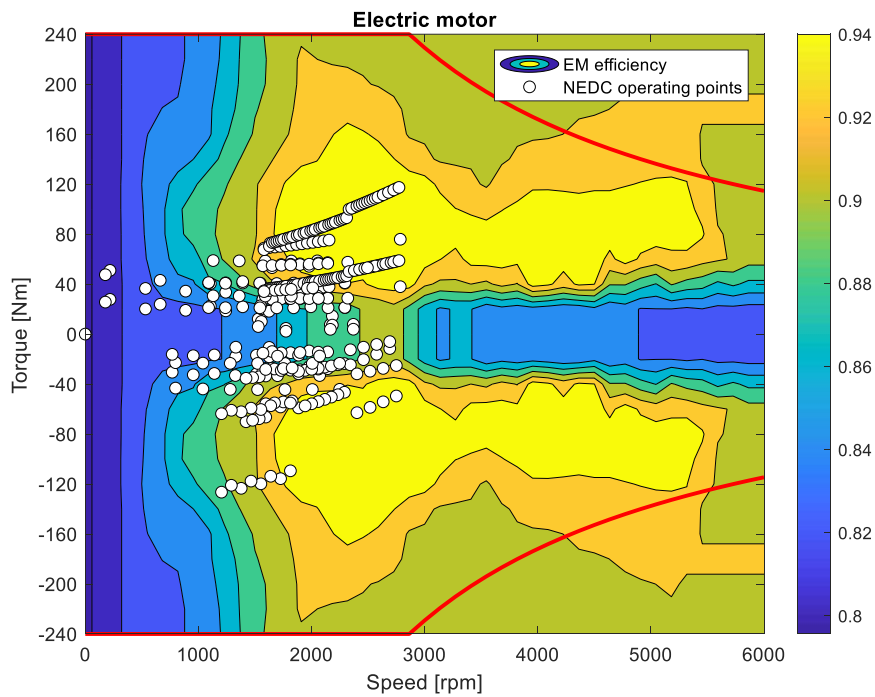


Figure 71

Figure 71 shows the operating points of the electric machine undergoing a CD test, it manages to work quite nimbly in the area of maximum efficiency.

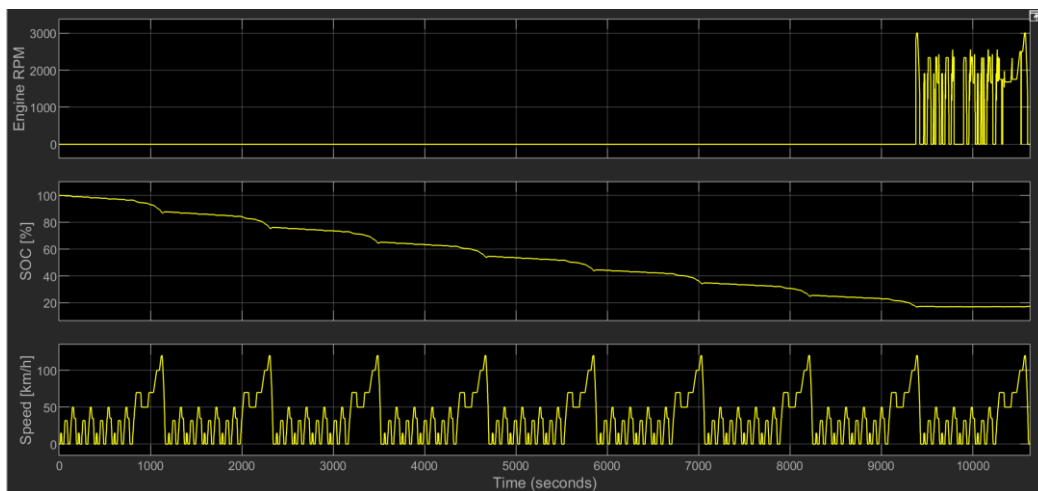


Figure 72

Figure 72 shows how ICE's first ignition occurs at the end of the 8th CD NEDC cycle. The next CD NEDC cycle, confirmed that the minimum SOC was reached, fulfilling the electricity balance criterion. The minimum SOC is around 16%. As might be expected, compared to the previous configuration the electric range is very similar, despite the presence of the gearbox, which could have brought the electric motor to work not to maximum efficiency, since this type of gearbox was designed for a traditional vehicle.

6.3 WLTP cycle CD test

For this configuration, the CD test along WLTP cycle is different from the previous one, concentrating the work points in an area between 1000 and 3000 rpm. As for the NEDC cycle, the characteristic of the electric machine is not taken advantage of beyond 3000 rpm, so little work is done in the area at maximum efficiency, concentrating the work points in an outflow zone around 88%.

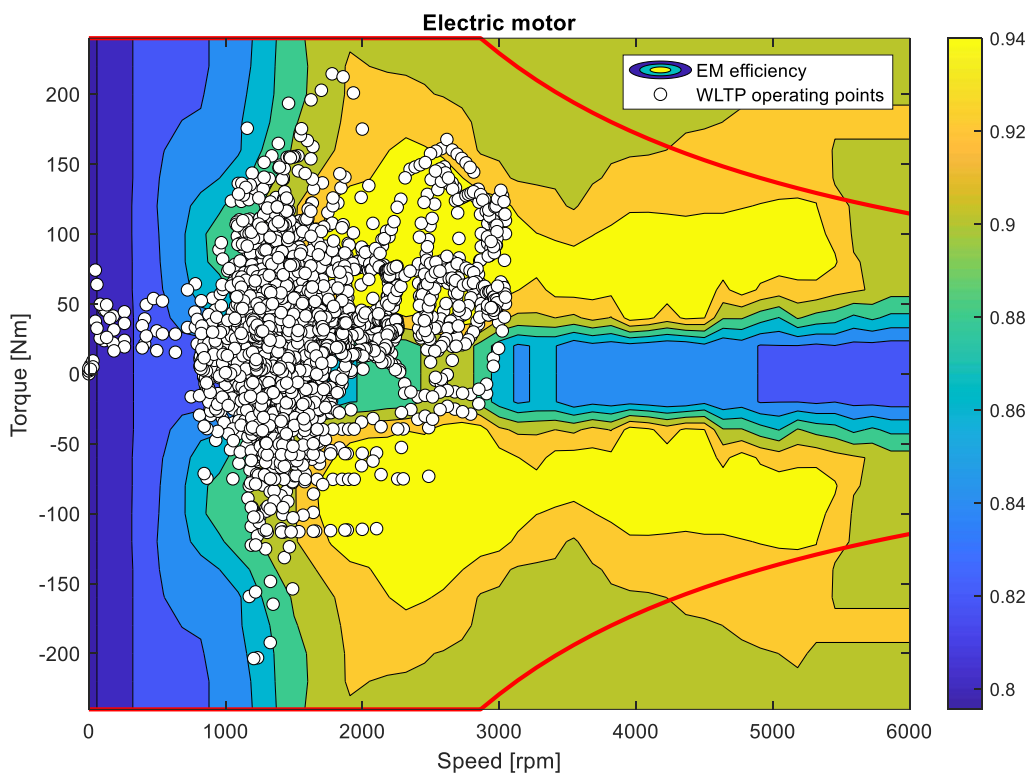


Figure 73

For this procedure, ICE is called to work during final phase of the 3rd WLTP cycle. In the next one you will reach the brake-off criterion. Like the hybrid series, where the thermal engine began to work at the end of the 3rd cycle.

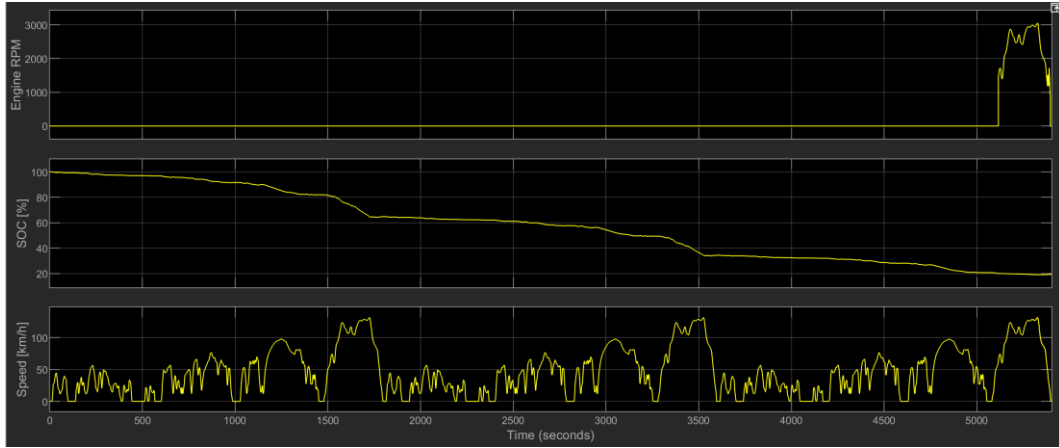


Figure 74

From the 74 figures it can be seen that the speed of the thermal engine, does not follow a trend imposed by the energy control system, but being mechanically constrained to the electric machine with a clutch, it is dragged from it in following the driving profile imposed.

6.4 NEDC cycle CS test

The next step is to perform a CS test along the NEDC cycle, presenting, as previously done, the operational points of ICE.

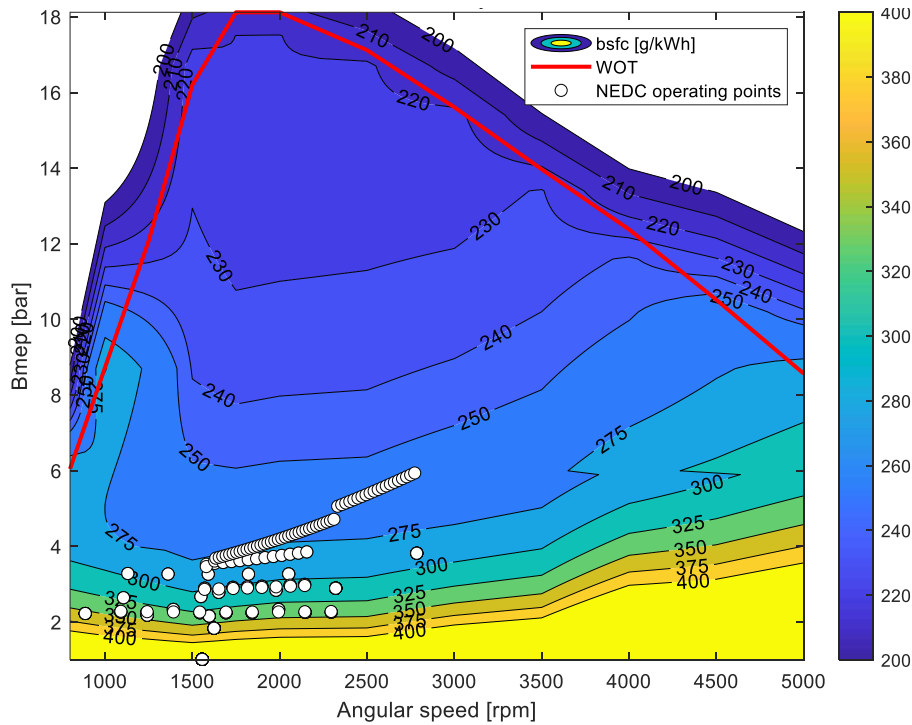


Figure 75

In this CS test, the thermal engine works in suboptimal bsfc points, thus negatively affecting CO₂ and FC emissions. For this configuration, a partition ratio value of the $k=0.5$ torque was used, i.e. the torque required for vehicle traction, and is provided in equal measure by both engines. You might think to use a value of k that allows the thermal engine to work in larger pairs but doing so would reduce too much the torque developed by the electric motor, making it work inefficiently and most importantly you would not be able to cope with the demand for power dictated by the driving cycle.

6.5 WLTP cycle CS test

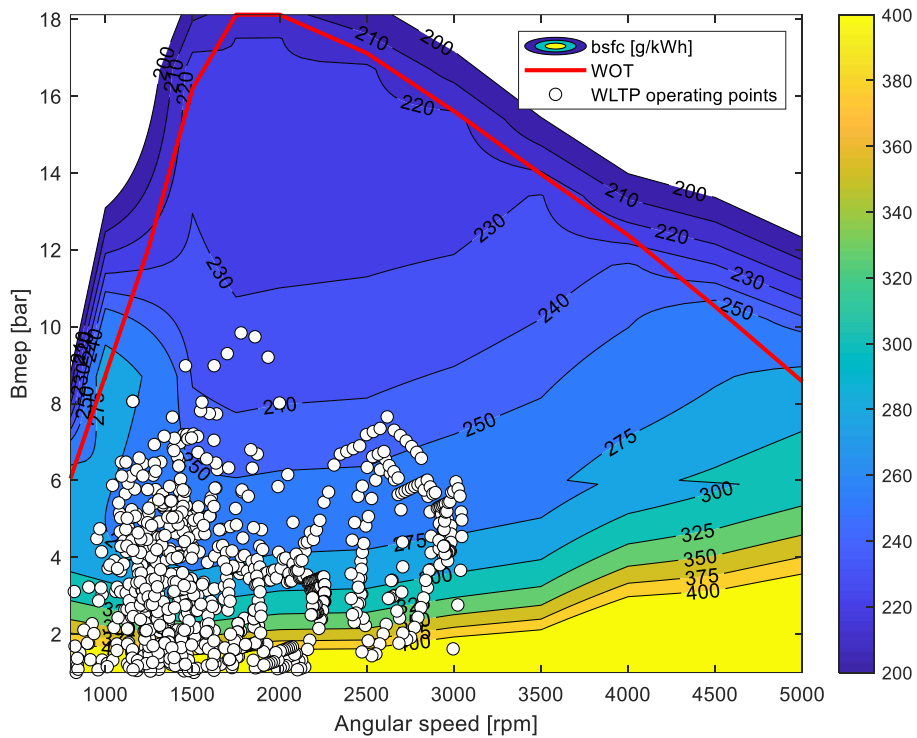


Figure 76

Even for the WLTP cycle, we can see that the thermal engine goes to work at the bottom points of the feature, where the bsfc is not particularly optimized. The partition factor of the pair was kept identical to that used for the NEDC cycle, to have a direct comparison of the results obtained.

One improvement could be to change the value of the partition ratio so that the engine can work with a higher load to eliminate part-load work zones.

6.6 CO₂ emissions, FC and electric range calculated for NEDC and WLTP cycle

Electric range defined in EU Regulations are reported in table 13.

Ranges [km]	NEDC	WLTP
D_{OVc}/R_{CDC}	88.24	69.81
D_e/AER	86.97	61,89

Table 13

Compared to the results shown for the series architecture you see how very similar they are. For the NEDC cycle, the parameter D_e earns about 2 km. By analyzing the data obtained for the WLTP cycle, we see that the R_{CDC} is identical, on the other hand, the AER is less than a very small amount, which is negligible. Even in this configuration looking at the AER which is the benchmark for the definition of the electric range, you were able to meet the project requirements.

Following the equations (3.1),(3.5) and (3.6) have been calculated CO₂ emissions and FC for this configuration:

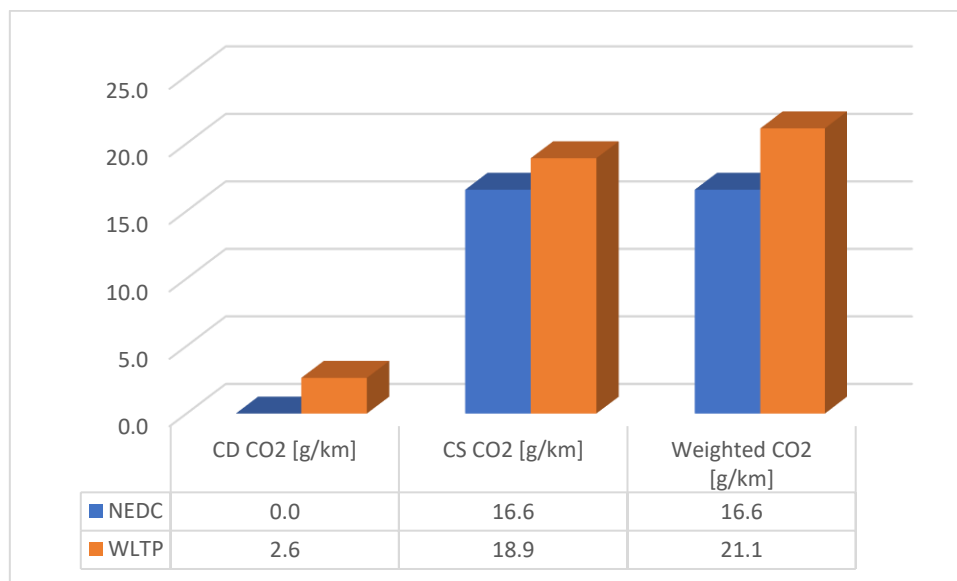


Figure 77

You can immediately see that the CO₂ emissions for the NEDC cycle are 3,6% higher than those estimated for the series configuration. The results obtained following the WLTP procedure are about 7,7% lower than those estimated for the series configuration.

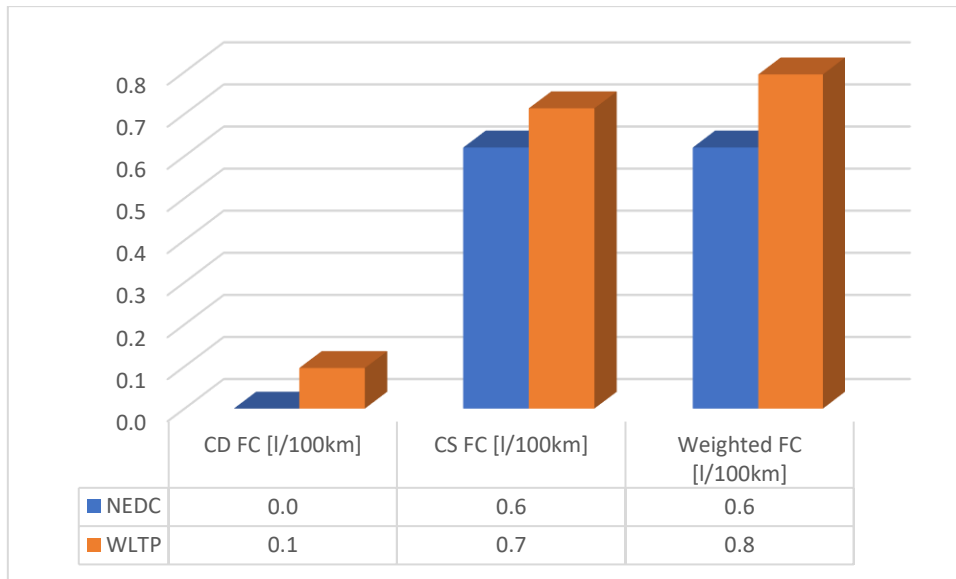


Figure 78

FC for the NEDC cycle, the results are identical because the value of D_{OVC} are very close . For the WLTP cycle, on the other hand, there is a slight reduction in FC, order of the 8.7%

6.7 Performance analysis

As previously done, the first performance analyzed is acceleration from 0 to 100 km/h. Initially the acceleration was evaluated in pure electric, but as shown in figure 79 the electric motor alone fails to develop the power needed for propulsion in the later stages of acceleration. The reason is to be found in the decrease of the size of the electric motor for this type of architecture and in the use of the gearbox present in the traditional vehicle.

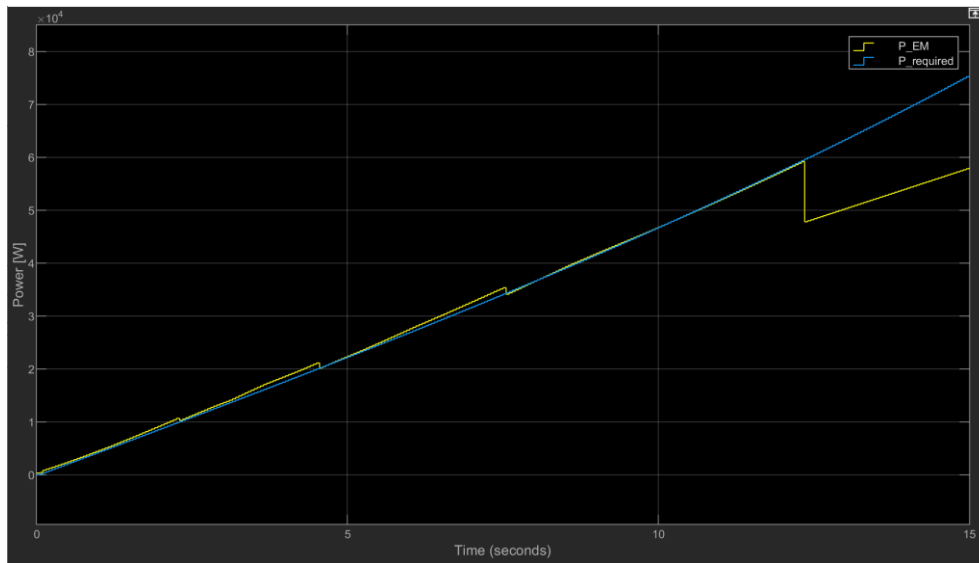


Figure 79

It was therefore necessary to have the thermal engine intervened during the acceleration of the vehicle, so that it provides a surplus of power to meet the demand for power for the vehicle's traction. In this way it is possible to reduce the time, in fact the acceleration takes place in about 11s, making the engine work in a way that produces a power of about 40 kW.

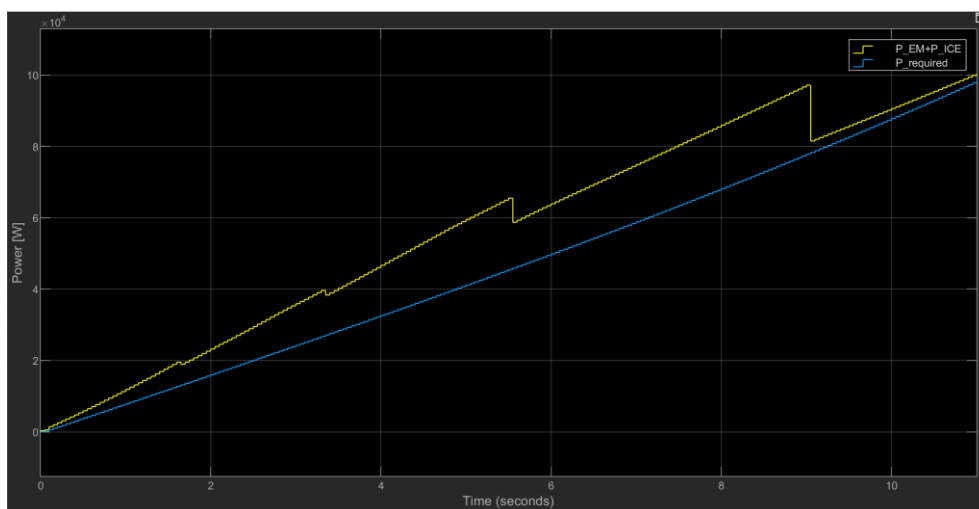


Figure 80

In the following figures the work points of both engine are shown, the electric motor in the final stages of acceleration is brought to work on its maximum torque curve.

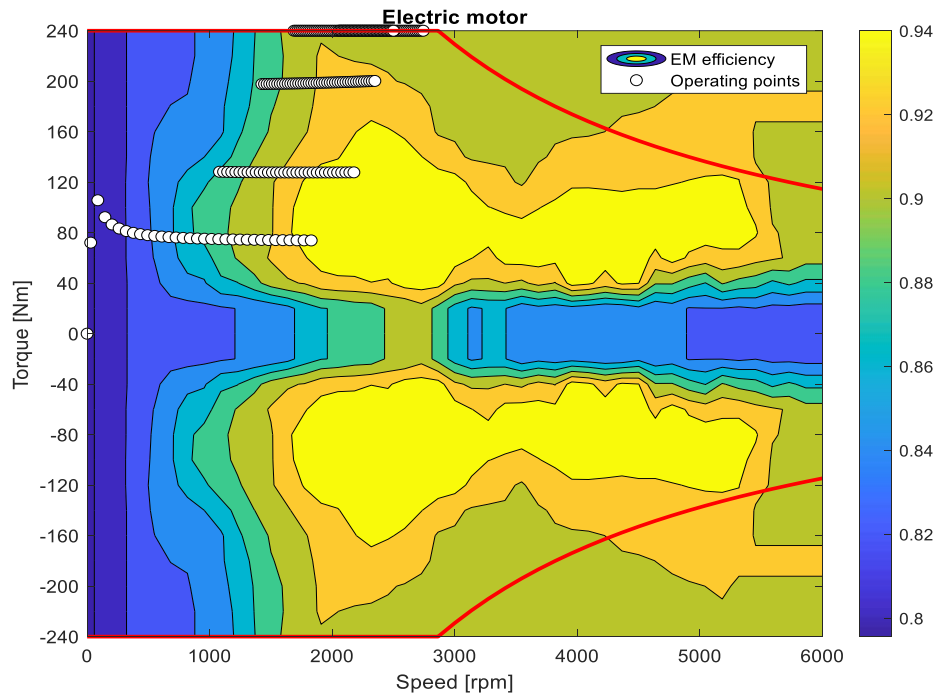


Figure 81

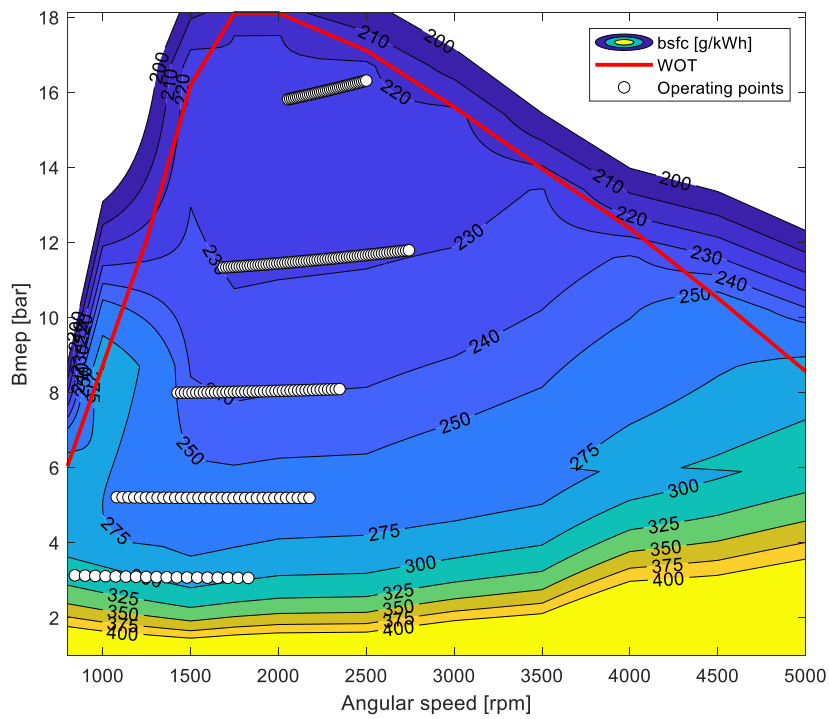


Figure 82

The second performance analysis concerns an emergency overtaking on suburban road. The parallel vehicle in question, performs much better than the series. The energy consumption and therefore the lowering of the state of charge during acceleration from 50 to 90 km/h, is slightly lower, therefore there will also be an improvement on the final SOC of the simulation which for the parallel hybrid stands at around 87% while for the hybrid series is about 84%.

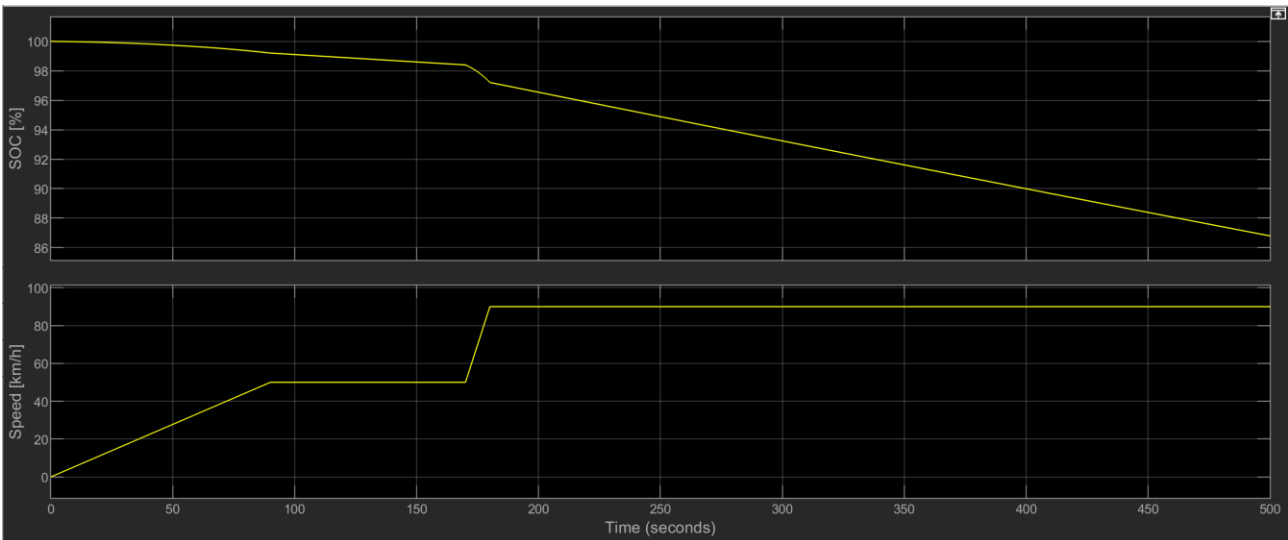


Figure 83

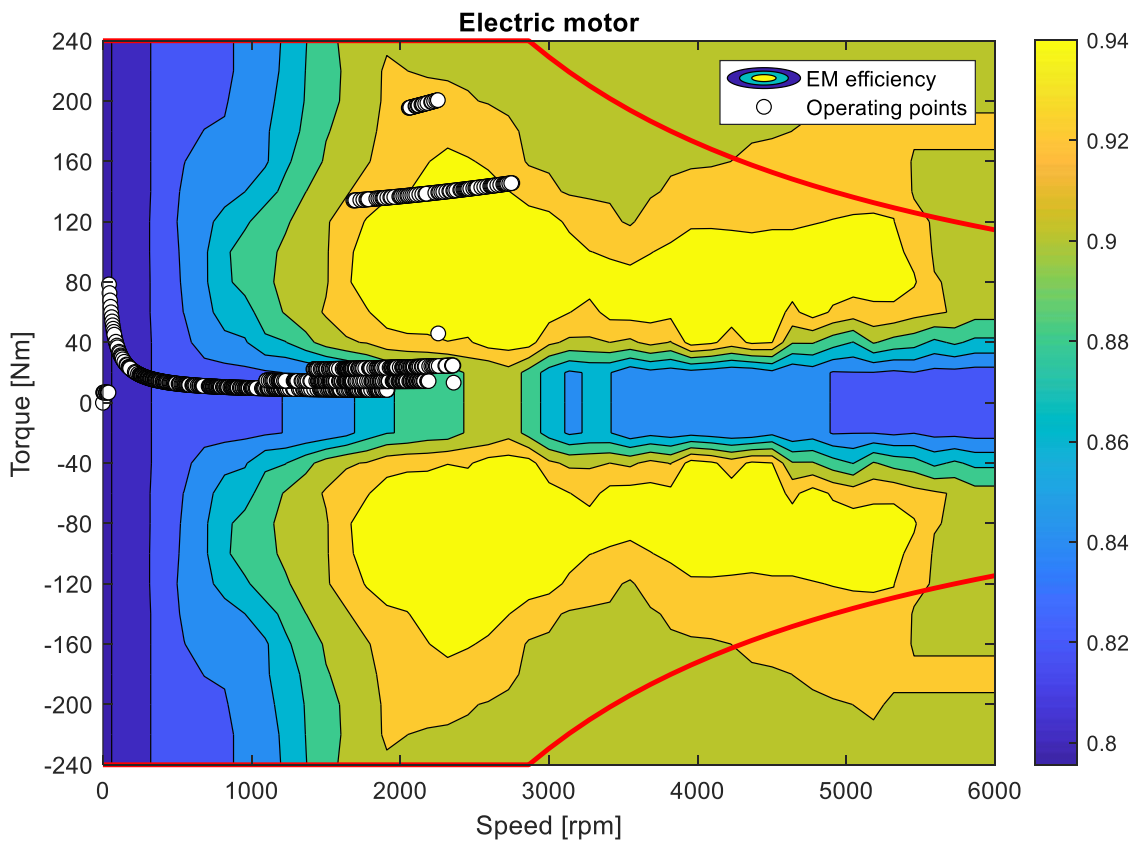


Figure 84

In this last simulation starting from a fully SOC you are asked to the driver of the vehicle to reach a speed of 140 km/h and to keep it up to a value of SOC considered acceptable.

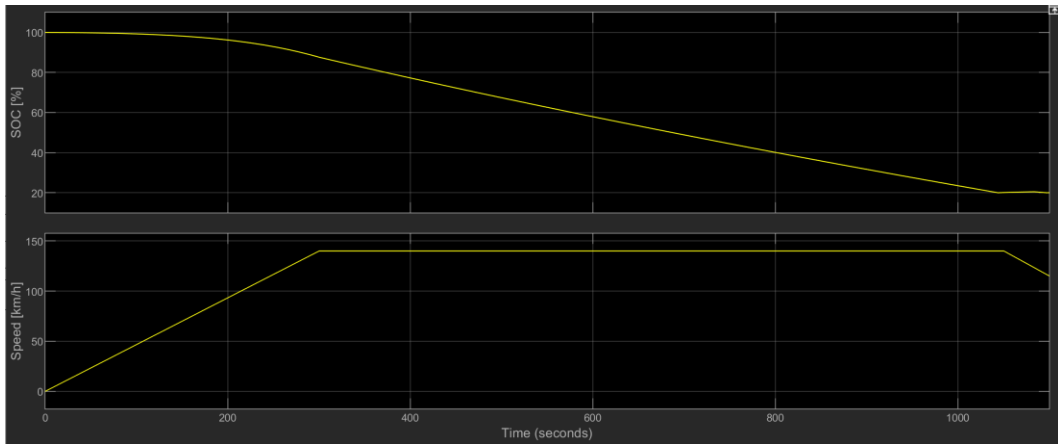


Figure 85

Figure 85 shows the trend of the SOC as a result of the driving profile below. The speed of 140 km/h is maintained for about 13 minutes, much better result than the series vehicle, up to a charge state of around 20%. Subsequently, the EMS puts the internal combustion engine into operation in CS mode, but accepts a reduction in the vehicle's speed.

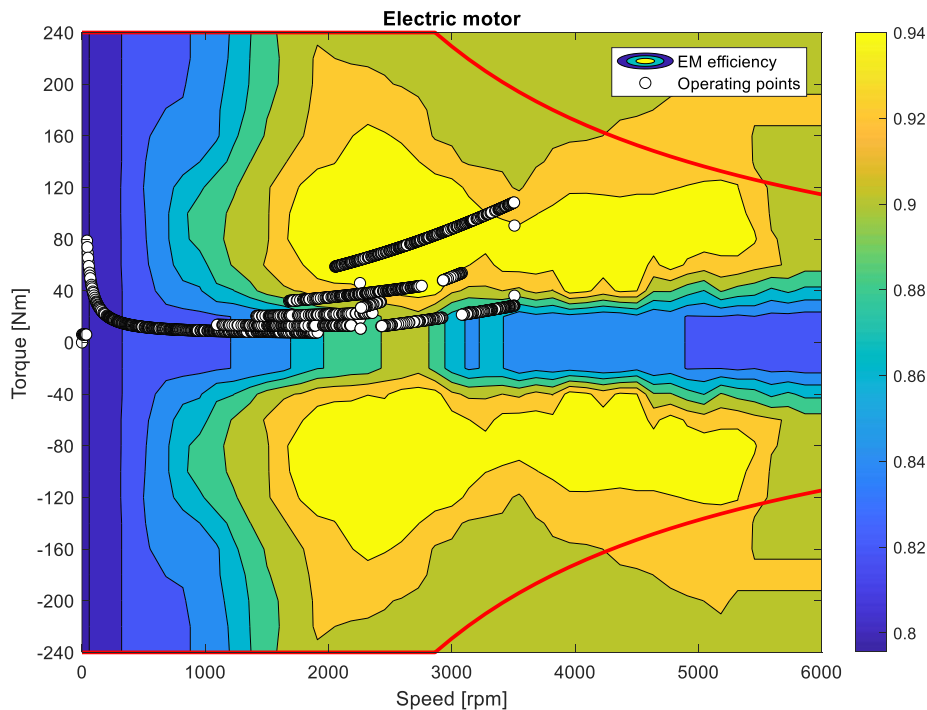


Figure 86

The operating points are slightly jagged due to the insertion of the gearbox.

Chapter 7: PHEV: Series-parallel powertrain

7.1 Presentation main component

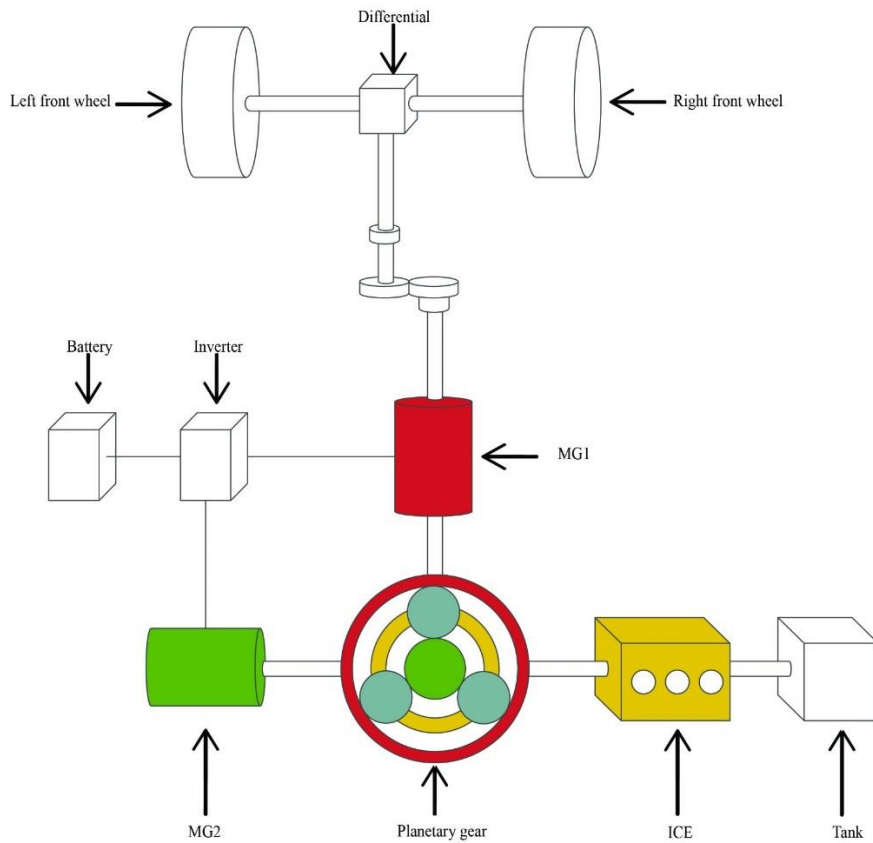


Figure 87

The latest configuration analyzed is a configuration that allows the vehicle to behave both as a series vehicle and as a parallel vehicle. As explained in the previous chapters, there are several design solutions that allow the coupling of the various components in order to obtain a complex hybrid, here you have chosen to use a particular configuration in which an planetary gear set is inserted. For this work the fundamental gear ratio is equal to 1.2. The differential gear ratio is 1.9 and the ratio of the transmission connecting the differential to the machine MG1 is 2.9.

This chapter avoided the presentation of the thermal engine since it is quite similar to the one used for parallel configuration, instead the two electric machines are presented, the one with the largest size will be identified as MG1 connected to the ring of the planetary gear, while the second electric machine of smaller size will be indicated with MG2 connected instead to the sun of the aforementioned planetary gear set.

Max torque MG2	119 Nm
Max Power MG2	21 kW

Table 14

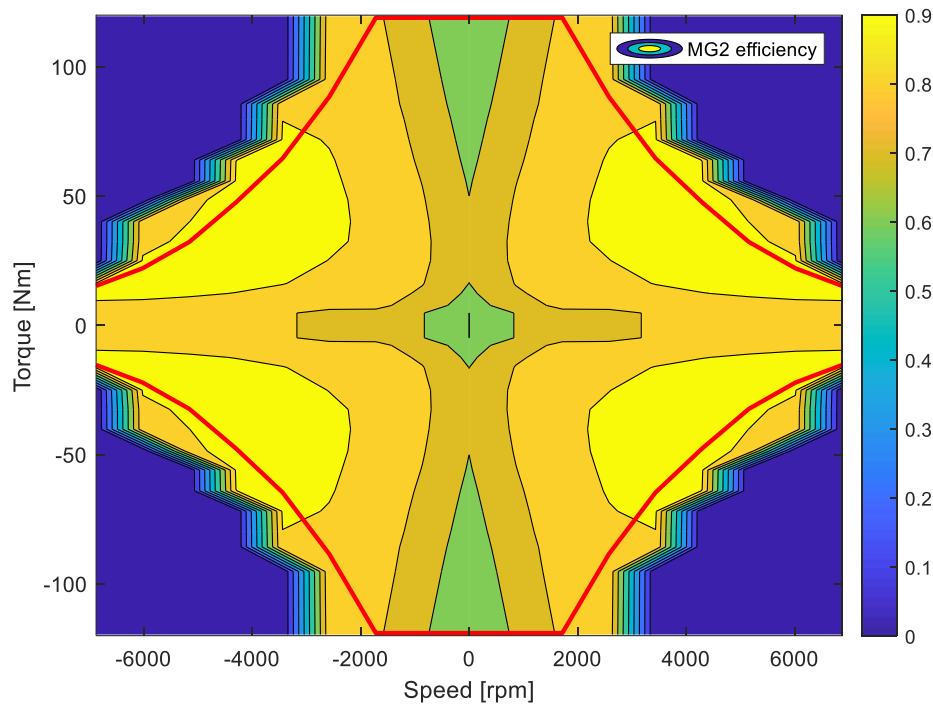


Figure 88

As you can see from Figure 88, this electric machine has 4 quadrant because by evaluating the relationship (3.8) that connects the angular speeds of the three power sources, you can see that, if you want to make nothing the speed of the ICE, the MG2 machine connected to the sun must rotate in the opposite direction to the MG2. This type of electric machine, will essentially play the role that the generator played in the series configuration, in fact you can notice the clear similarity of the feature. An electric car of this type was chosen to increase the electric range. It was seen that during the CD test, only the electrical component responsible for the traction, so in this architecture MG1 and MG2, will be the engines/generators during the CD test. Both machines can recharge batteries through regenerative braking but can both contribute to vehicle traction. For the MG2 machine in this thesis work, for reasons dictated by the Simulink environment, the convention was adopted in which $P_{EG} > 0$, first and third quadrant, indicates that the machine acts as a generator and is recharging the batteries, on the other hand when $P_{EG} < 0$ the machine participates in the propulsion of the vehicle by absorbing energy from the batteries.

The MG2 electric machine, is connected to the ring of the planetary gear set, which is connected via a fixed ratio to the differential and then to the wheels, will act as the main thruster, as was the case in the serial vehicle.

The feature presented in Figure 88 shows how the maximum torque and maximum power compared to other configurations have been reduced.

Max torque MG1	200 Nm
Max Power MG2	81 kW

Table 15

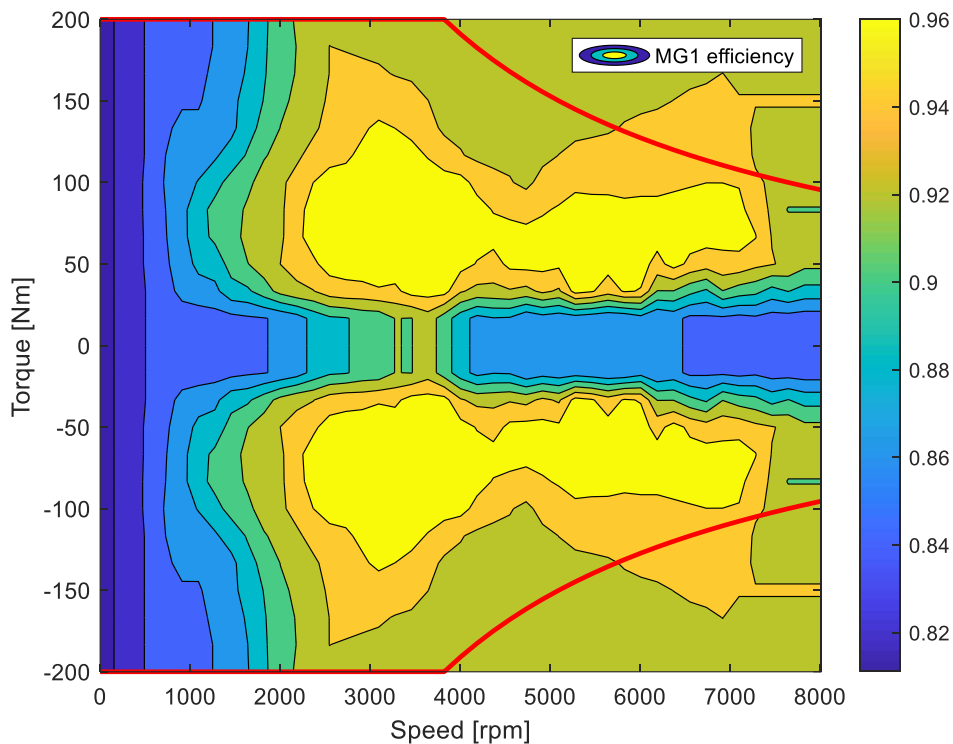


Figure 89

For the degree of hybridization, since this vehicle is able to work both as a hybrid series and as a parallel hybrid, 2 factors have been defined. One will refer to operation as a serious vehicle and the other to operation as a parallel vehicle. Through the (4.1) and the (5.1) were calculated:

$$R_{h,series} = 0.64$$

$$R_{h,parallel} = 0,39$$

For this powertrain, given the good results obtained it was decided to use the same type of battery with the same license plate characteristics used for the previous two configurations.

7.2 NEDC cycle CD test

Having changed the configuration of the powertrain compared to the main vehicle, to take into account the addition of three elements: battery pack, electric motor and electric generator, you choose to increase the mass tests for the NEDC and WLTP cycle by 220 kg, maintaining the coast down coefficients unchanged.

During the CD test, both electric machines are running to ensure pure electric traction without activating ICE for as many cycles as possible. This will inevitably require much more battery power, but on the other side it will be possible to recover more energy while braking since both machines can work as generators.

As we can see from the characteristic in figure 90, the operational points are the classic ones already seen for the NEDC cycle, the electric machine MG1 works smoothly along all the cycles traveled.

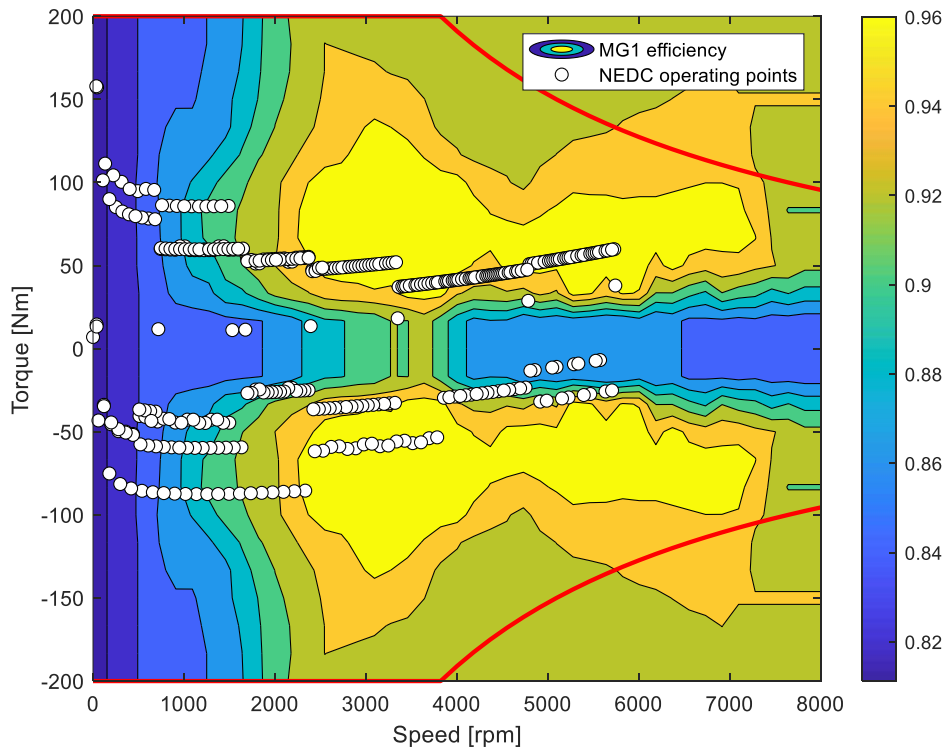


Figure 90

Figure 91 shows the work points of the MG2 electric machine. Most focus on dials at negative speeds, that is, when the two machines work at opposite speeds in order to hold the CARRIER connected to ICE. When ICE needs access, the MG2 machine adapts its speeds to make ICE work optimally.

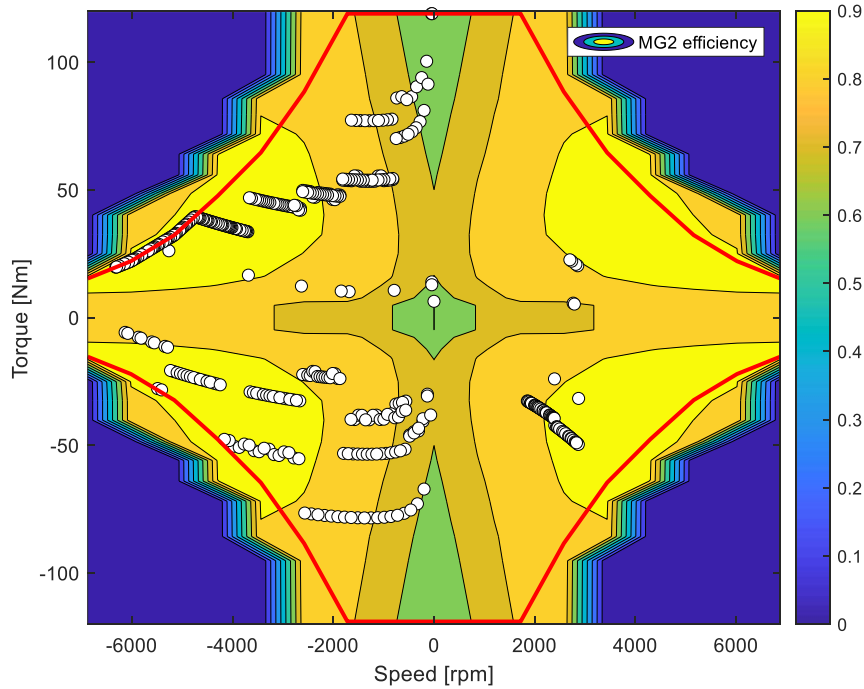


Figure 91

How easy it was to budget this type of architecture works without turning on the thermal engine for 9 NEDC cycles, maximum value achieved in this thesis work. The ICE lights up during the high-speed stretch of the tenth cycle at a charge state of about 19%, the next cycle will confirm that it has reached the electrical brake-off criterion. For the purposes of calculating the electric range, 10 cycles will be considered.

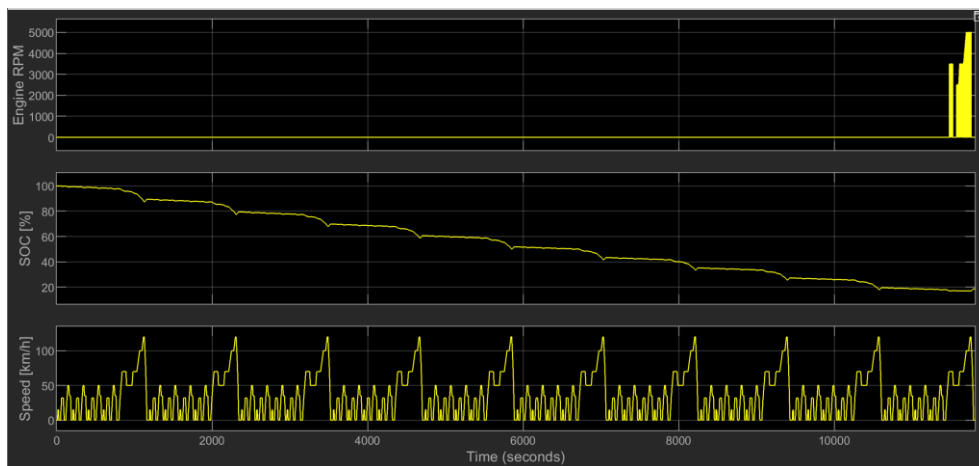


Figure 92

7.3 WLTP cycle CD test

The operating points are very similar to the series configuration, since the gearbox is not present, so the angular speed of the MG1 is directly proportional to that of the wheels via a fixed ratio.

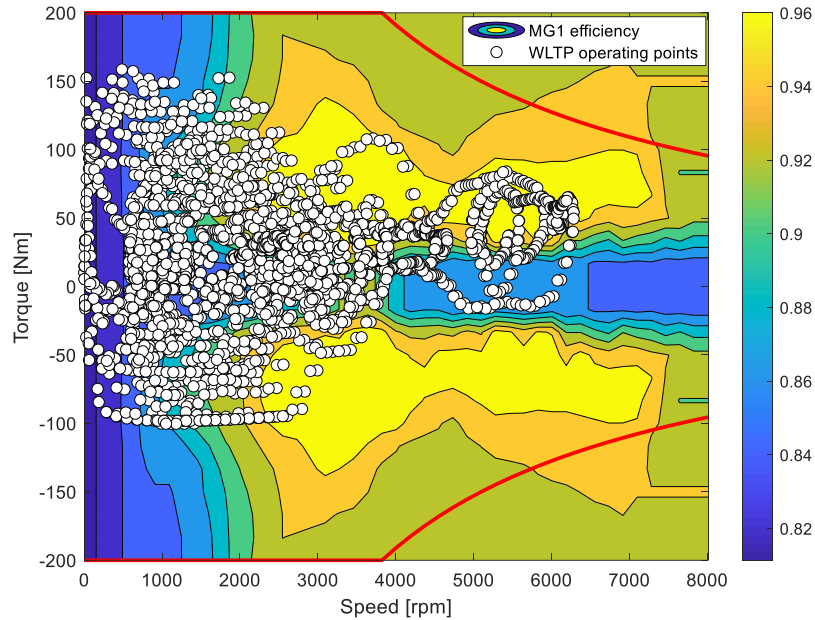


Figure 93

It is clear that the work points of the MG2 electric machine are much more jagged for the WLTP cycle. The work points of the positive speed zone indicate that the thermal engine has come into operation and therefore the MG2 machine adapts its speed.

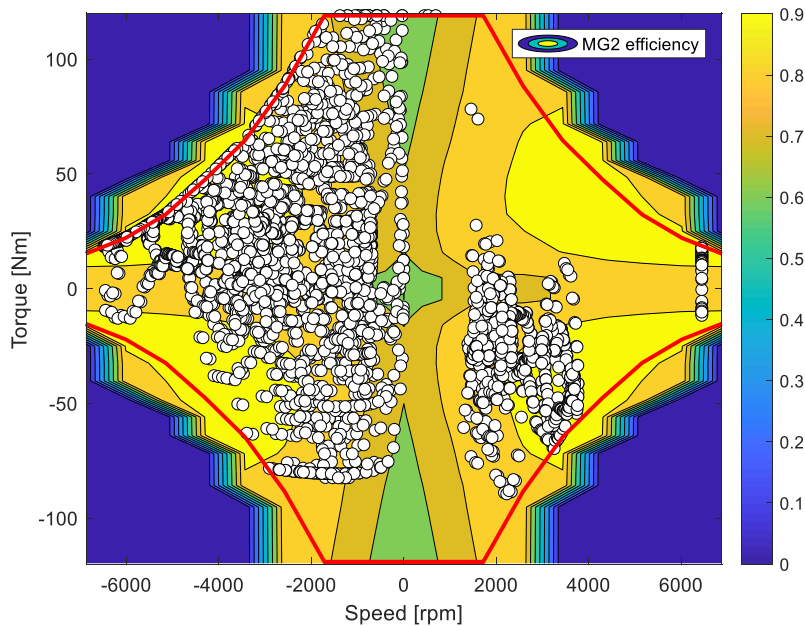


Figure 94

The ICE start to work during the 4th WLTP cycle, one cycle after respect parallel and series configuration. The speed of the thermal engine, very reminiscent of the trend seen for the parallel hybrid, this because despite there is no gearbox along the transmission line, the planetary gearbox behaves just a gearbox with ideally an infinite number of gears.

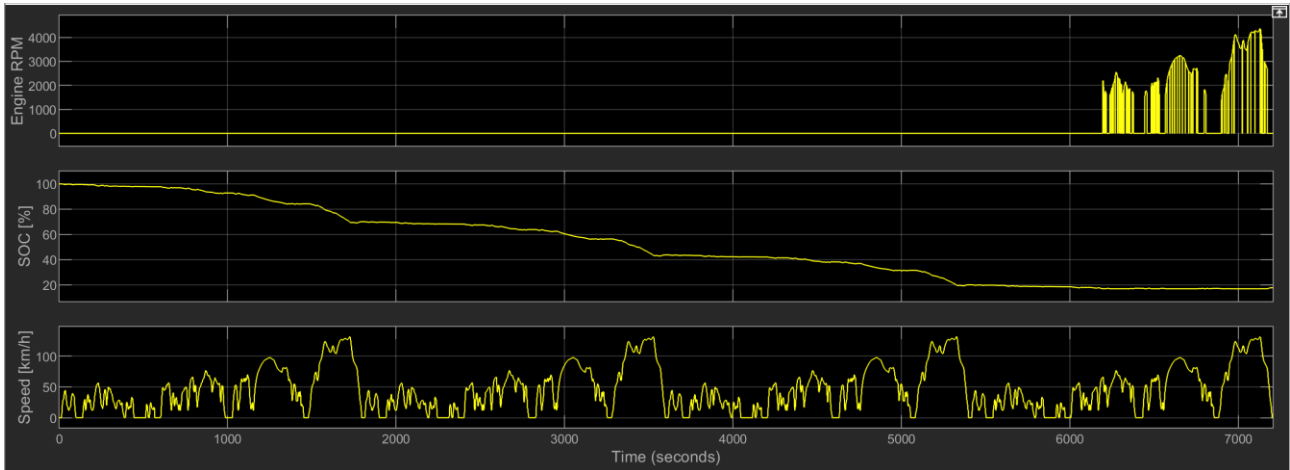


Figure 95

7.4 NEDC cycle CS test

The next step is to perform a CS test along the NEDC cycle, presenting, as previously done, the operational points of ICE and MG2.

ICE most of the time works with loads between 4 and 6 bar of bmep, for low rotation regimes you notice a peak, near the full load curve around the 8 bar. ICE working in this way allows the charge state to remain within a range of $\pm 1\%$ compared to the minimum state of charge, at the end of the CS test you notice a slight increase of the SOC up to about 18.6 %, due to the high-speed section of the NEDC cycle where ICE develops a greater power.

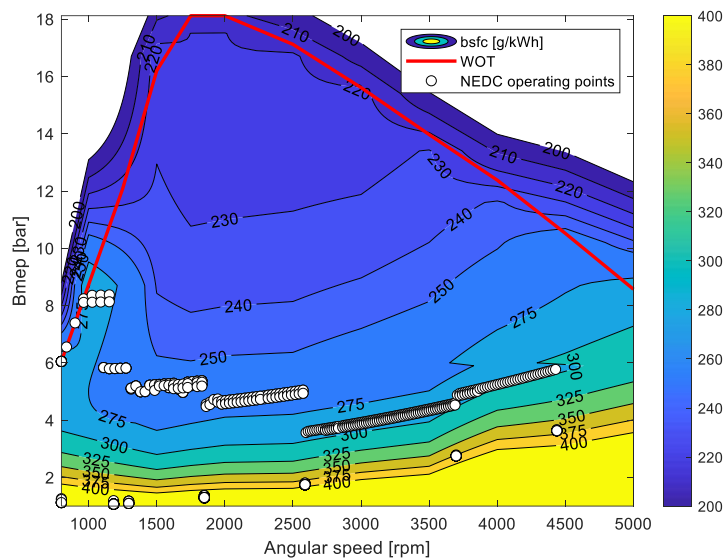


Figure 96

Once again you notice how the MG2 electric machine works on all the dials of the feature, most of the points are concentrated in the third quadrant, where $P_{MG2} > 0$ then you are transferring energy to the batteries.

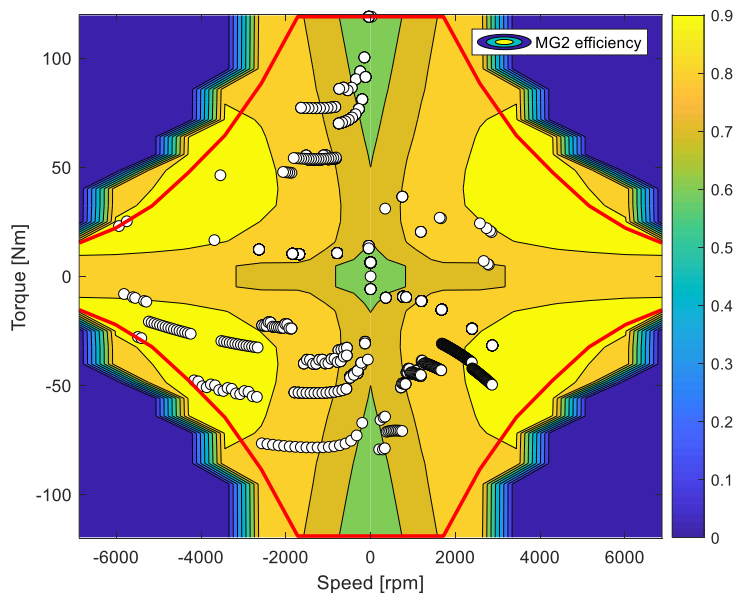


Figure 97

7.5 WLTP cycle CS test

For the WLTP cycle, cs testing was performed, without adopting particular control strategies, this is because, as done in the parallel architecture, the powertrain was allowed to work without consumption constraints, in order to evaluate the minimum performance in thermal CO₂ emissions and FC. The results that will be presented in the next chapter, therefore, are starting data from which, by adopting appropriate optimization control strategies (you know the guide profiles of the approval cycles), you can get additional benefits.

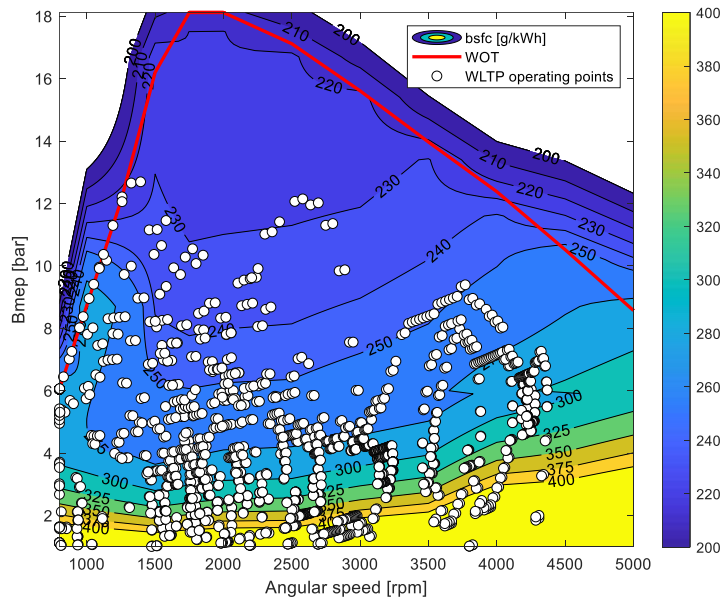


Figure 98

The MG2 electric machine essentially works, as for the NEDC cycle, on all four quadrant, obviously limiting the use in the first quadrant since doing so would result in ICE speeds too high.

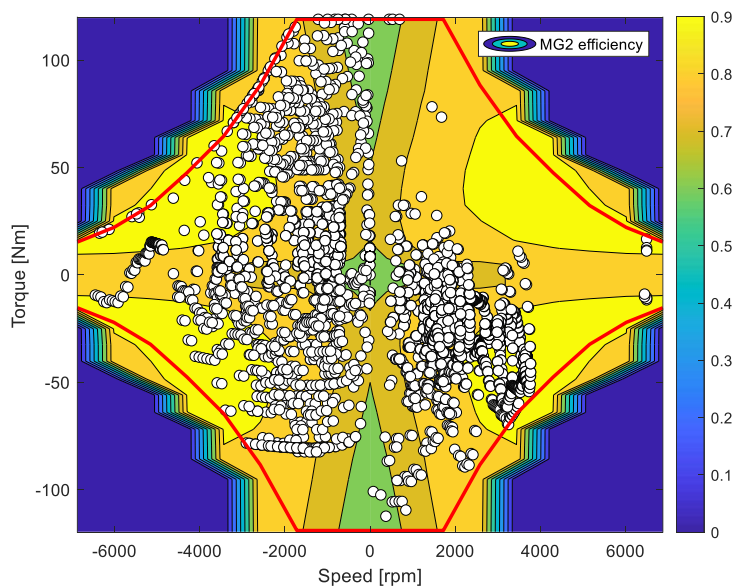


Figure 99

7.6 CO₂ emissions, FC and electric range calculated for NEDC and WLTP cycle

Electric range defined in EU Regulations are reported in table 16.

Ranges [km]	NEDC	WLTP
D _{OVc} /R _{CDC}	110	93,08
D _e /AER	103,9	72,9

Table 16

For this architecture, results were obtained significantly higher than the configurations previously analyzed, for the NEDC cycle, there was a gain on the electric range of about 25 km for the D_{OVc} and R_{CDC} and about 20 km for the D_e, while for the AER a gain of about 10 km.

These results, for completeness of treatment, were carried out simulations, not presented in this thesis work using a battery with a lower capacity but maintaining the same type of powertrain, the data are presented in Table 17:

Type	Li-Ion
Capacity	20 Ah
Nominal Voltage	345 V
Energy	6,9 kWh

Table 17

Using this battery, with an energy reduction of 37.27% it was still able to meet the project requirements for the range in pure electric and achieving results very similar to those obtained for the parallel vehicle in terms of CO₂ emissions and FC:

Ranges [km]	NEDC	WLTP
D _{OVc} /R _{CDC}	77,21	69,81
D _e /AER	69,83	56,81

Table 18

This configuration, looking at the data presented in subsequent graphs, significantly lowers CO₂ emissions and fuel consumption by about 50%. In this type of hybrid vehicle, we notice that the results obtained for the WLTP cycle, unlike the series and parallel powertrain, are lower than those obtained for the NEDC cycle. This result is particularly relevant because, as also studied by [23], the behavior of PHEV vehicles after the change in the approval procedures is not yet clear. In this case it was noted that the vehicle traveled an extra cycle during the WLTP in CD mode, this led to different FOTs from the first two architectures and therefore the subsequent CS test weighed less on the final results, according to the reports in the relevant legislation.

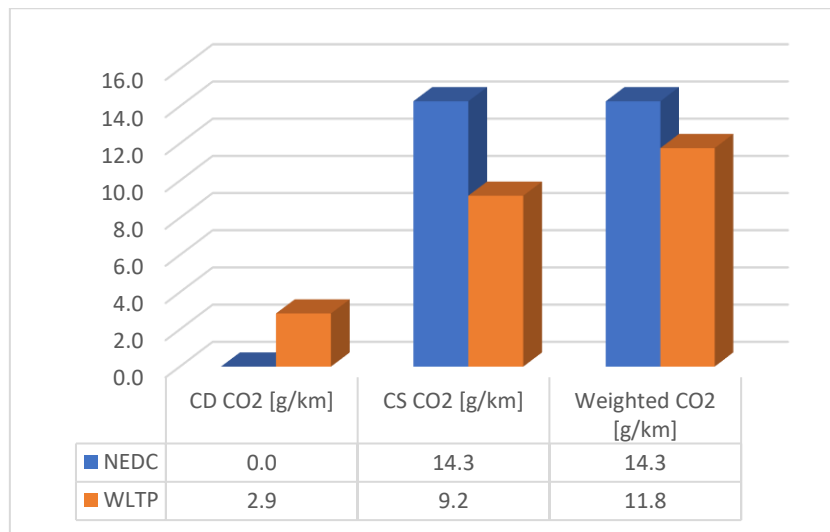


Figure 100

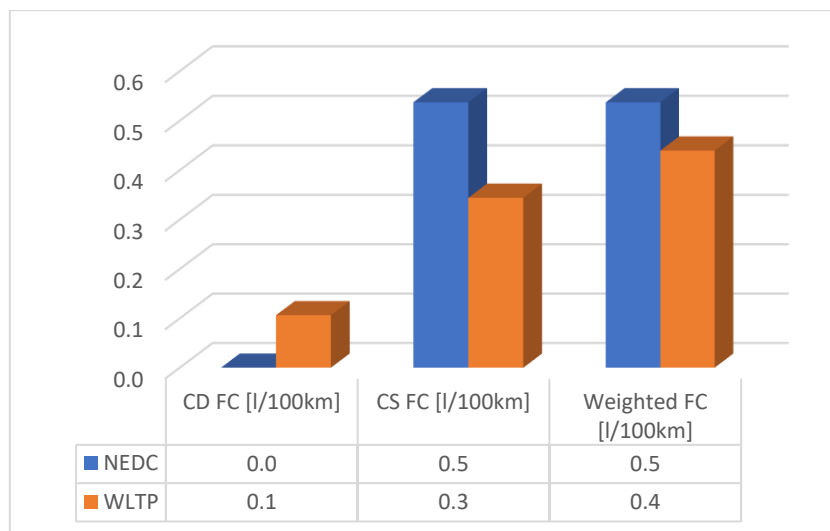


Figure 101

7.7 Performance analysis

The acceleration from 0 to 100 km/h of the vehicle was carried out in pure electric, making the two electric cars work so as not to turn on the thermal engine, therefore with a combination of speed such as to make the speed of the carrier null.

This configuration accelerates from 0 to 100 km/h in pure electric in 11 seconds, as was fair to expect is the best acceleration performance in pure electric of the three configurations analyzed.

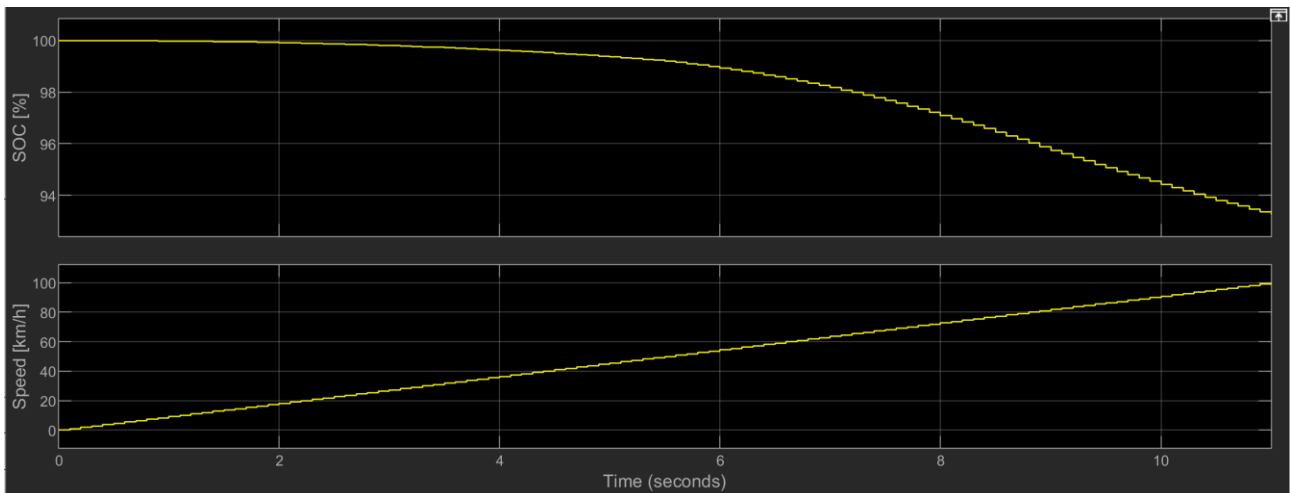


Figure 102

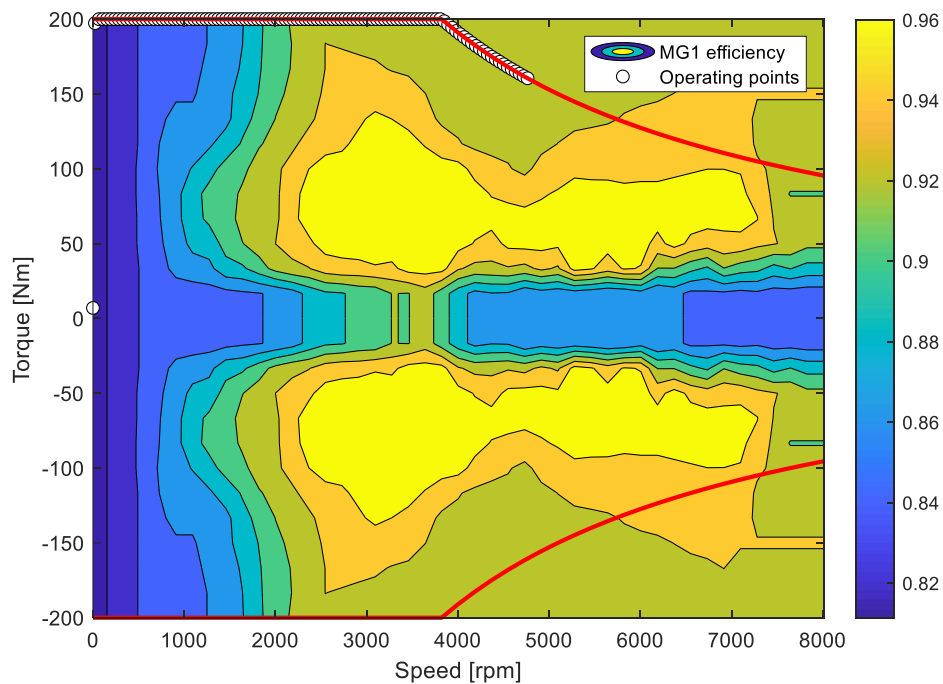


Figure 103

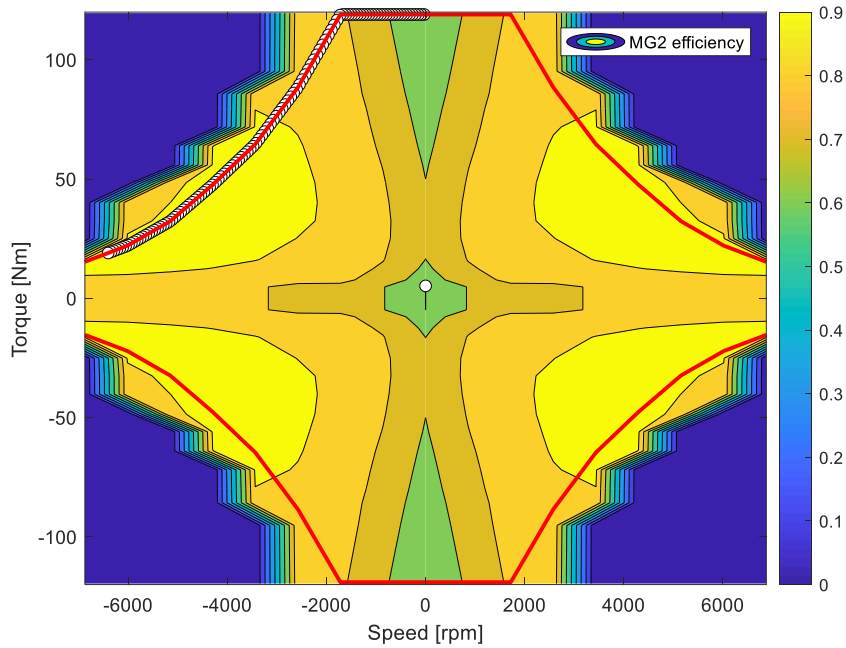


Figure 104

Figures 103 and 104 shows that both electric cars work along the maximum performance curve.

The second performance analysis concerns an emergency overtaking on suburban road. It was decided to entrust the propulsion for the duration of the manoeuvre to the electric machines alone, in fact it is noted that the state of charge drops in a much more marked way, having to power two machines that behave like engines, compared to previous architectures. The final charge status is just under 75%, about 10% less than the other two. This high energy absorption does not present serious problems since if you reach an SOC considered critical, just operate the thermal engine and bring the MG2 machine to work in the dials where it works as a generator. Once the thermal engine is operated, one might think to produce most of the power share needed for propulsion and consequently limit the power developed by the MG1 machine to make battery charging faster and more efficient.

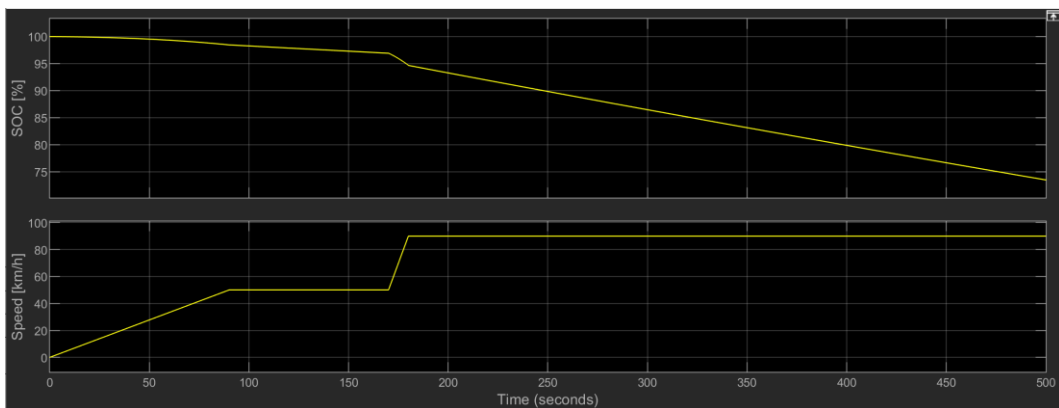


Figure 105

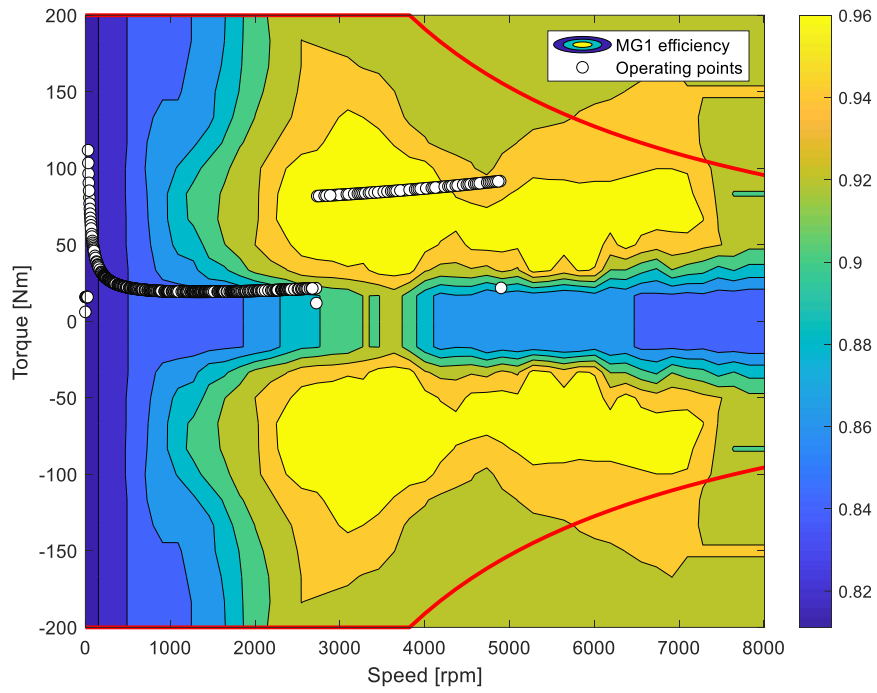


Figure 106

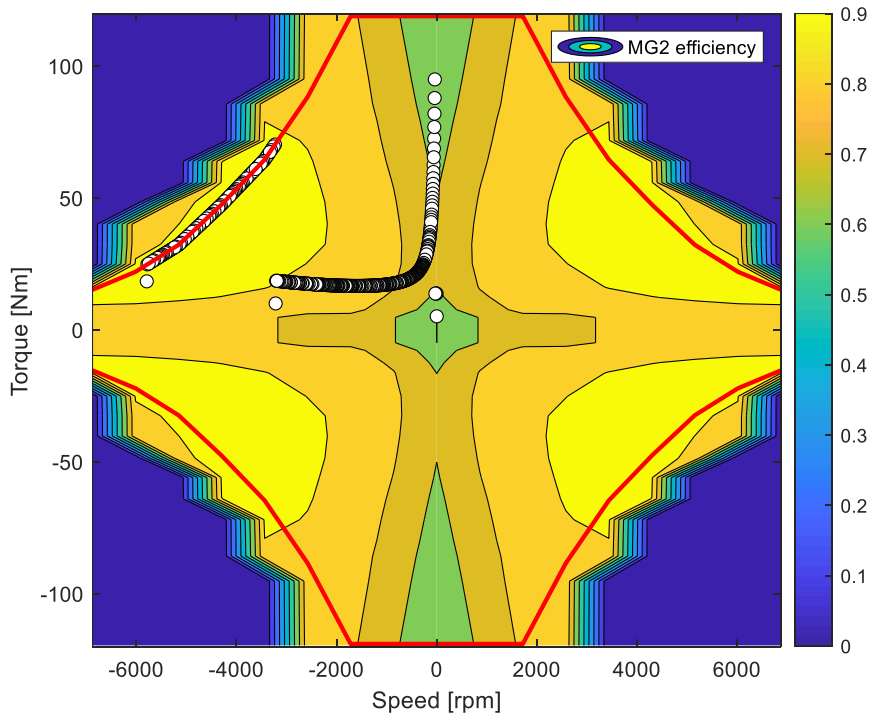


Figure 107

In this last simulation starting from a fully SOC you are asked to the driver of the vehicle to reach a speed of 140 km/h and to keep it up to a value of SOC considered acceptable.

The two electric machines work in order to meet the demand for power, the PSD manages to combine the power transfer, allowing the vehicle to maintain the constant speed of 140 km/h for about 19 minutes, then it reaches 20% of SOC and is activated the thermal engine in order to reduce the power transmitted by the MG1 machine, taking less energy from the batteries and at the same time making the MG2 work as a generator, as noted in the figure. 108.

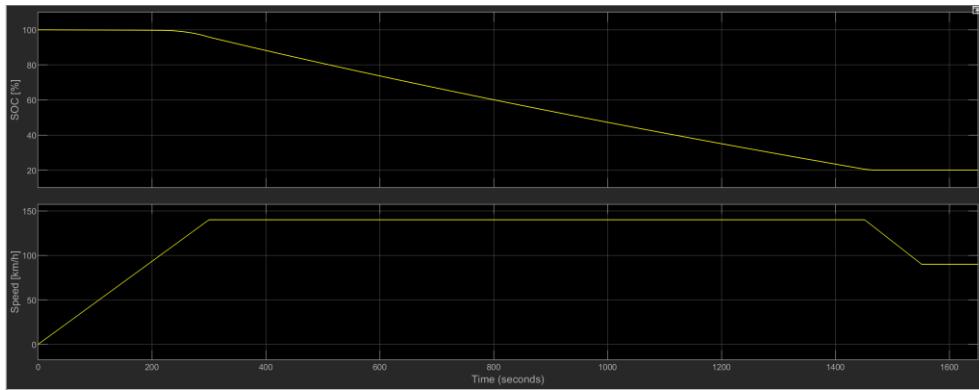


Figure 108

On the character of the MG1 machine you can see that there is a torque jump, this is due to the activation of the ICE that allows a reduction in the power delivered by MG1, the vehicle in this case is behaving like a parallel hybrid since ICE and MG1 provide along with the traction of the vehicle.

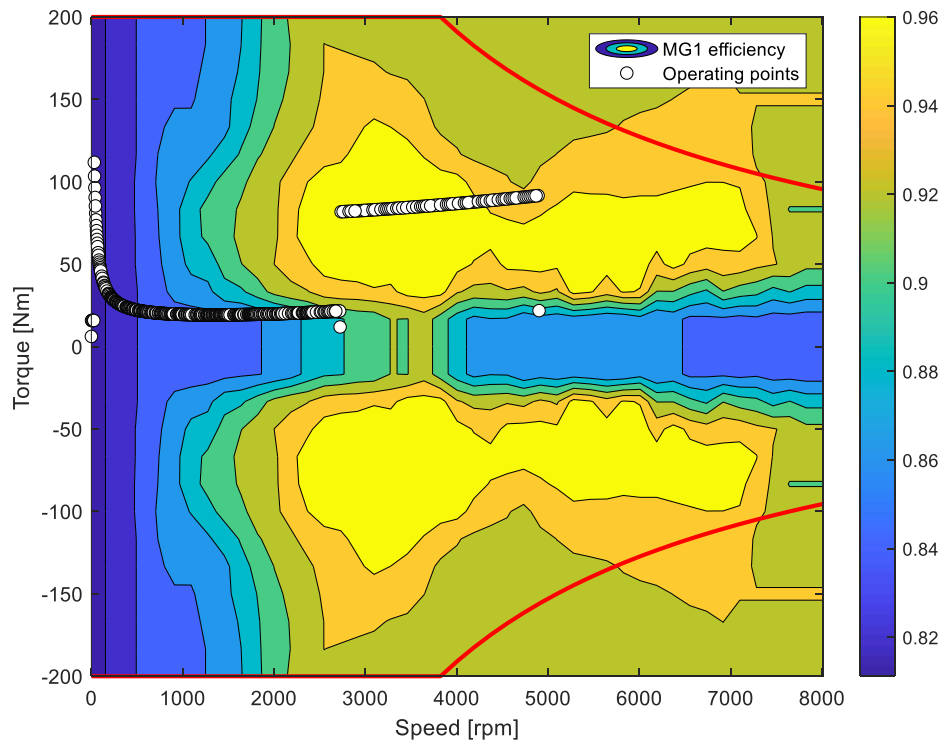


Figure 109

The MG2 electric machine works for most of the simulation in the third quadrant where the power is negative, so for the convention adopted is participating in the traction of the vehicle, when then the ICE is activated the rotation speed changes towards going to generate positive energy that following the electric path goes to provide energy to the batteries.

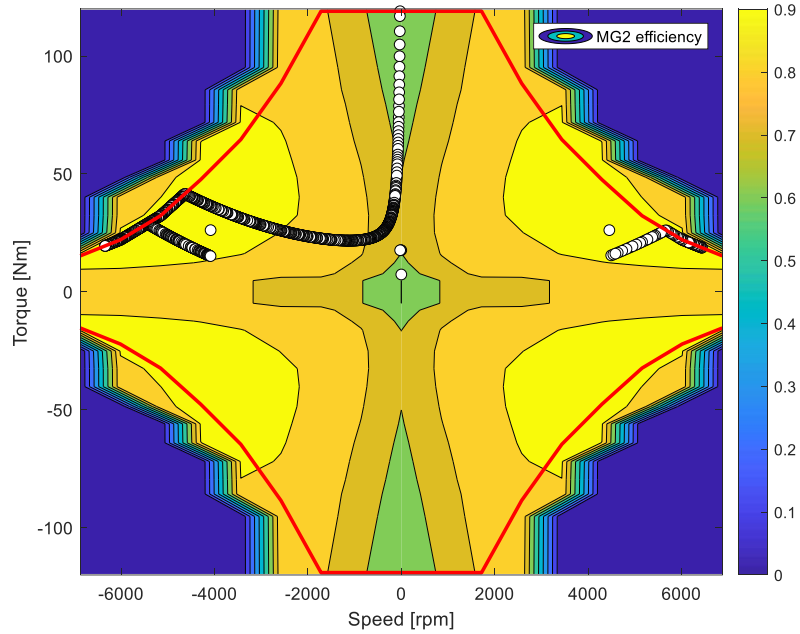


Figure 110

ICE is activated only in the later stages of the simulation, when the charge status reaches 20%.

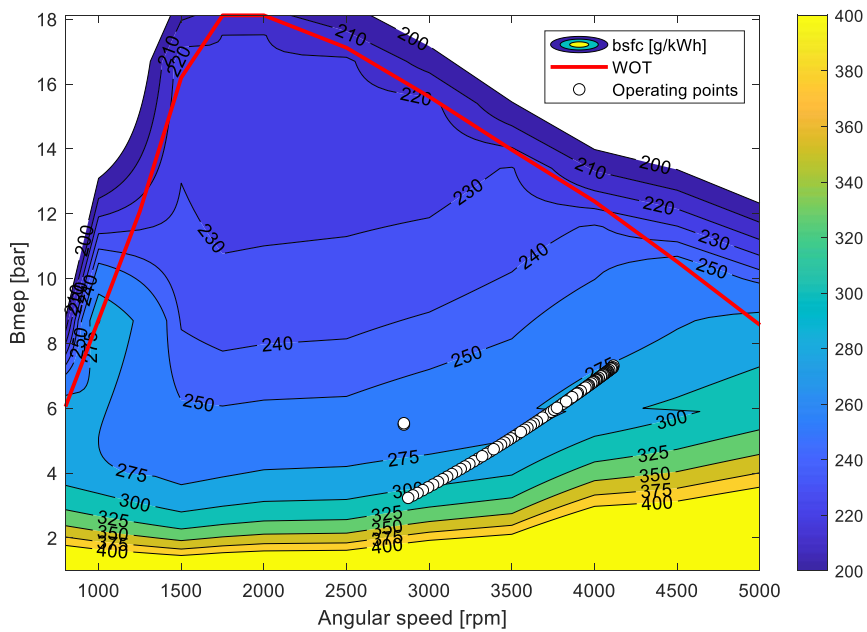


Figure 111

Chapter 8: Conclusions

The vehicle with series configuration lends itself adequately to the PHEV type, excellent behavior was found in pure electric driving, with SOC trends considered satisfactory during the simulations of the NEDC and WLTP driving cycles, but also during performance analysis. An undoubted advantage was to be able to reduce the size of the thermal engine by being freed from the speed of rotation of the wheels, thereby reducing consumption and CO_2 emissions. During these analyses, the various control strategies that can be adopted on this type of vehicle were not taken into account, the only strategy just mentioned was to activate the thermal engine when the SOC is lower than previously set SOC_{min} . From the simulations along the driving cycles, excellent electric range values emerged, a key parameter for PHEVs even more when you think of a model of the A or B segment, mainly used in cities where the average daily mileage is about 30-35 km. One disadvantage found in this type of architecture is that of the double conversion of power from the thermal engine to the electric generator, against a power developed by ICE of about 20 kW the generator manages to exploit only 60% the remaining 40% is not used due to the inevitable losses along the transmission line.

One of the goals of this thesis work was to understand the margin for reducing CO_2 and fuel consumption emissions. For this type of architecture, there was a reduction of η_c of about 86% for the NEDC cycle and 85% for the WLTP. For CO_2 emissions for the NEDC cycle there is an 86% reduction and for the WLTP cycle of about 87%.

The parallel architecture, as a whole, proves adequate for plug-in vehicles, the results of the simulations carried out are very satisfactory, in all the tests carried out there were improvements compared to the series configuration. It is worth remembering, however, that this type of configuration requires an important implementation of control strategies, having both thrusters mechanically connected to the wheels. In these simulations it was decided to use a constant torque distribution factor, but to make the work of both thrusters more efficient one might consider implementing control strategies for power-sharing, based on rules based on heuristic relationships. Optimization control strategies could also be used, but these require prior knowledge of the driving profile and could be used by manufacturers during NEDC and WLTP procedures. During the simulations, it was noted that the use of the gearbox present on the traditional vehicle inevitably leads to losses from the point of view of performance, so it goes without saying that in this architecture the gearbox plays a fundamental role and should be designed in such a way as to allow the electric machine to work in the best conditions in accordance with the needs of the thermal engine. All this leads to an increase in costs compared to a series architecture, which does not need a specially designed gearbox, but through a simple fixed ratio of reduction is able to make the electric machine work in areas of maximum efficiency.

The complex series-parallel configuration obtained using an planetary gearbox, from the simulations carried out turns out to be the best both from the point of view of emissions and consumption, and from the point of view of acceleration performance and maintaining a fairly high speed. By analyzing the data obtained during the simulations of the approval cycles, it was found that this configuration, boasting the highest electric range allowing the vehicle to obtain results on the WLTP approval cycle less than the NEDC, although the former is much more energy-aggressive than the second. This architecture has very wide room for improvement in terms of energy management, since by appropriately calibrating the speed of the MG2 machine connected to the sun of rotation, you can theoretically obtain infinite operating points for ICE, that is, to have a change with an infinite number of ratios. Many studies have been carried out in order to improve this type of architecture, including [24] in which a second epicyclic gear set is inserted as in figure 110 in order to obtain greater flexibility for the control of the two electric machines.

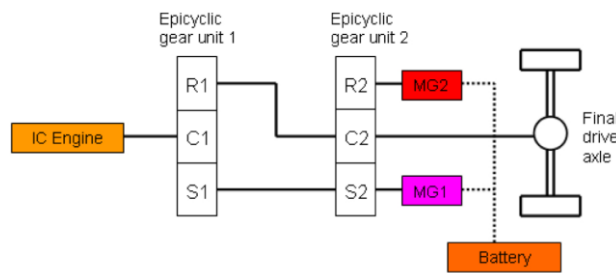


Figure 112

As a last comparison of the 3 architectures, energy efficiency regarding the WLTP cycle was calculated during CS testing, simulation in which all components of the hybrid powertrain are involved:

$$\eta_{tot} = \frac{E_{DC}}{E_{fuel} + E_{BT+} + E_{BT-}} \quad (8.1)$$

- E_{DC} : energia necessaria spesa per seguire il ciclo guida in [kW];
- E_{fuel} : energia ottenuta dalla combustione del carburante in [kW];
- E_{BT+} : energia erogata dalle batterie in [kW];
- E_{BT-} : energia restituita alle batterie attraverso la frenata rigenerativa

WLTP CS TEST			
	Series	Parallel	Complex
η_{tot}	0,36	0,42	0,45

Table 19

Note that the complex architecture is more efficient than other configurations for this particular case study, but it should be noted that no particularly elaborate control strategies have been implemented to make powertrains work better, so these results are liable to improvements.

Appendix A

Homologation driving cycle

Driving cycles are graphical and numerical representations of a vehicle's instant speed $v(t)$ as a function of time and are defined in different countries by competent bodies to assess vehicle performance in several respects: fuel consumption and pollutant emissions, both in design and on-road testing.

Some of these cycles have theoretical origin and can be formulated analytically, while others to describe a more realistic driving situation originate from speed measurements carried out directly on vehicles on real routes. Guide cycles can belong to two distinct categories:

- Transient driving cycles: these are the cycles that involve changes in parameter movements (speed, acceleration, grade, etc.)
- Modal driving cycles: these are cycles characterized by the succession of short time intervals during which the acceleration of the vehicle is constant

The driving cycles that find the most applications are:

- European driving cycle: NEDC, WLTP and RDE;
- American driving cycle: FTP-72, FTP75, US06, SC03, HFEDS, HD-UDDS, IM240, LA-92, NYCC;
- Japanese driving cycle: 10 mode, 11 mode, 15 mode, 10-15 mode, JC08;

In addition to the driving cycles introduced in the automotive sector there are driving cycles that also affect the motorcycle and heavy-duty and off-road vehicles

The NEDC cycle combines a series of 4 ECE-15 cycles, which correspond to a type of urban driving, followed by an EUDC cycle representative of suburban driving, at higher speeds.

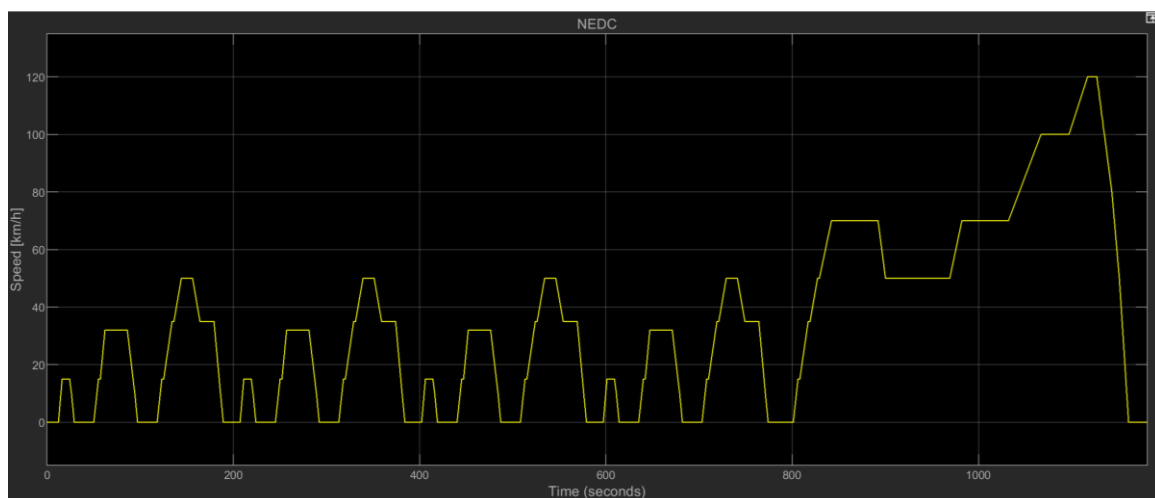


Figure 113

From September 1, 2017, the Worldwide harmonised HarmonisEd Light-Duty Vehicles Test Procedure (WLTP) was introduced, which provides more realistic consumption data thanks to significantly more dynamic test parameters than the NEDC cycle. This can be divided into four different phases, each representing a different driving mode.

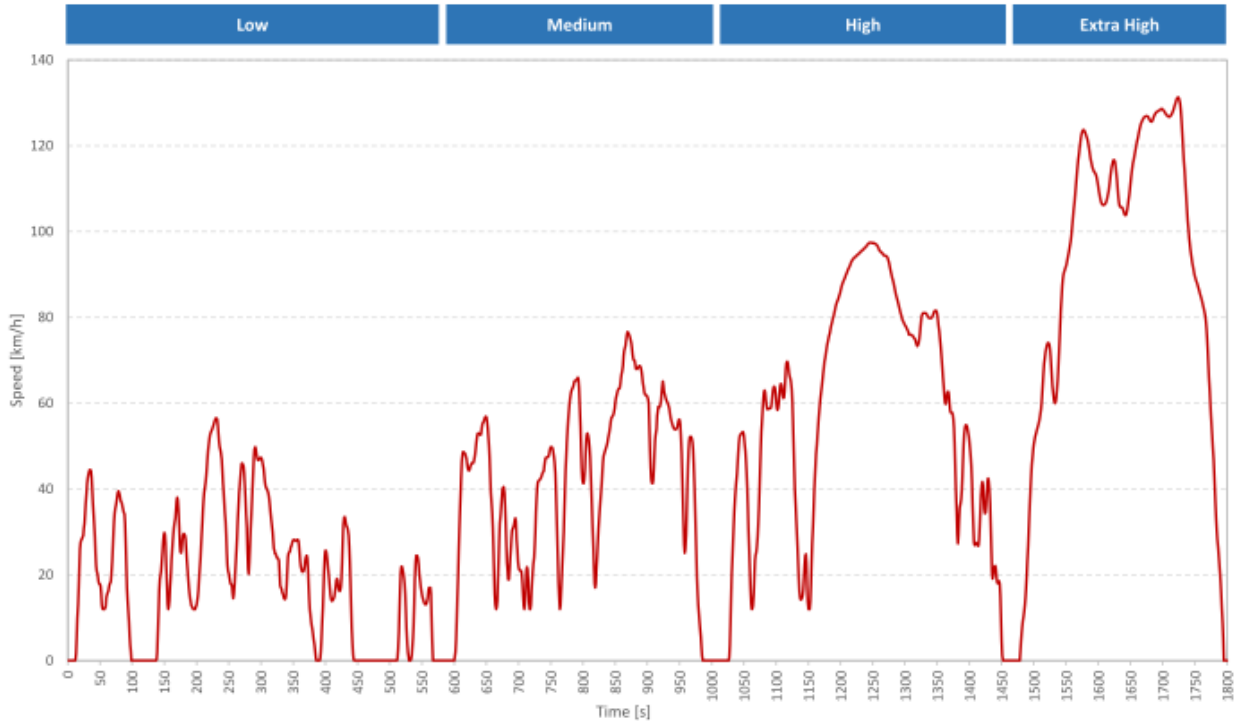


Figure 114

The main differences between the two types of tests are reported., a summary of the main procedural differences between NEDC and WLTP procedures is presented in [25].

Parameters	NEDC	WLTP
Duration (s)	1180	1800
Distance (km)	11.03	23.27
Average speed (km/h)	33.6	46.5
Maximum speed (km/h)	120.0	131.3
Stop duration (%)	23.7	12.6
Constant driving (%)	40.3	3.7
Acceleration (%)	20.9	43.8
Deceleration (%)	15.1	39.9
Average positive acceleration (m/s^2)	0.59	0.41
Maximum positive acceleration (m/s^2)	1.04	1.67
Average positive “speed*acceleration” (m^2/s^3)	1.04	1.99
Maximum positive “speed*acceleration” (m/s^2)	9.22	21.01
Average deceleration (m/s^2)	-0.82	-0.45
Minimum deceleration	-1.39	-1.50

Table 29

In addition to the WLTP, measures have been carried out in Europe since September 2017 according to the RDE test method. Unlike NEDC and WLTP, emissions are not measured on the test bench, but in road traffic. The RDE measurement process requires the vehicle to take several routes, one third in urban areas, one on suburban roads and one on motorways with random accelerations and braking, of course always in compliance with the rules, in figure 115 is show an example of RDE cycle. The car is equipped with Portable Emission Measurement System (PEMS) detectors that measure emissions. The duration of the test is between 90 and 120 minutes with an external temperature of between -7°C and 35°C .

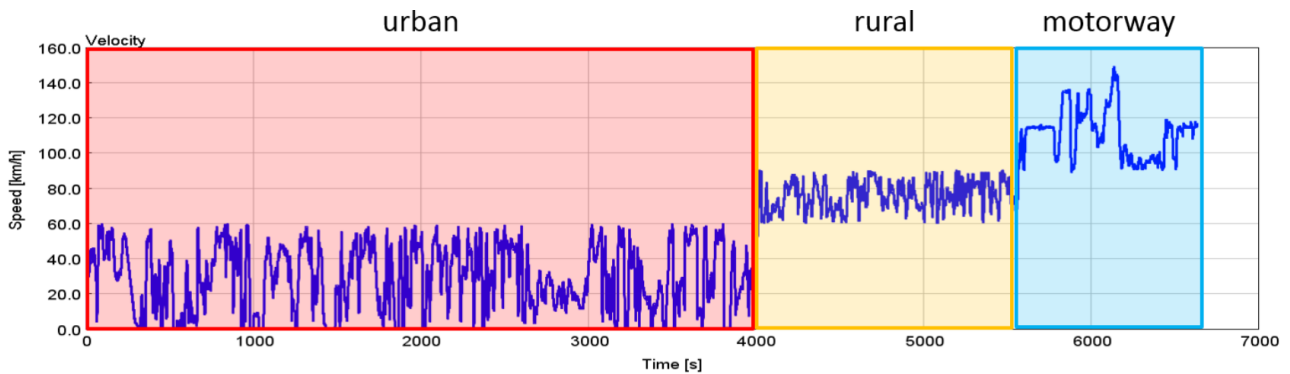


Figure 115

Bibliography

- [1] E. E. G. V. Initiative, «EGVI 10 YEARS IMPACT ASSESSMENT,» Aprile 2019;
- [2] Regulation (UE) 2019/631 of European Parliament and of the Council 17/04/2019
- [3] “Trasport & Enviroment” “Electric surge: Carmakers’ electric car plans across Europe 2019-2025”;
- [4] Notes of the course “Controllo delle emissioni di inquinanti” Prof. E. Spessa;
- [5] S. Sasaki “Toyota's newly developed hybrid powertrain” Proc. of the 10th International Symposium on Power Semiconductor Devices and ICs, 1998. IEEE-ISPDS 98. Kyoto (JP) Jun 03-06 1998;
- [6] J. M. Miller “Hybrid electric vehicle propulsion system architectures of the e-CVT type” IEEE Transaction on Power Electronics, Vol. 21, No. 3, May 2006, page(s) 756-767;
- [7] M.J. Hoeijmakers J.A. Ferreira “The Electric Variable Transmission” IEEE Transactions on Industry Applications, Publication Date: July-Aug. 2006 Vol. 42, Issue 4 page(s): 1092 – 1100. ISSN : 0093-9994;
- [8] G. Holmes and M. R. Schmidt, “Hybrid Electric Powertrain Including a Two-Mode Electrically Variable Transmission,” U.S. Patent 6 478 705 B1, Nov. 12, 2002.X. Ai;
- [9] G.Y Ehsami M., GaoY., e Ehmadi A. “ Hybrid Electric Vehicles, ” Modern Electric, Hybrid Electric and Fuel Cell Vehicles, CRC Press, 2011;
- [10] L. Guzzella, A. Sciarretta “ Vehicle Propulsion System ” Springer Press Third Edition;
- [11] Regulation (UE) 2017/1151 of European Parliament and of the Council 1/07/2017;
- [12] QSS_ToolBox manual, ETH Zurich;
- [13] Lynwander, P., 1983, Gear Drive Systems: Design and Application. Marcel Dekk;
- [14] C. Ferraresi, T. Raparelli, “Meccanica applicate” Clut Press, Third Edition;
- [15] Notes of the course “Propulsori termici” Prof. F. Millo;

- [16] K. Khan, B. Zhou; "Real Time Application of Battery State of Charge and State of Health Estimation" Michigan Technological University, SAE International 2017-01-1199;
- [17] Notes of the course "Propulsori termici", Fuel Consumption, CO₂ and NO_x Emissions of a Passenger Car over the NEDC and WLTC driving cycles, prof. F. Millo;
- [18] J. Meisel, W. Shabbir, S. A Evangelou "Control of PHEV and HEV Parallel Powertrains using a Sequential Linearization Algorithm", SAE International 2015-01-1219;
- [19] Regulation (UE) 2017/1151 of European Parliament and of the Council 1/07/2017;
- [20] UNECE Regulation 101, revision 3, "Uniform provisions concerning the approval of passenger cars powered by an internal combustion engine only, or powered by a hybrid electric powertrain;
- [21] UNECE Global Technical Regulation No.15, Worldwide Harmonized Light Vehicles Test Procedure. UNECE Geneva, Switzerland, 2016;
- [22] C. Cubito, L. Rolando, F. Millo, B. Ciuffo, S. Serra, G. Trentadue, M. G. Otura and G. Fontaras "Energy management Analysis under Different Operating Modes for a Euro-6 Plug-in Hybrid Passenger Car, SAE international 2017-01-1160;
- [23] J. Pavlovic, A. Tansini, G. Fontaras, B. Ciuffo, M. G. Otura, G. Trentadue, R. S. Bertoa, F. Millo "The impact of WLTP on the Official Fuel Consumption and Electric Range of Plug-in Hybrid Electric Vehicles in Europe", SAE international 2017-01-1160;
- [24] A. Elmarakbi, D. Dixon, R. Trimble and Q. Ren; "Modelling and Analyzing Hybrid Electric Vehicles with Single and Dual Epicyclic Power Split Transmission", SAE International, 2013-01-9119;
- [25] J. Pavlovic, B. Ciuffo, G. Fontaras, G. Marotta et al, "An insight into procedural differences between NEDC and WLTP and their possible impact on CO₂ emissions from the type-approval: Case of vehicles with internal combustion engines", under review for Energy Policy;